Unclassified
SECURITY CLASSIFICATION

(2)

AD-A208 866

MENTATION PAGE

Form Approved
OMB No. 0704-0188

1a. [illegible]	1b. RESTRICTIVE MARKINGS
2a. S [illegible]	3. DISTRIBUTION/AVAILABILITY OF REPORT Approved for public release; distribution is unlimited.
2b. DECLASSIFICATION/DOWNGRADING SCHEDULE	
4. PERFORMING ORGANIZATION REPORT NUMBER(S) UTRC89-13 ✓	5. MONITORING ORGANIZATION REPORT NUMBER(S) AFOSR-TR- 89-0715
6a. NAME OF PERFORMING ORGANIZATION United Technologies Research Center	6b. OFFICE SYMBOL (If applicable)
6c. ADDRESS (City, State, and ZIP Code) East Hartford, CT 06108	7a. NAME OF MONITORING ORGANIZATION AFOSR/NA
	7b. ADDRESS (City, State, and ZIP Code) Building 410, Bolling AFB DC 20332-6448
8a. NAME OF FUNDING/SPONSORING ORGANIZATION AFOSR/NA	8b. OFFICE SYMBOL (If applicable) NA
	9. PROCUREMENT INSTRUMENT IDENTIFICATION NUMBER F49620-88-C-0051
8c. ADDRESS (City, State, and ZIP Code) Building 410, Bolling AFB DC 20332-6448	10. SOURCE OF FUNDING NUMBERS PROGRAM ELEMENT NO. 61102F; PROJECT NO. 2308; TASK NO. A2; WORK UNIT ACCESSION NO.

DTIC ELECTE JUN 06 1989 S C E

11. TITLE (Include Security Classification)
(U) The Determination of Rate-Limiting Steps During Soot Formation

12. PERSONAL AUTHOR(S)
Colket, M. B., Hall, R. J., Sangiovanni, J. J. and Seery, D. J.

13a. TYPE OF REPORT	13b. TIME COVERED	14. DATE OF REPORT (Year, Month, Day)	15. PAGE COUNT
Annual	FROM 2/1/88 TO 1/31/89	1989 - April 27	83

16. SUPPLEMENTARY NOTATION

17. COSATI CODES			18. SUBJECT TERMS (Continue on reverse if necessary and identify by block number)
FIELD	GROUP	SUB-GROUP	Toluene, Benzene, pyrolysis, oxidation, polyaromatic hydrocarbons, soot formation, shock tube

19. ABSTRACT (Continue on reverse if necessary and identify by block number)

A single-pulse shock tube has been used to examine toluene pyrolysis and the rich oxidation of benzene ($\phi > 7.5$) diluted in argon over the temperature range of 1200 to 2000K and at total pressures of ten to thirteen atmospheres. Dwell times were about 500 microseconds. Collected gas samples were analyzed using gas chromatography for hydrogen, carbon oxides and C_1- to C_{14}- hydrocarbons. Low molecular weight products during benzene oxidation include cyclopentadiene and vinylacetylene and support literature proposals for oxidation of benzene. High molecular weight products are dominated by species containing mixtures of five- and six-membered rings. During toluene pyrolysis very rapid production of polyaromatic hydrocarbons occurs between 1400 and 1450K, consistent with temperatures at which particle inception occurs in diffusion flames.

(Cont.d)

20. DISTRIBUTION/AVAILABILITY OF ABSTRACT	21. ABSTRACT SECURITY CLASSIFICATION
☒ UNCLASSIFIED/UNLIMITED ☒ SAME AS RPT. ☐ DTIC USERS	Unclassified
22a. NAME OF RESPONSIBLE INDIVIDUAL Julian M Tishkoff	22b. TELEPHONE (Include Area Code) (202) 767-[illegible]	22c. OFFICE SYMBOL AFOSR/NA

DD Form 1473, JUN 86 — Previous editions are obsolete. — SECURITY CLASSIFICATION OF THIS PAGE

Unclassified

ABSTRACT (Cont'd.)

Simplified modeling techniques of soot formation have been explored. The most successful model is one based on the MAEROS code. Using experimentally determined benzene production rates from a premixed ethylene, laminar flame and known rates for carbon addition to particles, production rates for soot are predicted accurately.

UTRC89-13

THE DETERMINATION OF RATE – LIMITING STEPS DURING SOOT FORMATION

Annual Report

Table of Contents

List of Figures

UTRC89-13

THE DETERMINATION OF RATE-LIMITING STEPS DURING SOOT FORMATION

Annual Report

I. Summary

A single-pulse shock tube has been used to examine toluene pyrolysis and the rich oxidation of benzene ($\phi > 7.5$) diluted in argon over the temperature range of 1200 to 2000K and at total pressures of ten to thirteen atmospheres. Dwell times were about 500 microseconds. Collected gas samples were analyzed using gas chromatography for hydrogen, carbon oxides and C_1- to C_{14}-hydrocarbons. Low molecular weight products during benzene oxidation include cyclopentadiene and vinylacetylene and support literature proposals for oxidation of benzene. High molecular weight products are dominated by species containing mixtures of five- and six-membered rings. During toluene pyrolysis very rapid production of polyaromatic hydrocarbons occurs between 1400 and 1450K, consistent with temperatures at which particle inception occurs in diffusion flames.

Simplified modeling techniques of soot formation have been explored. The most successful model is one based on the MAEROS code. Using experimentally determined benzene production rates from a premixed ethylene, laminar flame (Harris, Weiner and Blint) and known rates for carbon (as acetylene) addition to particles, production rates for soot are predicted accurately.

II. Introduction

There is increasing experimental evidence that important rate-limiting steps to soot formation are the production and growth of aromatic rings. Detailed modeling and comparison to experimental data has led to a good understanding of mechanisms and rates for the production of benzene (and phenyl radical). Existing mechanisms for the formation of naphthalene (plus related species) and higher order aromatics are principally thermochemical estimates and no experimental verification of these steps (mechanisms or rate constants) are available. Another large uncertainty in soot formation mechanisms is the effect of oxidation. Under many conditions, growth of polyaromatic hydrocarbons (PAH's) may be quite fast but is counterbalanced by oxidation. Therefore, the net production rate of PAH's and therefore of soot is only a small fraction of the "gross" production rate of PAH's. Oxidation processes (mechanisms and rates) of aromatic hydrocarbons at elevated temperatures (> 1200K) are unfortunately very poorly known.

To investigate these important and competitive phenomena, an experimental and modeling program is being performed. The experimental phase of the program involves the use of a single-pulse shock tube to thermally stress mixtures of gases, which are then quenched, and the reaction products are analyzed. This program is focusing on detection of two- and three-ringed products in order to test mechanisms proposed for the formation of these species. In support of this work and under corporate sponsorship, the gas sampling system has been modified to collect and detect high molecular weight species. To examine the competitive oxidation processes, rich oxidation of benzene has been investigated. Furthermore, in order to help confirm detailed chemical kinetic modeling, species concentrations will be measured in real time by coupling a time-of-flight mass spectrometer to the end wall of the shock tube.

Two types of modeling are being performed as part of this contract. Detailed chemical kinetic modeling is being used for comparison to experimental data and to test reaction mechanisms and rate constants for formation of multi-ringed species and for oxidation processes. Secondly, using

concepts developed from this work and from the literature, simplified models are being examined which may be useful in describing the formation and growth of soot. Since this latter work is relatively new and the results are extremely encouraging, details of the calculations are provided in this report.

III. Results

A. Modifications to Experimental Facilities

A primary goal of this program is to collect experimental data on the production of high molecular weight species during pyrolysis and "oxidative pyrolysis" of hydrocarbons. In order to collect this data, the sampling system was modified. The system was modified under corporate sponsorship and several designs and calibration procedures were tested. Schematics of the original and final sampling system are compared in Figures 1a and 1b. In the original system, lines were heated to 80°C, whereas for the modified system, all lines were heated to 150°C, and better monitoring procedures were established to avoid "cold" spots. In addition, high temperature solenoids were installed in the modified system. An important change was moving the sampling collection volume to after, rather than before, the gas sampling loops. This was required in order to minimize the number of valves between the shock tube and the sampling loops, since each valve resulted in some loss of the high molecular weight products. This design is not ideal since it does not allow for mixing any non-uniformities in the collected sample. Nevertheless, comparison of data obtained using the modified system compares well with data obtained using the original sampling arrangement. In addition, an enhancement in the calibration technique was developed. All species with molecular weights of about 100 g/mole and below could be adequately calibrated using premixed gaseous samples in bottles which could be interchanged using quick disconnect fittings. Accuracy of analysis for these species is approximately $\pm$ 3 to 6 percent. This uncertainty is size dependent with the larger uncertainty assigned to the heavier species (e.g., benzene, toluene, styrene, etc.). For yet larger species, solid samples were dissolved in toluene and then injected into an atmosphere of argon and allowed to mix at high temperature in a mixing volume for about one-half hour (See Fig. 1b). Subsequently, the gas was analyzed and calibration factors were determined relative to the toluene response. Uncertainties were approximately $\pm$ 10 to 30 percent, again depending on the size of the molecule. The largest species for which a calibration was obtained was phenanthrene. Attempts to observe pyrene failed. The very large uncertainties for the heaviest species suggests that profiles of these species are semi-quantitative.

A second goal of this program is to observe species concentrations in real-time rather than just analyzing end gases from the single-pulse shock tube. In order to perform this research, a time-of-flight mass spectrometer (CVC) will be coupled to the end wall of the shock tube, and data collected using a high speed data acquisition system (LeCroy). The development and installation of this equipment is behind schedule due to ordering problems, and further delayed since the mass spectrometer has not yet been delivered, although it is now well past the manufacturer's delivery date. This work is being performed under corporate sponsorship.

B. Experimental Results

Since the end of the previous AFOSR contract in November 1987, twenty separate mixtures have been shock heated and products analyzed by gas chromatography. The mixtures are listed in Table I. Six of the mixtures were examined as part of the first year of this AFOSR program; the remainder were tested under corporate sponsorship. For these tests, dwell times were typically 500 microseconds and total pressures (balance argon) were 9 to 13 atmospheres.

In the following paragraphs, results on toluene pyrolysis and benzene oxidation are discussed.

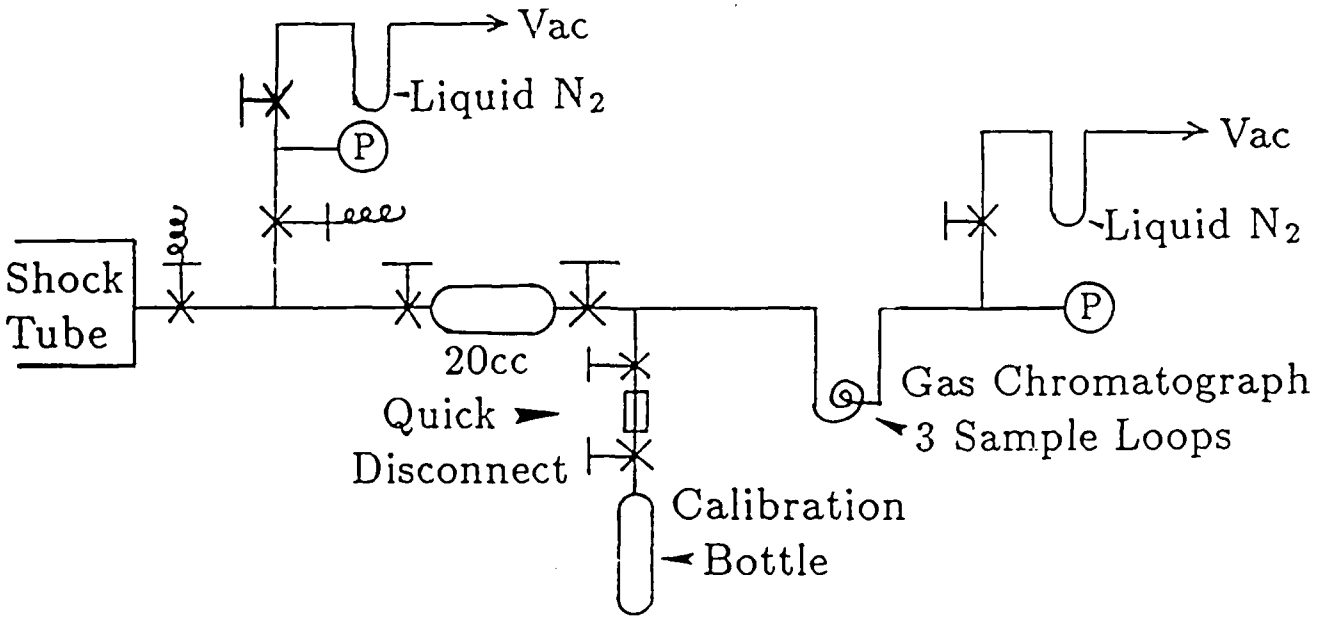

Figure 1a. Original Sampling System

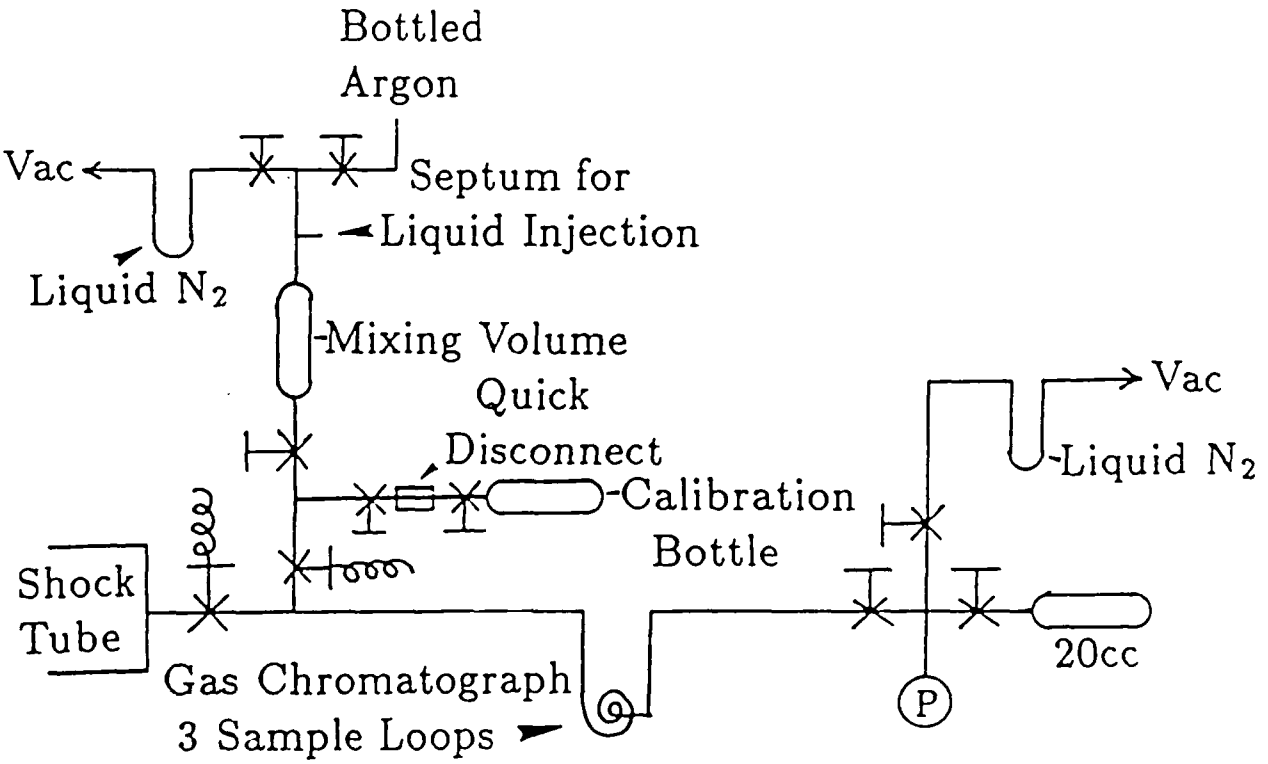

Figure 1b. Modified Sampling System

Table I

Series of Experiments Completed During the First Year of AFOSR Program

Reactants	Initial Concentrations
Toluene	1%
Benzene	1.1%
Benzene/oxygen	1.1/0.22%
Benzene/oxygen	0.11/0.022%
Benzene/oxygen	1.1/1.1%
Dicyclopentadiene	0.125%
*Acetylene/ethene	1.1/2.2%
*Acetylene/ethene	0.125/0.25%
*Toluene/methanol	1.0/0.15%
*Toluene/hydrogen	1.0/3.1%
*Methylcyclohexane	1%
*Methanol	4%
*Natural Gas/oxygen	4/1%
*Methane/oxygen	4/1%
*Cyclopentadiene	1.4%
*Cyclopentadiene	0.1%

* Performed under corporate sponsorship

The data on dicyclopentadiene has not been analyzed due to the complexity of the gas chromatogram. Corporate sponsored work subsequently demonstrated that dicyclopentadiene could be successfully decomposed (by refluxing) into cyclopentadiene, which is then mixed with argon and shock heated in the single-pulse shock tube. Work on cyclopentadiene will continue in the second year of the AFOSR program.

1. Toluene Pyrolysis

One of the first mixtures analyzed for this program was 1% toluene, since several previous runs with this mixture have been performed and provide a reference set of data. The newly obtained data is in excellent agreement with the results presented previously (Ref. 1) for the lower molecular weight compounds (< 128 g/mole). In addition, because of the enhanced sampling system, profiles on a variety of PAH's were also obtained in this recent series of experiments. Some of the aromatic compounds produced from pyrolysis of 1% toluene are shown in Figure 2. Profiles of toluene, benzene, indene, and naphthalene shown in Figure 2 agree well with the earlier data. The remaining profiles are new information. The low temperature formation of bibenzyl is from recombination of benzyl radicals; although, due to uncertainty in the thermochemistry of benzyl, it is unknown whether the bibenzyl could be produced at high temperatures or in the quenching waves. Hopefully, detailed modeling will assist in deciphering this data. The other products shown in Figure 2 represent a relatively small portion of the total number of high molecular weight species, although the mass contained in these selected species represents about 75% or more of the total mass of the species observed. Possible reactions describing the production of selected species are proposed in Figure 3. Analysis of this data and detailed modeling is continuing. The result that PAH's are produced very rapidly at 1400 to 1500K is consistent with concepts developed from diffusion flames which indicate inception occurs at 1300 to 1500K.

2. Benzene Oxidation

The oxidation of benzene was also examined during this past year. Prior to the oxidation runs, a pyrolysis experiment was performed. However, based on the product distribution and comparison with previously obtained data, it is believed that an impurity of a small amount of oxygen (~ 1000 ppm) affected the recent "pyrolysis" experiments. Benzene decay and light product formation (methane, acetylene, diacetylene, cyclopentadiene, and vinylacetylene) are shown in Figures 4 - 6 for the two oxidation runs at high benzene concentrations and for the previous benzene pyrolysis experiments. In these figures, the measured concentrations of reactants rather than the percent calculated from partial pressure mixing (Table 1) are listed. The effect of oxygen clearly is to cause decay of benzene at lower temperatures as well as to enhance the low temperature production of the dominant product, acetylene. In addition, oxygen causes the low temperature formation of cyclopentadiene and vinylacetylene, which strongly supports the mechanistic arguments proposed by Venkat et al (Ref. 2) for benzene oxidation. Oxygen only slightly affects the production of diacetylene. This species is a byproduct of the thermal decomposition of phenyl radical which is slow due to its high activation energy (~ 70 kcal/mole). The slight enhancement in the production of diacetylene with increasing oxygen presumably is due to an increase in phenyl radical concentration (via radical attack on benzene).

Dominant polyaromatic hydrocarbons produced during the rich oxidation of benzene (1.25% benzene, 0.3% oxygen) are shown in Figure 7. A large number of other high molecular weight products were also produced, although many of these are unidentified. It is estimated, however, that the total mass contained in unidentified species is less than 30% of the mass for all the high molecular weight compounds. The dominant PAH products are similar to those observed during pyrolysis of toluene. In both cases, a predominance of both five- and six-membered rings is observed. The presence of species containing five-membered rings is not surprising, based on previous

Figure 2

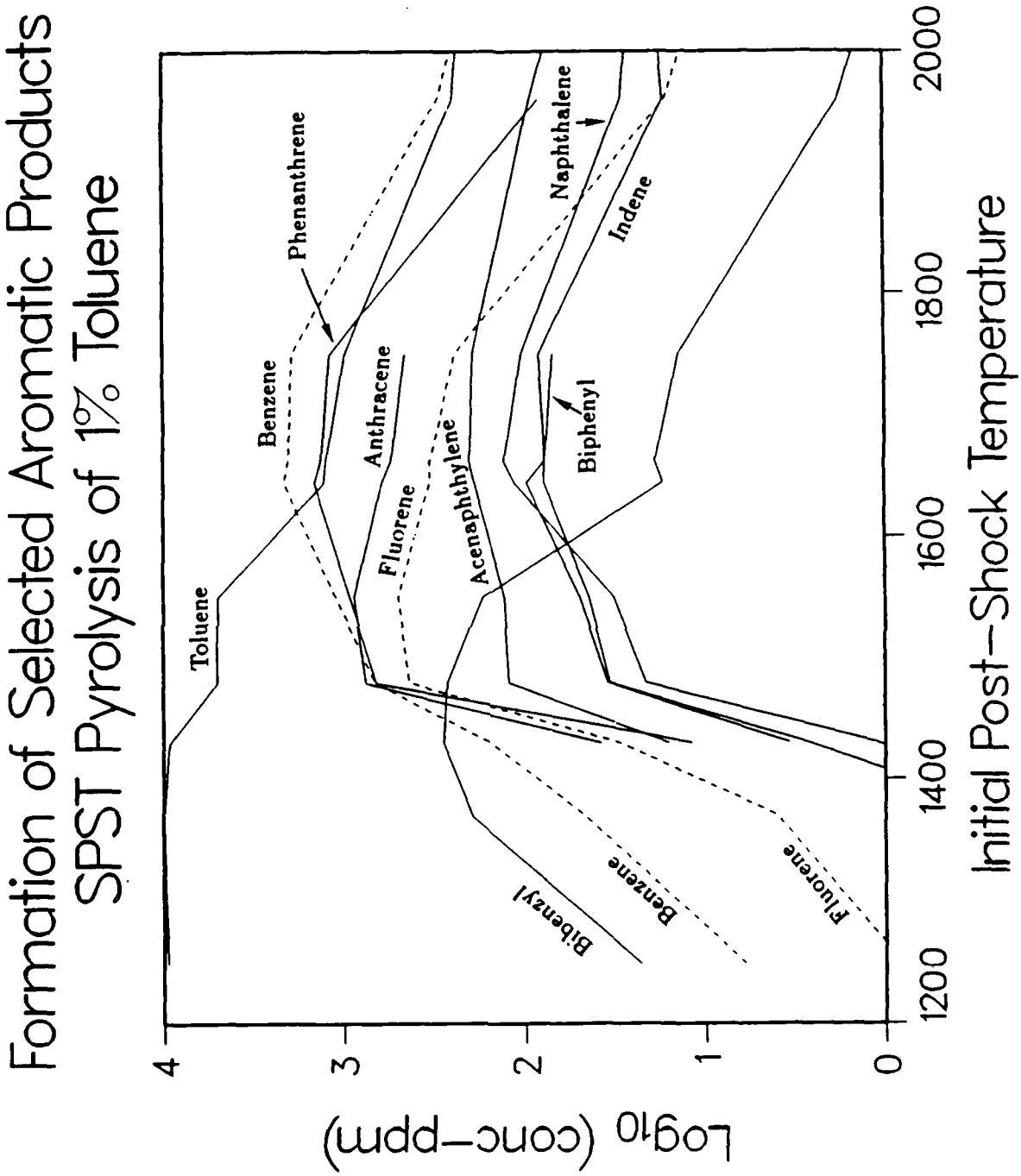
Formation of Selected Aromatic Products
SPST Pyrolysis of 1% Toluene
Log10 (conc-ppm)
Initial Post-Shock Temperature
Toluene
Benzene
Phenanthrene
Anthracene
Fluorene
Acenaphthylene
Naphthalene
Indene
Biphenyl
Dibenzyl
Benzene
Fluorene
0
1
2
3
4
1200
1400
1600
1800
2000

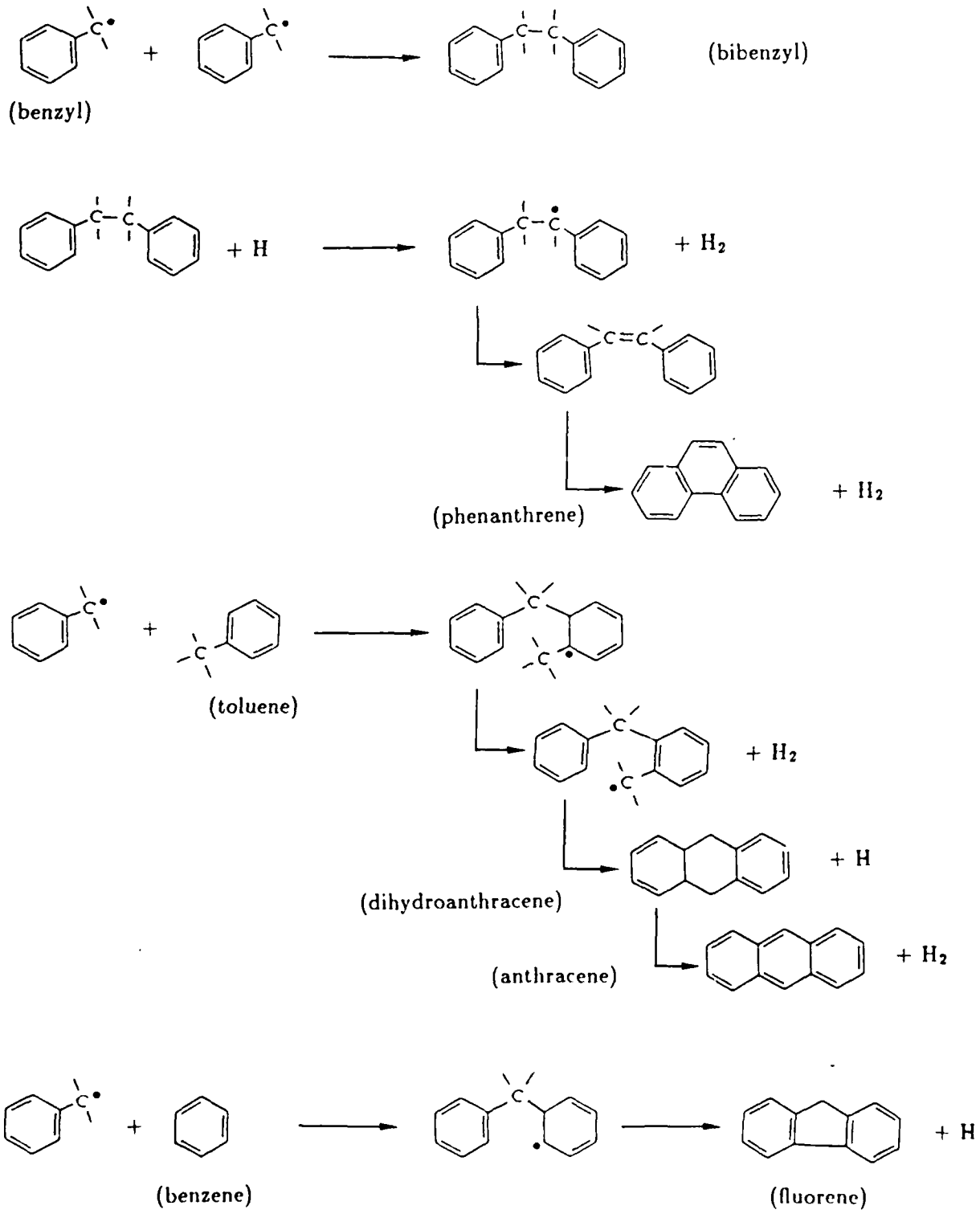

Fig. 3. Possible Reactions for Formation of PAH

Figure 4

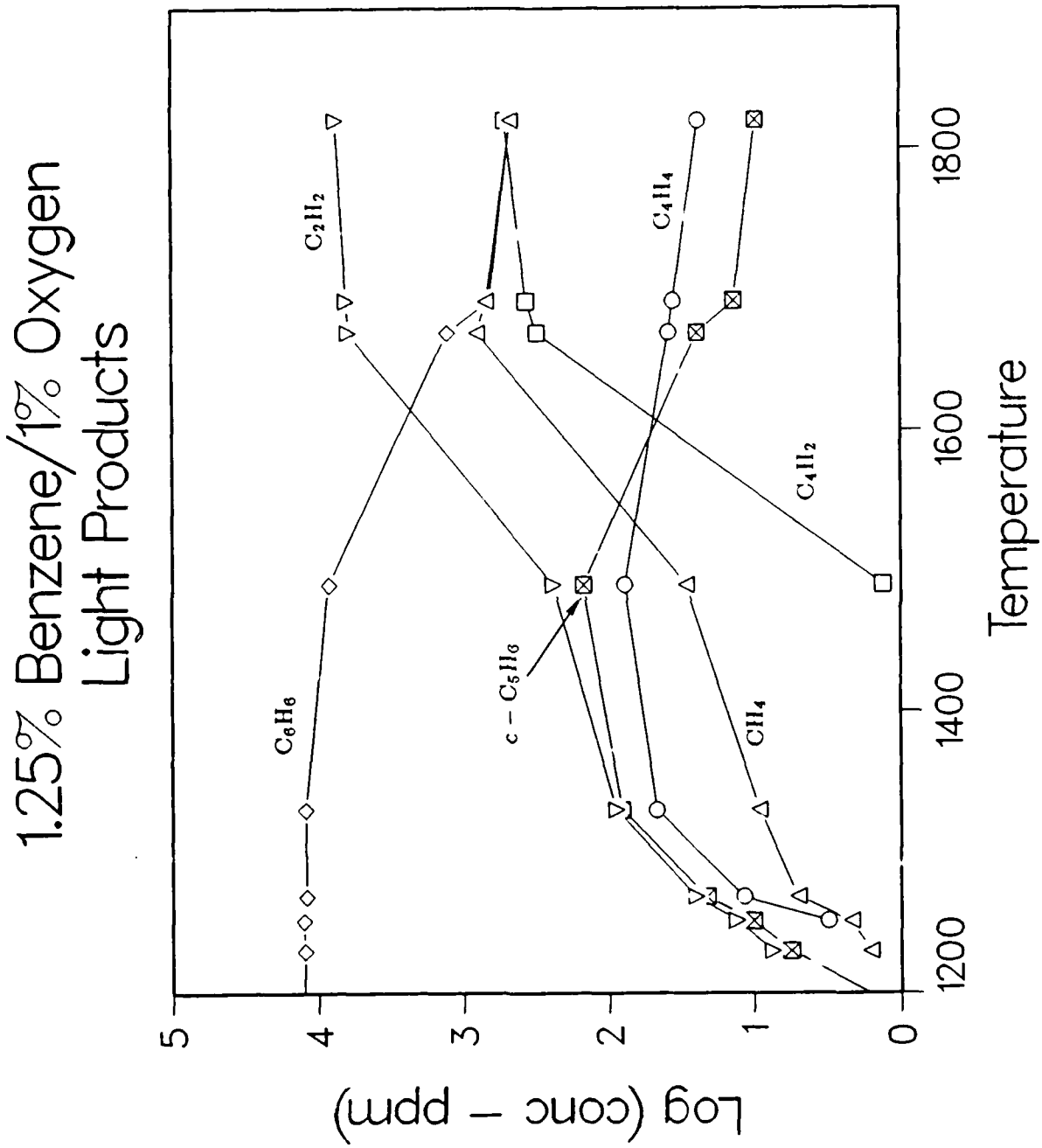
1.25% Benzene/1% Oxygen
Light Products
Log (conc – ppm)
Temperature
5
4
3
2
1
0
1200
1400
1600
1800
C_6H_6
C_2H_2
$c-C_5H_6$
CH_4
C_4H_4
C_4H_2

Figure 5

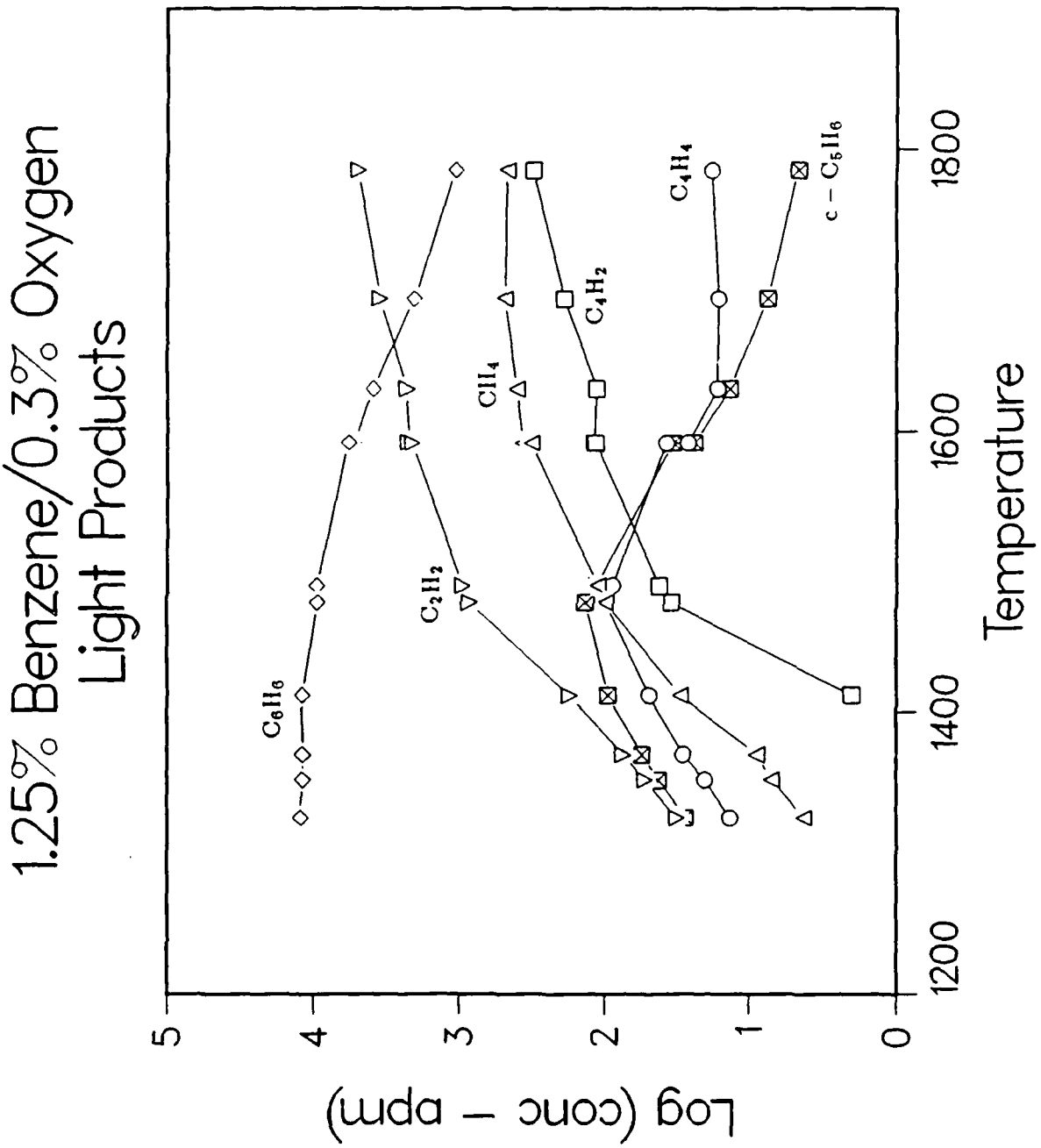
1.25% Benzene/0.3% Oxygen
Light Products
Log (conc – ppm)
Temperature
5
4
3
2
1
0
1200
1400
1600
1800
C_6H_6
C_2H_2
CH_4
C_4H_2
C_4H_4
c – C_6H_6

Figure 6

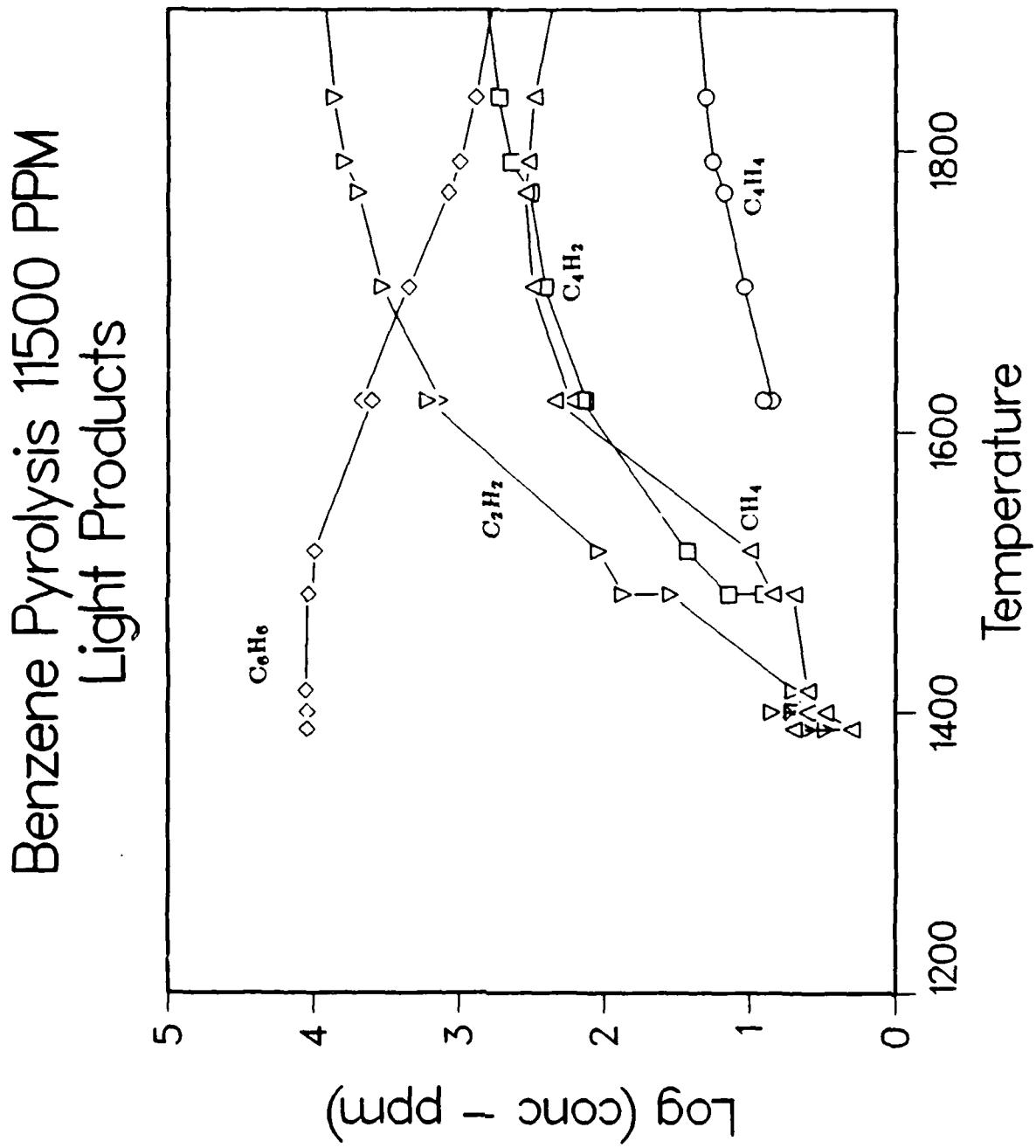
Benzene Pyrolysis 11500 PPM
Light Products
Log (conc – ppm)
5
4
3
2
1
0
1200
1400
1600
1800
Temperature
C_6H_6
C_2H_2
C_4H_2
CH_4
C_4H_4

Figure 7

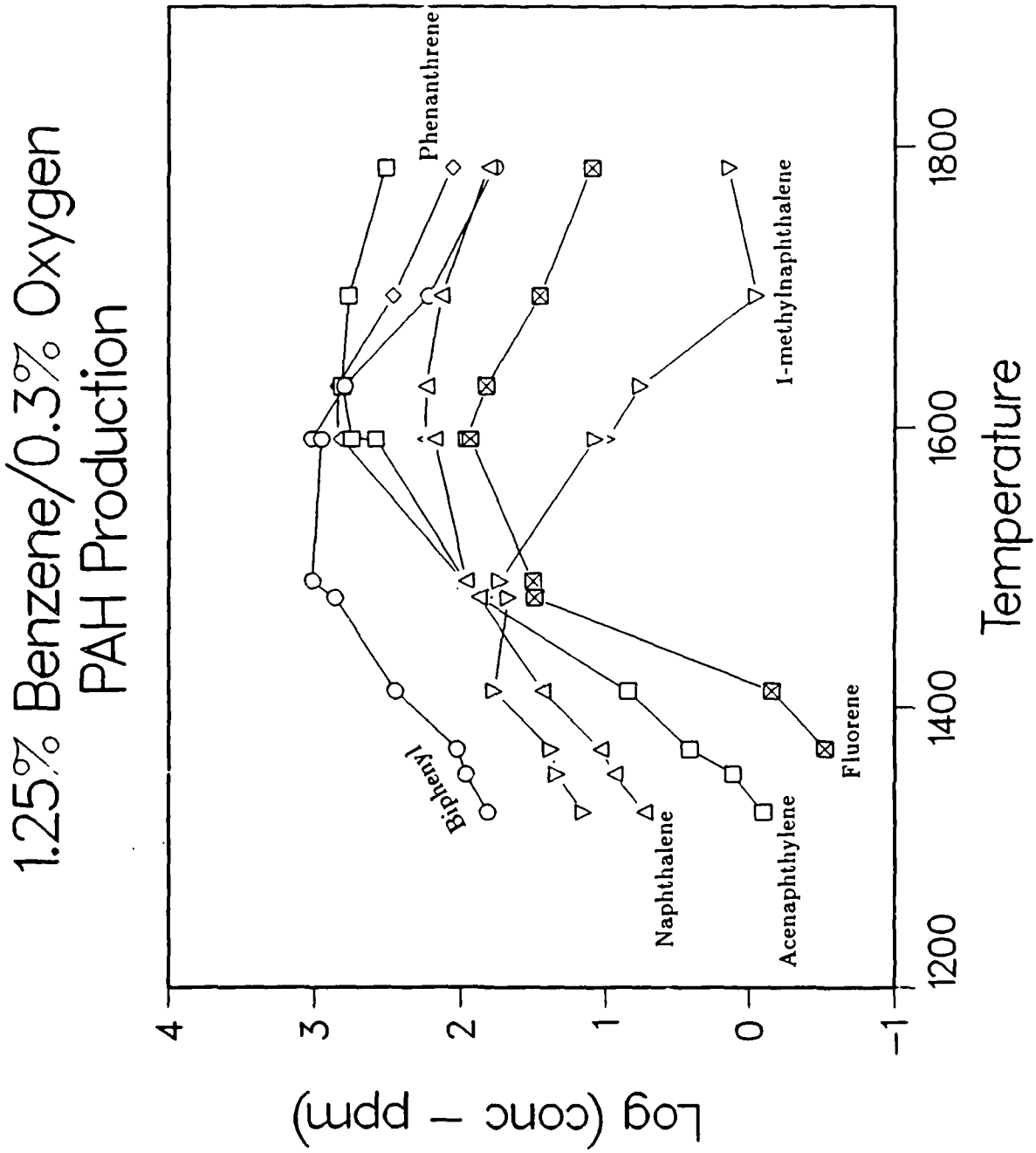
1.25% Benzene/0.3% Oxygen
PAH Production
Log (conc – ppm)
4
3
2
1
0
-1
1200
1400
1600
1800
Temperature
Phenanthrene
1-methylnaphthalene
Biphenyl
Naphthalene
Acenaphthylene
Fluorene

studies in flames; however, existing models for PAH growth and soot formation neglect the potential importance of these species. Profiles and identities of PAH species during the oxygen-contaminated experiment on benzene pyrolysis were similar to those in Figure 7, although they were shifted to higher temperatures. The profiles of PAH's for the less rich oxidation (1% oxygen) were severely depressed, although a carbon balance (which includes formation of carbon monoxide and carbon dioxide) indicates significant loss of mass. The implication is that with the larger amounts of oxygen, the growth of PAH's is significantly accelerated. These results are considered preliminary and need to be verified in future experiments.

C. Model of Soot Particle Formation

1. Model Soot Inception Kinetics/Nucleation Calculations

Soot inception kinetics have been modeled by considering a mechanism of stepwise acetylene addition of the form

$$\dot{A}_i + H_2 \rightleftharpoons A_i + H \quad (0)$$

$$\dot{A}_i + C_2H_2 \rightleftharpoons A_iC_2H + H \quad (1)$$

$$A_iC_2H + H \rightleftharpoons \dot{A}_iC_2H + H_2 \quad (2)$$

$$\dot{A}_iC_2H + C_2H_2 \rightarrow \dot{A}_{i+1} \quad (3)$$

Here A_i is a closed ring aromatic species (A_1=benzene, A_2=naphthalene, $\dot{A}_1$=phenyl, etc.); the mass of A_i is 78+(i-1)50 a.m.u.

Setting the time derivatives of radical, intermediate concentrations equal to zero (steady state approximation) results in the following set of coupled rate equations for the concentrations of the closed ring species.

$$\frac{d[A_1]}{dt} = \frac{-[A_1]}{T_1} + Q$$

$$\frac{d[A_2]}{dt} = \frac{-[A_2]}{T_1} + \frac{[A_1]}{T_2}$$

$$\frac{d[A_3]}{dt} = \frac{-[A_3]}{T_1} + \frac{1}{T_2}([A_2] + r[A_1])$$

$$\vdots$$

$$\frac{d[A_i]}{dt} = \frac{-[A_i]}{T_1} + \frac{1}{T_2}([A_{i-1}] + r[A_{i-2}] + ...r^{i-1}[A_1])$$

where Q is the benzene source rate and

$$\frac{1}{T_1} = k_{-0}[H]\left\{1 - \frac{k_0[H_2]}{k_1[C_2H_2] + k_0[H_2] - \frac{k_1 k_{-1}}{k_{-1}+k_2}[C_2H_2]}\right\}$$

$$\frac{1}{T_2} = \frac{k_1 k_2 k_3 (k_0 k_{-0})[C_2H_2]^2[H][H_2]}{(k_{-1}+k_2)(k_{-2}[H_2] + k_3[C_2H_2])\left\{k_1[C_2H_2] + k_0[H_2] - \frac{k_1 k_{-1}[C_2H_2]}{k_{-1}+k_2}\right\}^2}$$

$$\text{and } r = \frac{T_1/T_2}{k_{-0}[H]T_1 - 1}$$

If Q is assumed constant in time, the analytic, recursive solutions for the first few closed ring species are

$$[A_1] = Q\ T_1(1 - e^{-t/T_1})$$

$$[A_2] = \left(\frac{T_1}{T_2}\right)[A_1] - Q\left(\frac{T_1}{T_2}\right) t\ e^{-t/T_1}$$

$$[A_3] = \left(\frac{T_1}{T_2} + r\right)[A_2] - Q\left(\frac{T_1}{T_2^2}\right) t^2/2\ e^{-t/T_1}$$

$$[A_4] = \left(\frac{T_1}{T_2} + 2r\right)[A_3] - r\left(\frac{T_1}{T_2} + r\right)[A_2] - Q\left(\frac{T_1}{T_2^3}\right)\frac{t^3}{6}e^{-t/T_1}$$

It is convenient to resort to numerical integration of the rate equations, because the analytic solutions become complicated and we want eventually to consider the effects of agglomeration reactions of the form

$$A_i + A_j \xrightarrow{\beta_{ij}} (A_i)(A_j) \equiv A_{ij} \qquad \text{(large } i,j)$$

The A_{ij} can participate in the stepwise acetylene addition mechanism and agglomerate to form higher order aggregates, and the kinetic master equations have been suitably modified to include terms for these additional processes. The following provisional rate coefficient data were employed in our simulations:

$$k_0 = 5.1 \times 10^{12}\ e^{-5020/T}\ \text{(moles/cc/sec)}$$

$$k_{-0} = 2.51 \times 10^{14}\ e^{-8081/T}$$

$$k_1 = 10^{12}\ e^{-2013/T}$$

$$k_{-1} = 7.6 \times 10^{13}\ e^{-3030/T}$$

$$k_2 = 2.51 \times 10^{14}\ e^{-8081/T}$$

$$k_{-2} = 1.51 \times 10^{13}\ e^{-5404/T}$$

$$k_3 = 2 \times 10^{12}\ e^{-2013/T}$$

The following species concentration parameters were estimated from the Harris papers (Ref. 3 - 5):

$$[C_2H_2] = 2.3 \times 10^{-7} \text{ moles/cc}$$
$$[H_2] = 5.2 \times 10^{-7}$$
$$[H] = 7.4 \times 10^{-9}$$
$$Q = 4.9 \times 10^{-7} \text{ moles/cc/sec}$$

For these parameters at T=1600K, $T_1 \simeq 1.3$ millisec, and $T_1/T_2 \simeq 0.3$. A simulation of the time evolution of the closed ring concentrations without aggregation is shown in Figure 8. It is seen that the time to achieve steady state for the N-th closed ring species is approximately NT_1. Thus the time required to form a 1000 a.m.u. particle for which $N \simeq 20$ would be 20 - 30 milliseconds, which is about an order of magnitude too slow for the process of soot inception. The steady state ratio of $[A_i]/[A_{i-1}](i < 2)$ is$(T_1/T_2 + r)$; thus, the steady state concentration of the i-th closed ring is

$$[A_i] \simeq QT_1\left(\frac{T_1}{T_2}\right)\left(\frac{T_1}{T_2} + r\right)^{i-2}$$

When Q is assumed to have a reasonable shut-off time of one millisecond, the time histories of the closed ring species are as shown in Figure 9. Note the qualitative resemblance to the experimental measurements of Bittner and Howard (Ref. 6). While some uncertainty attaches to the rate coefficients and species concentrations which go into this calculation, the indication is that our simple stepwise acetylene addition mechanism is too slow to explain observed soot inception rates in the absence of agglomerative or other mechanisms. Implicit in the foregoing analysis has been the assumption that the rate coefficients $k_0 - k_3$ do not scale with the order of A_i. In fact, there are qualitative arguments one can make that these rates should increase monotonically with i. As i increases, the number of sites available for H-atom abstraction and acetylene addition increases, and so should the rate coefficient. Preliminary estimates are that the scaling could be fairly strong, leading to significant shortening of the time required to form large mass species. This question will be further addressed in the future; the implication is that the rate-limiting step will prove to be the formation rate of the first few closed ring species.

Reactions of the form

$$\dot{A}_i + A_j \rightleftharpoons A_iA_j + H$$
$$\dot{A}_i + \dot{A}_j \rightleftharpoons A_iA_j$$

could also be important. The sequence

$$\dot{A}_1 + A_1 \rightleftharpoons A_1A_1 + H$$
$$A_1A_1 + H \rightleftharpoons A_1\dot{A}_1 + H_2$$
$$A_1\dot{A}_1 + C_2H_2 \rightleftharpoons A_3 + H$$

for example, could provide an alternative fast mechanism for the production of A_3. These reactions are presently being incorporated into the steady state analysis to see if they lead to accelerated production of A_3.

When physical agglomeration processes are allowed, our preliminary calculations show that the production of higher mass species can be significantly accelerated, but the results are sensitive to

Figure 8

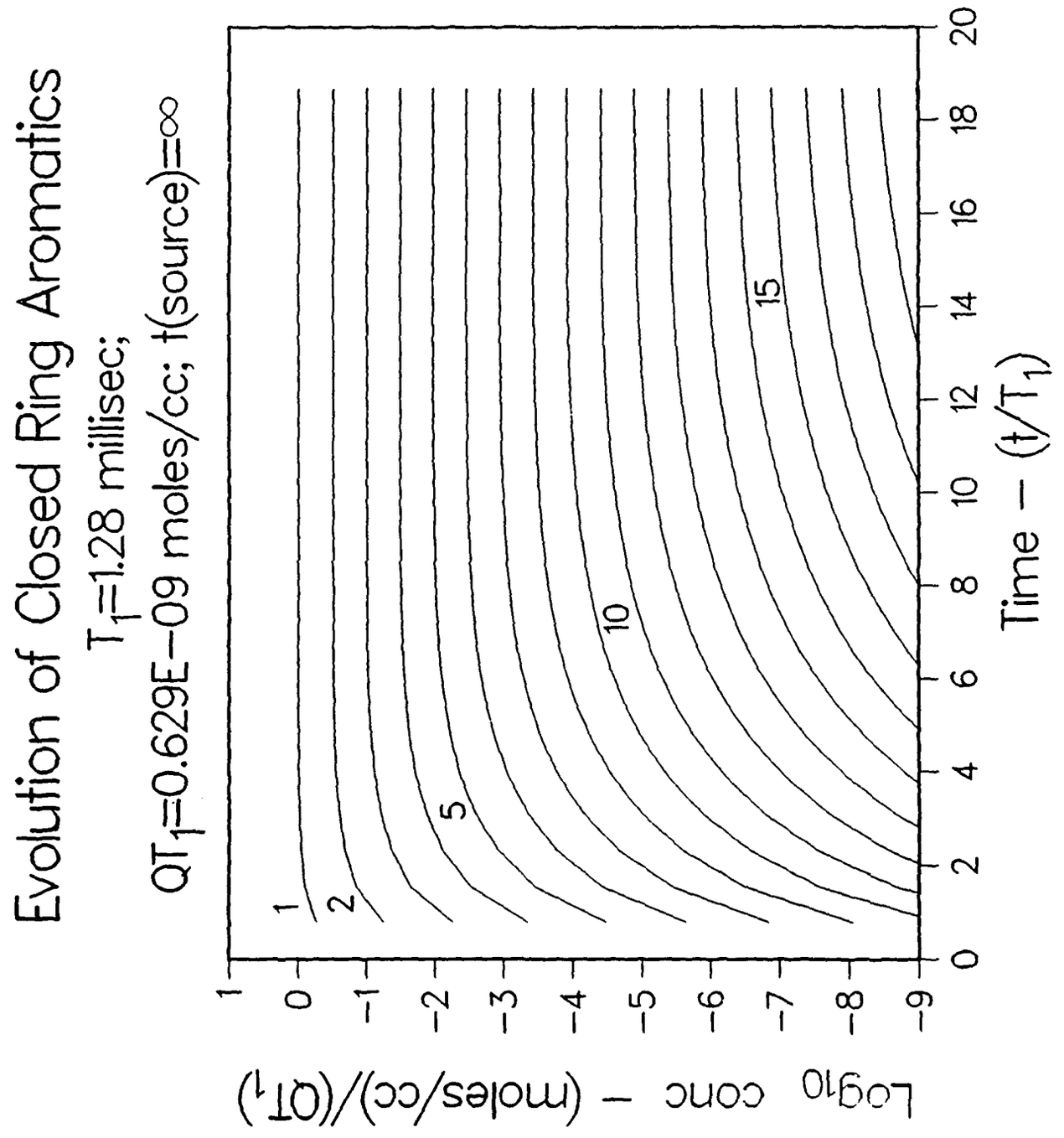
Evolution of Closed Ring Aromatics
T1=1.28 millisec;
QT1=0.629E-09 moles/cc; t(source)=∞
Log10 conc – (moles/cc)/(QT1)
Time – (t/T1)
1
2
5
10
15
1
0
-1
-2
-3
-4
-5
-6
-7
-8
-9
0
2
4
6
8
10
12
14
16
18
20

Figure 9

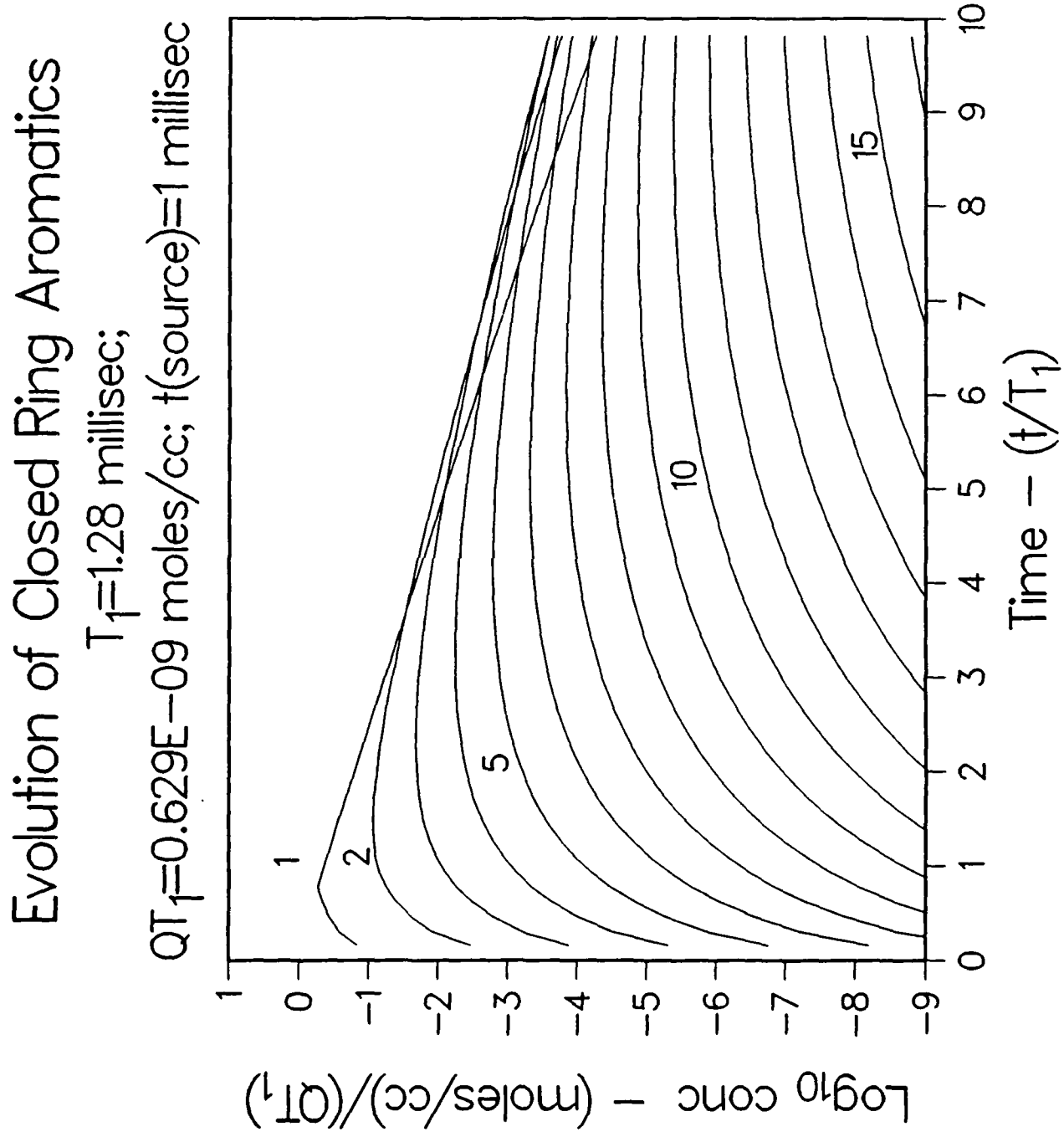
Evolution of Closed Ring Aromatics
T1=1.28 millisec;
QT1=0.629E-09 moles/cc; t(source)=1 millisec
Log10 conc – (moles/cc)/(QT1)
Time – (t/T1)
1
2
5
10
15
1
0
-1
-2
-3
-4
-5
-6
-7
-8
-9
0
1
2
3
4
5
6
7
8
9
10

the model for the sticking probabilities. The question of scaling of these probabilities with particle size is one that will have to be addressed with some care if the calculations are to be meaningful. The results of more extensive agglomeration calculations will be presented in a future report.

Finally, we also considered the stepwise mechanism

$$\dot{A}_i + H_2 \rightleftharpoons A_i + H$$
$$\dot{A}_i + C_2H_2 \rightleftharpoons A_i\dot{C}_2H_2$$
$$A_i\dot{C}_2H_2 + C_2H_2 \rightleftharpoons A_i\dot{C}_4H_4$$
$$A_i\dot{C}_4H_4 \rightarrow A_{i+1} + H$$

Given reasonable estimates for the rate coefficients in a steady state analysis, however, the characteristic formation times are much too long for this to be the correct inception mechanism.

2. Soot Aerosol Dynamics Simulations

After the inception or nucleation stage, soot particles continue to grow as isolated spheroids, reaching a size of 40-100 nm; at later times, these spheroids fuse to form chainlike clusters or aggregates. Prior to the aggregation phase, the growth of the primary spheroids occurs through surface deposition of gas phase hydrocarbons and coalescing collisions in which colliding spheroids stick together and form a new spheroid.

In order to model the growth of primary soot spheroids, the most recent version of an aerosol dynamics code, MAEROS (Ref. 7), has been appropriately modified. This is a sectional model in which the particle size range of interest is divided into discrete classes, or intervals. A set of master equations for the rate of change of particle number density in each size class is then integrated numerically, accounting for the processes of nucleation, surface growth, and coalescence. Each size class has a source term representing nucleation, but in our simulations this is set equal to zero for all but the smallest size class. Surface growth is assumed to occur primarily through acetylene deposition, using the Harris-Weiner growth rate expression (Ref. 3). In this formulation, the rate of mass addition to a particle is proportional to the particle surface area, and is linear in the acetylene vapor concentration. The effective surface growth rate given by Harris and Weiner is time dependent, and we have chosen an early, or young, soot value. Provision is made for acetylene vapor depletion, and oxidation is accounted for by modifying the surface growth term to allow for oxidative mass removal at a rate given by the well-known Nagle and Strickland-Constable expression (Ref. 8). The latter is plotted in Figure 10. It can be seen that for oxygen concentrations above roughly 5%, and temperatures below approximately 2000K, the effective oxidation rate becomes essentially independent of oxygen concentration. Coalescence rate coefficients are calculated in the MAEROS program using the Fuchs-Sutugin expression (Ref. 9), which spans the Knudsen number range from free-molecule to continuum. A coalescence sticking probability is input to the computer code. Kennedy (Ref. 10) and Harris and Kennedy (Ref. 11) have shown that soot particle collision rates can be significantly enhanced by long-range Van der Waals forces. These forces between electrically neutral dielectrics have their origins in quantum fluctuations as embodied in the Heisenberg uncertainty principle, which create instantaneous dipole moments in the colliding bodies. We have written a computer program to calculate the collision rate enhancements arising from these forces. The program is based on the Lifshitz(Ref. 12), Langbein (Ref. 13), and Marlow (Ref. 14) theory, and is similar to the calculation outlined by Kennedy (Ref. 10). All dielectric constant parameters are the same as those given in Reference 10. Calculated enhancement factors for soot particles in the free-molecule regime at 1600K are shown in Figure 11. It can be seen that the enhancements are a function mainly of the radius difference between particles, and for the smallest particles reach a value of about 2.4.

Figure 10

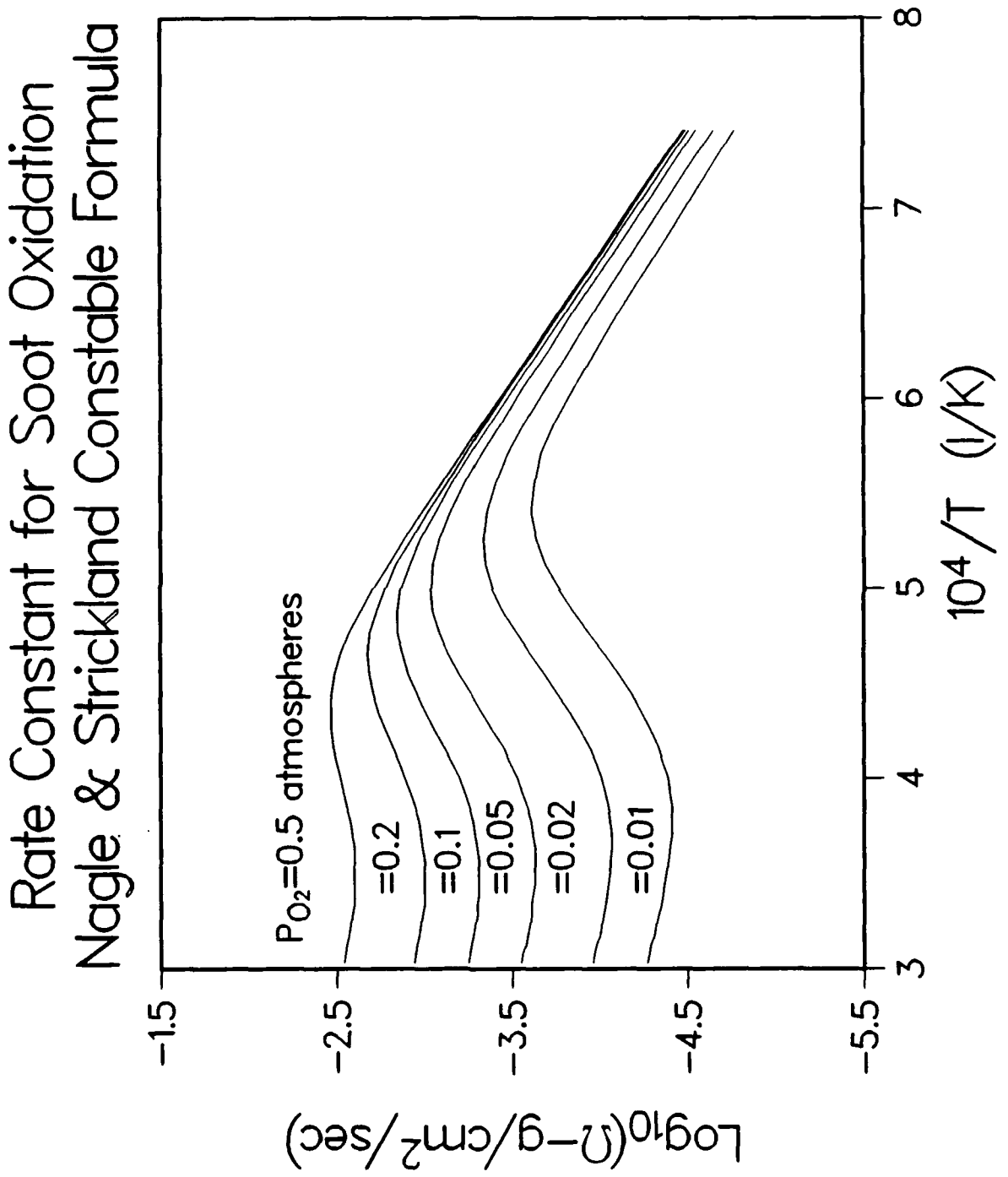
Rate Constant for Soot Oxidation
Nagle & Strickland Constable Formula
P_{O_2}=0.5 atmospheres
=0.2
=0.1
=0.05
=0.02
=0.01
$Log_{10}(\Omega$-g/cm^2/sec)
-1.5
-2.5
-3.5
-4.5
-5.5
3
4
5
6
7
8
10^4/T (1/K)

Figure 11

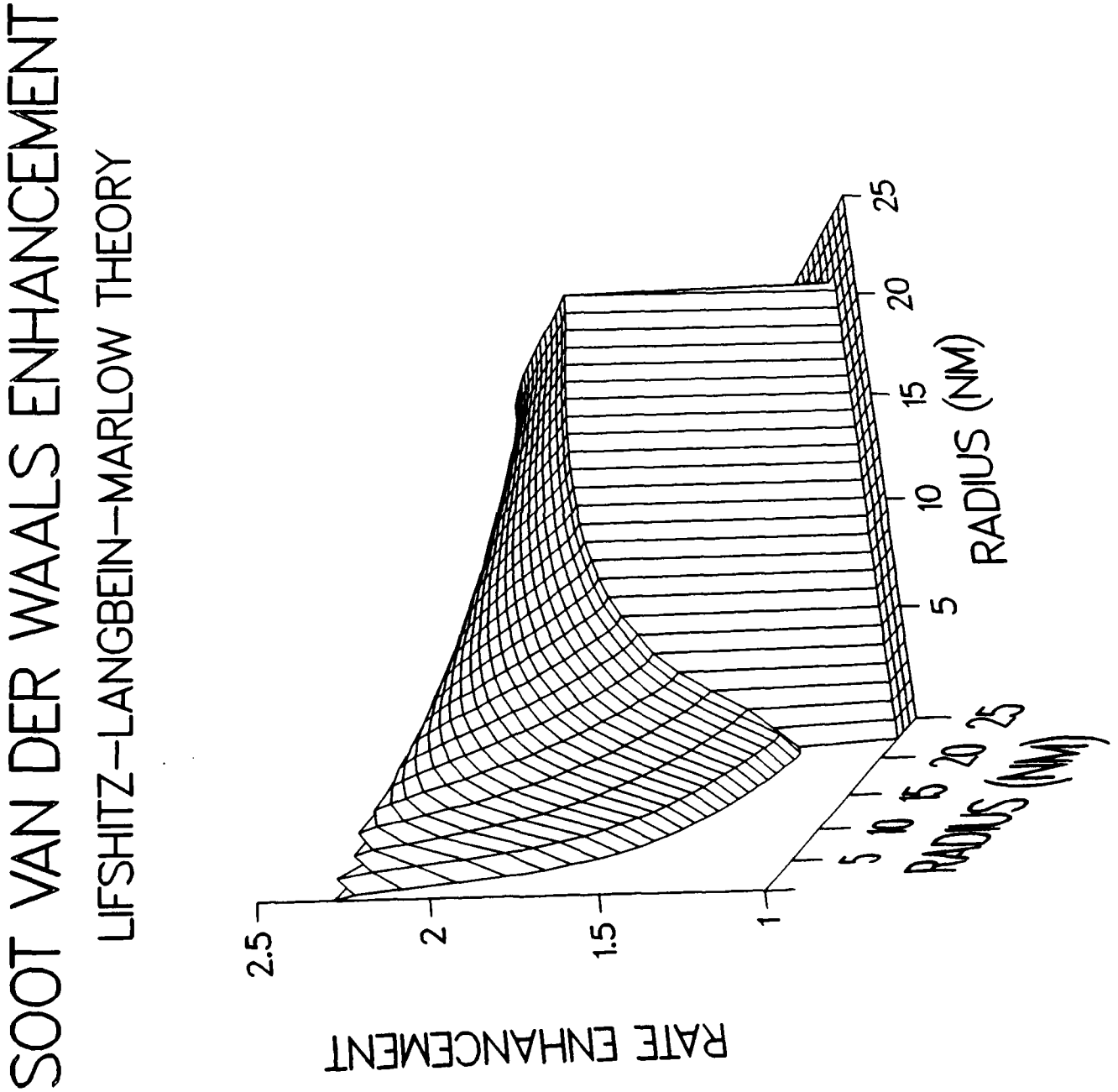
SOOT VAN DER WAALS ENHANCEMENT
LIFSHITZ–LANGBEIN–MARLOW THEORY
RATE ENHANCEMENT
2.5
2
1.5
1
RADIUS (NM)
5
10
15
20
25
RADIUS (NM)
5
10
15
20
25

The most important approximation made in our soot aerosol dynamics simulations has been to set the lower limit of size range at the approximate size (.5nm - 5Å) of a benzene molecule, and to extrapolate the Harris-Weiner surface growth rate expression to this size class. The nucleation rate for this size range is taken to be the local benzene production rate, and the nucleation rate is set equal to zero for all other size classes. This clearly is an approximation, and a more careful coupling of soot inception kinetics with aerosol dynamics simulations might be needed in the future, but, as will be seen, its use leads to some encouraging results.

The MAEROS code has the advantage of computational efficiency; for the size range .5 to 1000 nm, with 15 - 20 size classes, the computation times are on the order of VAX-minutes. There is, however, some sensitivity of the results to number of size classes; a change from 20 to 15 changes the calculated numbers by about 10%. Calculations with a larger number of size intervals are planned, but require non-trivial code modifications. It may ultimately be desirable to use a code employing moving sectional boundaries, because of reduced numerical diffusion error; we are planning to check our results by having F. Gelbard run our cases on an unreleased version of MAEROS that uses the moving sectional grid technique. All calculations to follow have been performed with the maximum 20 size classes presently allowed in the program. In these calculations, the benzene source rate and acetylene concentration were taken as before from S. Harris flame conditions (Ref. 3 - 5) in order to attempt to reproduce the measured soot volume fraction profiles reported in Reference 3.

Figure 12 shows the calculated evolution of the soot number density distribution with time. It is apparent that the dynamics model predicts the appearance of 10 - 100 nm particles on a time scale of about 10 milliseconds. It is also clear that after about four milliseconds, the shape of the distribution has taken on an invariant form. This is the "self-preserving" size distribution (Ref. 15), as can be seen in Figure 13, where the same data are plotted as a function of the normalized variables $n'(v)\bar{v}/N$ and $v/\bar{v}$, where v is particle volume, $\bar{v}$ is average particle volume, and $N = \int_0^\infty n'(v)dv$. A self-preserving form is expected for coalescence-dominated kinetics (Ref. 15); our calculations show that it can still be expected even in the presence of nucleation and surface growth.

The calculated soot volume fraction is plotted as a function of time in Figure 14 for various values of the coalescence sticking probability, which has been assumed here to be size-independent. For very low values of the sticking probability, coalescence does not proceed rapidly, and the relative surface area of the particles remains high. Surface deposition proceeds rapidly when there are large numbers of small particles, and the total soot volume fraction increases to large values. When sticking probability is increased, coalescence becomes important and a smaller number of larger particles is formed. Coalescence in itself conserves volume fraction, but the reduced relative surface area of the larger particles reduces mass addition by surface growth. Thus, the calculated volume fraction decreases as seen with increasing sticking probability. Only for the very low values of sticking probability is significant depletion of the acetylene vapor predicted. It is interesting to note that there is excellent agreement with experiment for sticking probabilities in the expected range 1 - 2. Both the magnitude and time dependence of the Reference 3 results, which were obtained from absorption measurements, are seen to be reproduced well. At the present time, the success of a model which omits the fine details of the inception kinetics is possibly fortuitous, but certainly encouraging. These results support previous work indicating that the rate-limiting process of soot formation is the formation of the first few rings. The extrapolation of the Harris-Weiner surface growth rate to the smallest molecule/particle size classes appears to effectively reproduce the effects of more detailed inception kinetics; this result (supported by recent calculations of Howard, Harris, and Frenklach) might form the basis of a very simple and powerful model for soot formation. Further examination of these questions is planned. Another point of interest is whether the aging of the acetylene surface deposition rate reported in Ref. 3 is really due to temperature effects and an activation energy for the process.

Calculated Evolution of Soot Size Distribution Coagulation & Surface Growth from Maeros Code Harris Surface Growth Rate and Flame Conditions

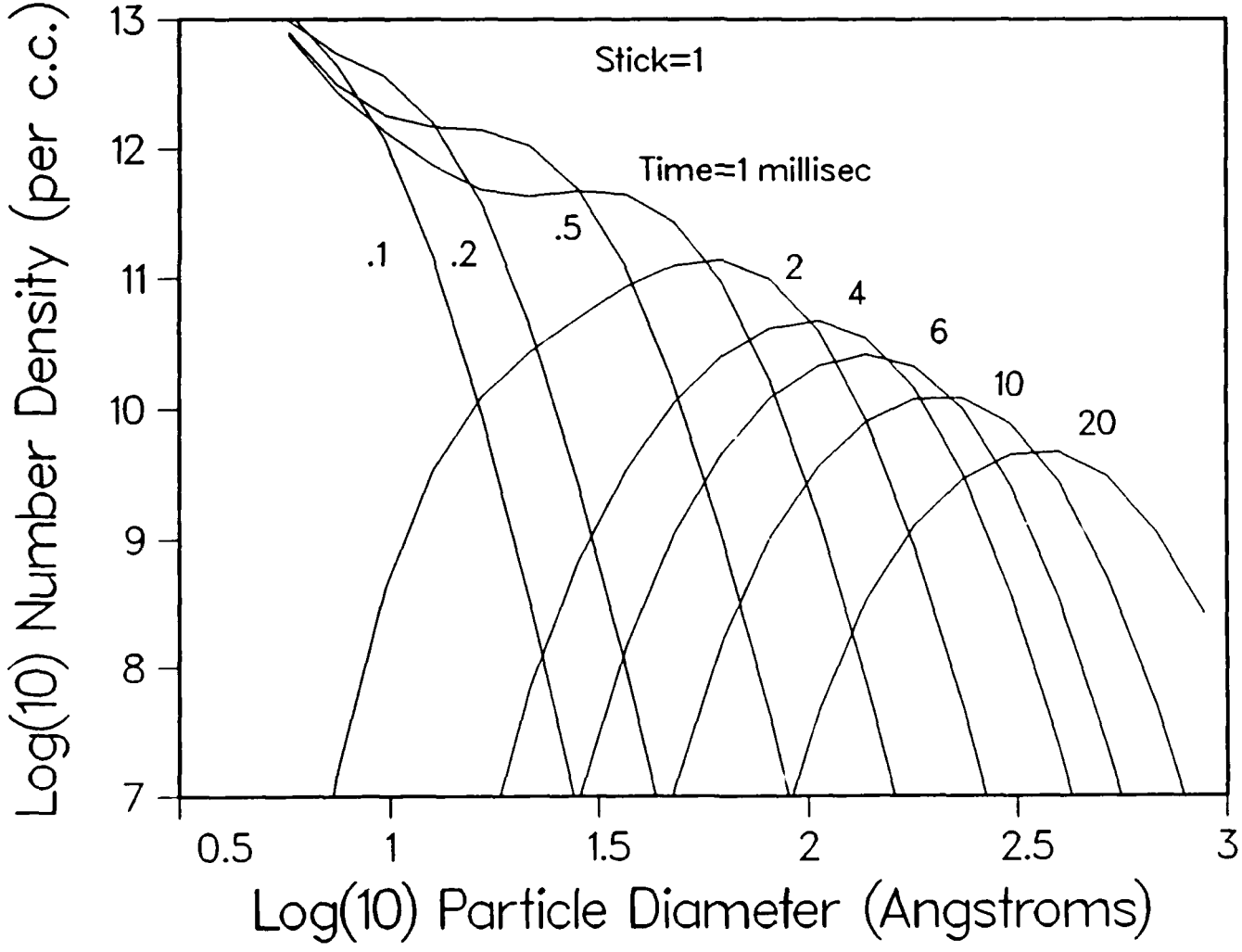

Figure 12

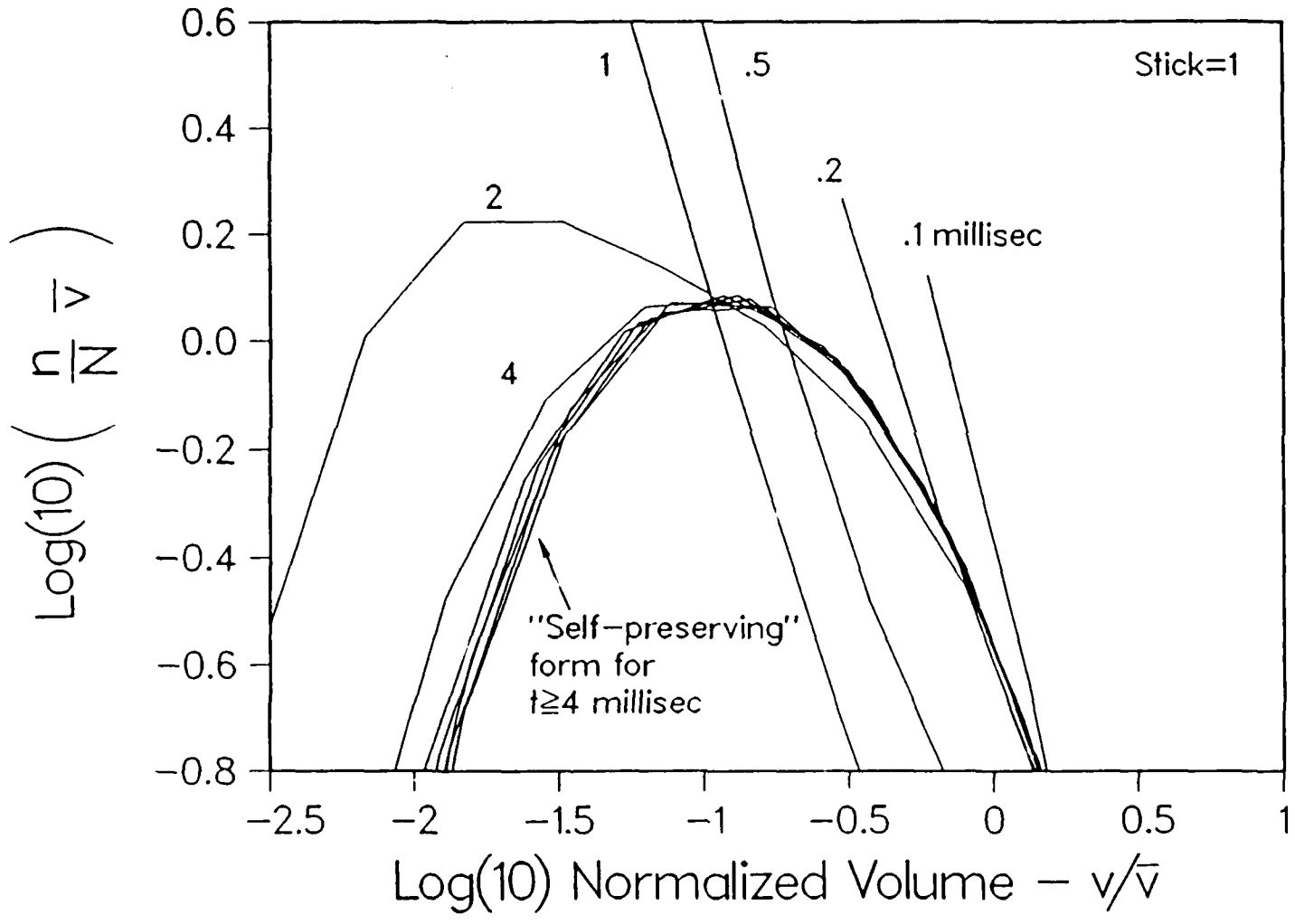
Size Class Distributions from MAEROS Code
Harris Surface Growth Rate and Flame Conditions
Stick=1
1
.5
.2
.1 millisec
2
4
"Self-preserving"
form for
t≧4 millisec
0.6
0.4
0.2
0.0
−0.2
−0.4
−0.6
−0.8
−2.5
−2
−1.5
−1
−0.5
0
0.5
1
Log(10) (n/N v̄)
Log(10) Normalized Volume — v/v̄

Figure 13

Figure 14

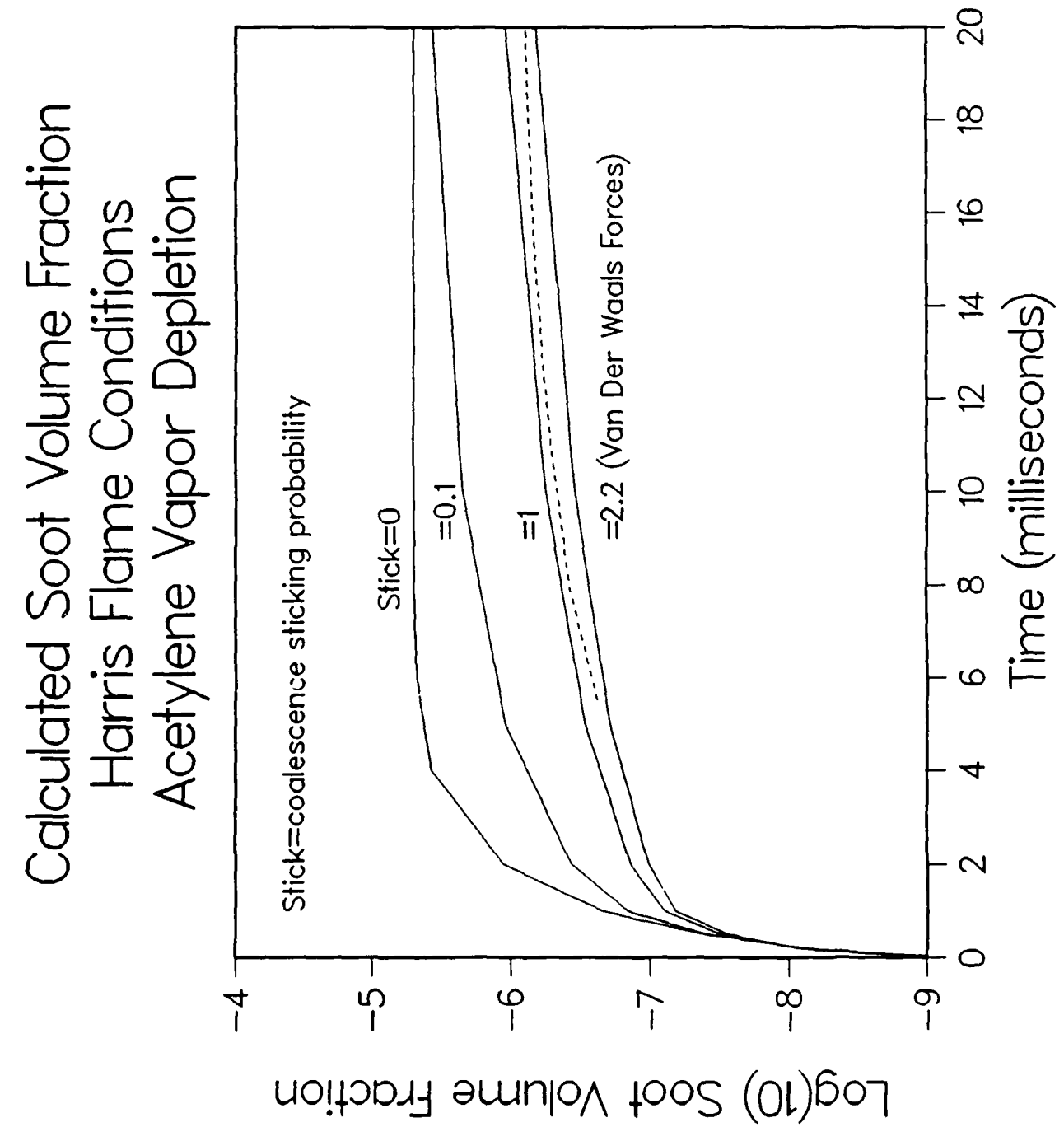
Calculated Soot Volume Fraction
Harris Flame Conditions
Acetylene Vapor Depletion
Stick=coalescence sticking probability
Stick=0
=0.1
=1
=2.2 (Van Der Waals Forces)
Log(10) Soot Volume Fraction
-4
-5
-6
-7
-8
-9
0
2
4
6
8
10
12
14
16
18
20
Time (milliseconds)

Figure 15

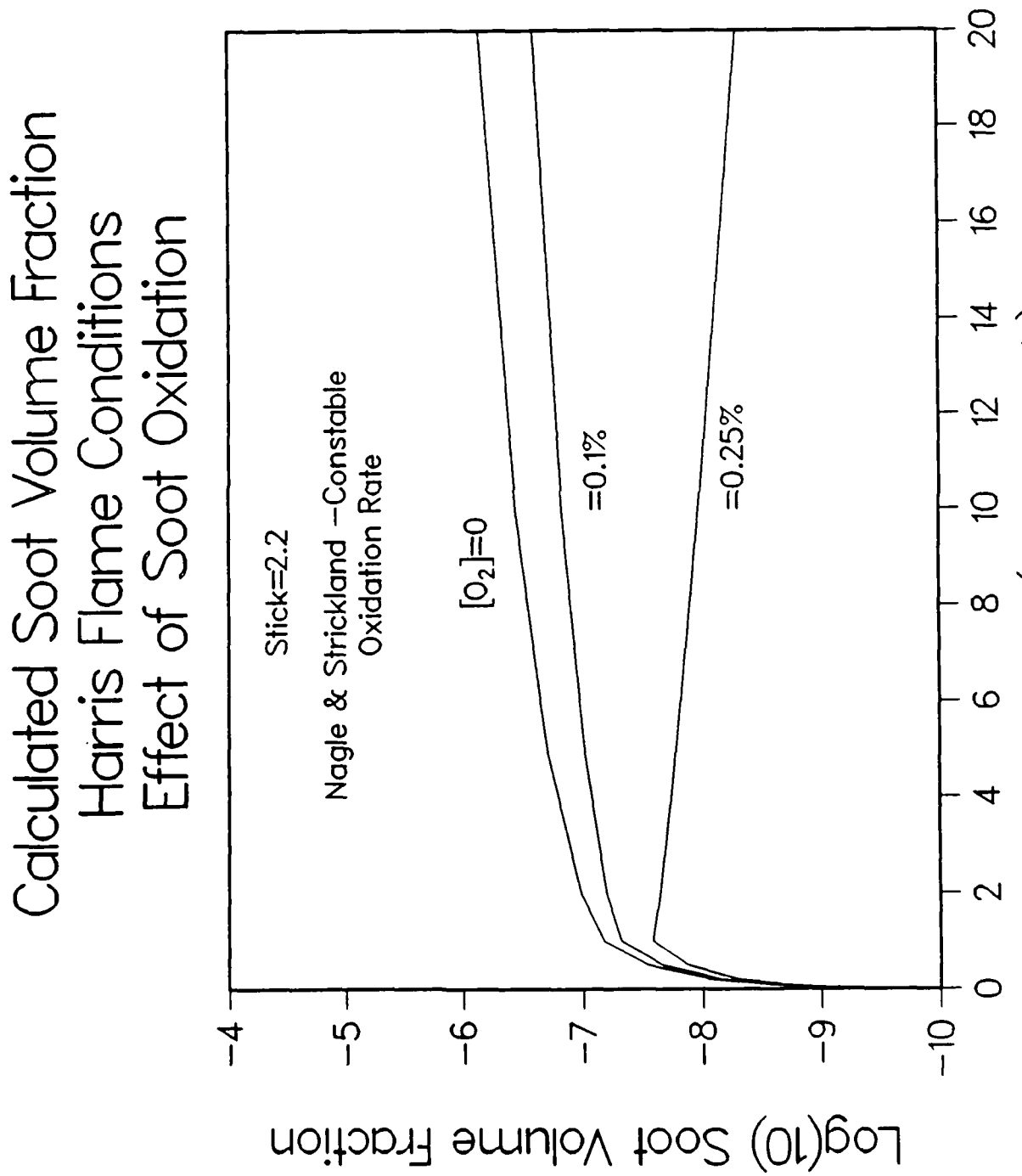
Calculated Soot Volume Fraction
Harris Flame Conditions
Effect of Soot Oxidation
Stick=2.2
Nagle & Strickland –Constable
Oxidation Rate
[O2]=0
=0.1%
=0.25%
Log(10) Soot Volume Fraction
Time (milliseconds)
-4
-5
-6
-7
-8
-9
-10
0
2
4
6
8
10
12
14
16
18
20

Performing the soot growth calculations with oxygen present shows that even modest amounts of oxygen can have rather drastic effects on the predicted amount of soot formed. Figure 15 displays the calculated soot volume fraction versus oxygen concentrations. Given the Harris-Weiner acetylene surface growth rate and the Nagle and Strickland-Constable surface oxidation rates, it appears not to be possible to form soot for oxygen concentrations beyond roughly 0.2% at a temperature of 1600K. No depletion of the oxygen by the oxidation process has been allowed for in these calculations, however.

IV. List of Publications

A paper entitled "The Pyrolysis of Acetylene Initiated by Acetone" by M. B. Colket, H. B. Palmer and D. J. Seery has been published in *Combustion and Flame,* Vol. 75, pp. 343-366, 1989. This work was initiated under contract F49620-85-C-0012, and revisions to the manuscript were performed under this contract. See Appendix C for reprint.

A paper entitled "The Pyrolysis of Acetylene and Vinylacetylene in a Single-Pulse Shock Tube" by M. B. Colket was published in the *Twenty-First Symposium (International) on Combustion,* The Combustion Institute, pp. 851-864, 1986. See Appendix D for reprint. Research for this publication was performed under contract F49620-85-C-0012.

A manuscript entitled "Oxidative Pyrolysis of Ethene in a Single-Pulse Shock Tube" by M. B. Colket and D. J. Seery will be written late in 1989 and submitted to the *Twenty-Third Symposium (International) on Combustion,* Jan. 1990.

A manuscript entitled "A Simplified Model for the Production of Soot in a Premixed Flame" by R. J. Hall and M. B. Colket will be written in 1989 and submitted to *Combustion Science and Technology.*

V. Meeting Interactions and Presentations

1. A round table discussion on "Current Problems in Soot Formation During Combustion, Especially the Mechanism of Soot Formation" was held in Göttingen, West Germany on March 29-30, 1989. The meeting was organized by Professor H. Gg. Wagner and was attended by about twenty engineers/scientists currently involved with understanding soot formation phenomena. Financial support was provided by the Commission for Condensation Phenomena of the Academy of Sciences in Göttingen, West Germany.
2. Eastern Section of the Combustion Institute, Clearwater Beach, Florida, Dec. 5-7, 1988. M. Colket presented an invited talk entitled "The Role of Oxidative Pyrolysis in Preparticle Chemistry". See Appendix A.
3. Brookhaven National Laboratory, Upton, New York, November 9, 1988. M. Colket presented an invited seminar entitled "Kinetic Mechanisms for the Pyrolysis of Unsaturated Hydrocarbons". Financial support provided by BNL.
4. Department of Energy - Office of Basic Energy Sciences Combustion Research Meeting held at Lake Geneva, Michigan, June 1-3, 1988. M. Colket was invited by W. H. Kirchhoff to be an observer and participant at this D.O.E. contractor's meeting. The meeting was attended under corporate sponsorship.

References

1. Colket, M.B. and Seery, D.J., "Mechanisms and Kinetics of Toluene Pyrolysis", poster presentation at the Twentieth Symposium (International) on Combustion, Ann Arbor, MI, 1984.
2. Venkat, C., Brezinsky, K., and Glassman, I., *Nineteenth Symposium (International) on Combustion*, The Combustion Institute, Pittsburgh, PA, p. 143.
3. S.J. Harris and A.M. Weiner, *Combustion Science & Technology,* 131, 155 (1983).
4. S.J. Harris and A.M. Weiner, "A Picture of Soot Particle Inception", in press.
5. S.J. Harris, A.M. Weiner and R.J. Blint, "Formation of Small Aromatic Molecules in a Sooting Ethylene Flame", from preprints of papers presented at 194th National Meeting of American Chemical Society, Div. of Fuel Chemistry, New Orleans, LA, 31 August - 4 September 1987, Vol. 32, p. 488.
6. J.D. Bittner and J.B. Howard, "Pre-particle Chemistry in Soot Formation", in *Particulate Carbon - Formation During Combustion,* D.C. Siegla and G.W. Smith, eds., p. 109, Plenum Press, 1981.
7. F. Gelbard, *MAEROS User Manual,* NUREG/CR-1391, (SAND80-0822) 1982. The version of the code which we use is "MAEROS2X".
8. J. Nagle and R.F. Strickland-Constable, *Proceedings of the Fifth Carbon Conference,* Vol. 1, Pergamon Press, 1963, p. 154.
9. N.A. Fuchs and A.G. Sutugin, in *Topics in Current Aerosol Research,* G.M. Hidy and J.R. Brock, eds., Vol. 2, pp. 34-35, Pergamon Press, 1971.
10. I.M. Kennedy, *Combustion & Flame,* 68, 1 (1987).
11. S.J. Harris and I.M. Kennedy, *Combustion Science & Technology,* 59, 443 (1988).
12. E.M. Lifshitz, *Sov. Phys. JETP,* 2, 73 (1956).
13. D. Langbein, *J. Phys. Chem. Solids,* 32, 1657 (1971).
14. W.H. Marlow, *J. Chem. Phys.,* 73, 6284 (1980).
15. F.S. Lai, S.K. Friedlander, J. Pich and C.M. Hidy, *J. Colloid Interface Sci.,* 39, 395 (1972).

Appendix A

The Role of Oxidative Pyrolysis In Pre-particle Chemistry

The Role of Oxidative Pyrolysis in Preparticle Chemistry

M. B. Colket III
United Technologies Research Center

Presentation to the Eastern Section of the Combustion Institute
Clearwater Beach, Fla., Dec. 5-7, 1988

The specific steps leading to soot formation have been described recently by Glassman[1]. In his review article, Glassman unites the individual efforts and results of a great many dedicated researchers and presents a cohesive story of the processes leading to soot formation. His analysis focuses on flame structure and temperature as two of the most important parameters in controlling soot formation: increasing temperature in a diffusion flame enhances soot formation since fuel pyrolysis rates are increased; yet, in premixed flames, increasing temperature decreases soot formation since competitive oxidation processes are enhanced. In the present article, oxidation processes are considered. First, global effects due to the presence of oxygen are reviewed. Secondly, the oxidation of radical intermediates critical to soot formation, i.e., vinyl and phenyl, are examined, and then the phenomena of soot-oxidation are briefly discussed.

Oxygen is often found in the fuel side of diffusion flames. For example, probe sampling[2,3] has demonstrated the existence of oxygen at concentrations near 1% in the interior fuel jet of a coannular flame. The oxygen may be from finite rate chemistry (diffusion of O_2 through the flame front), leakage at the burner lip or partial mixing (turbulent, diffusion flame). The effect of oxygen has been shown to vary depending on fuel-type[4]: for ethene, oxygen addition enhances soot formation, but for alkanes, soot formation remains the same or actually decreases. This effect has been explained[4] by the fact that, at 1400 K, oxygen addition noticeably enhances the pyrolysis rate and radical production for ethene but barely changes these rates in the case of the pyrolysis of an alkane. Thus, oxygen addition to ethene accelerates the chemistry but has little (or only a dilution) effect for alkanes, which have substantially weaker C-C and C-H bonds. This result is qualitatively consistent with shock tube results on soot scattering[5] and ring formation[6] which showed that both soot and aromatic production are enhanced at lower temperatures when small amounts of oxygen are added to the pyrolysis of unsaturated hydrocarbons. Numerical modeling[7] confirms the acceleration in chemistry due to the presence of oxygen.

Quantitative prediction of soot production, should it become a reality, will require knowledge of competition between processes associated with ring formation and fragmentation. As an example of the uncertainty associated with these processes, consider reactions involving the vinyl radical which has been suggested to be a primary radical leading to the formation of aromatic rings.

$$C_2H_3 + C_2H_2 \rightleftharpoons C_4H_5 \rightleftharpoons C_4H_4 + H \quad (1)$$

$$C_2H_3 + C_2H_4 \rightleftharpoons C_4H_7 \rightleftharpoons C_4H_6 + H \quad (2)$$

$$C_2H_3(+M) \rightleftharpoons C_2H_2 + H(+M) \quad (3)$$

$$C_2H_3 + O_2 \rightarrow HCO + H_2CO \quad (4)$$

$$C_2H_3 + O_2 \rightleftharpoons HO_2 + C_2H_2 \quad (5)$$

The relative rates of these reactions will define the fate of the vinyl radical, i.e., does it undergo growth, does it decompose to acetylene, or is it oxidized. Unfortunately, there is a relatively large amount of uncertainty in these rate constants and the accuracy of models may therefore be in question.

The rate constant for Reaction 1 has recently been measured[8] to be $10^{12.3}$ exp(-5.0 kcal/mole/RT) cm^3/mole/sec and recent predictions[9] and most literature values are reasonably close to this determination near 1200 K. Two values for k_2[8 10] differ by an order of magnitude although the direct measurement by Fahr and Stein[8] is probably the more reliable value.

Values for k_3 vary over three orders of magnitude. Very few experimental rate constants have been determined and these experiments have been subject to alternative interpretation or large uncertainty. A reasonable estimate for k_3 should be derivable from a measurement of the reverse process and detailed balancing. Unfortunately, the heat of formation of vinyl radicals has been under much discussion recently and values range from 61 to 72 kcal/mole (see Ref. 9). This uncertainty leads to a range in the calculation of k_3 of more than two orders of magnitude at 1200 K.

Information regarding Reaction 4 has been obtained only at low temperatures[11] and interpretation of these results has recently been questioned[9]. There is no experimental confirmation of this reaction or a rate determination at combustion temperatures. Inclusion of this reaction and its low temperature rate constant[11] in detailed chemical models indicates that this reaction and its rate constant are critical in the modeling of hydrocarbon oxidation. This and similar reactions could also play a very important role in arresting growth to higher molecular weight species. Reaction 5 is perhaps of lesser importance, and its rate constant is also poorly known. Published values (see Ref. 12) range two orders of magnitude. Evidence for its existence is minimal and rate constants have been inferred from detailed modeling.

Considering these large uncertainties and the importance of these vinyl radical reactions to the rich combustion of hydrocarabons and pre-particle kinetics, a series of experiments were performed in a single-pulse shock tube (SPST) coupled with gas chromatographic analysis[13]. Experimental results for a mixture of 3.5% ethene, 0.52% oxygen and the balance argon are shown in Figs. 1a-1d for total pressures near 10 atm and average dwell times of 550 microseconds. Profiles were also obtained for cis- and trans-2-butene, as well as C_5- and C_6- species. Although not shown in Fig. 1, they were included in the mass balances shown in Figs. 1a and 1b. Similar experiments were also performed with no added oxygen (but there was an oxygen impurity of about 1000 ppm) and for 2.0% oxygen. The pyrolysis products were virtually the same as those obtained by Skinner and Sokoloski[14] although decomposition rates were faster. The principle effect of oxygen addition is to accelerate the kinetics with little overall change to the product distribution, although carbon oxides, ketene, and acetaldehyde were also detected. An increased rate of aromatic production was observed at lower temperatures when oxygen was added to the ethene, which is consistent with calculations[7]. The production of aromatics has in turn been correlated with soot production[15].

An analysis of the data indicated that information on the vinyl radical could be obtained from the yields of 1,3-butadiene (via Reaction 2). If one assumes that (1) butadiene decomposition is negligible at low extents of reaction (<1200 K), (2) all oxidized products arise principally from Reaction (4), and (3) these products are rapidly converted to carbon monoxide, then the relative rates of Reactions 2 and 4 can be written

$$\frac{R_4}{R_2} = \frac{k_4}{k_2}\frac{[O_2]}{[C_2H_4]} = \frac{1}{2}\frac{d[CO]/dt}{d[C_4H_6]/dt} \qquad (A)$$

where the factor of one-half arises from the production of both formyl and formaldehyde (or two CO's) in Reaction 4. Integrating this expression over the length of the experiment and rearranging gives:

$$\frac{k_4}{k_2} = \frac{1}{2}\frac{[CO]_f}{[C_4H_6]_f}\frac{[C_2H_4]_i}{[O_2]_i} \qquad (B)$$

where the subscripts i and f refer to the initial and final concentrations, respectively. If assumptions (1) or (2) are *invalid*, then Eq. (B) represents an upper limit ratio. Alternatively, if the

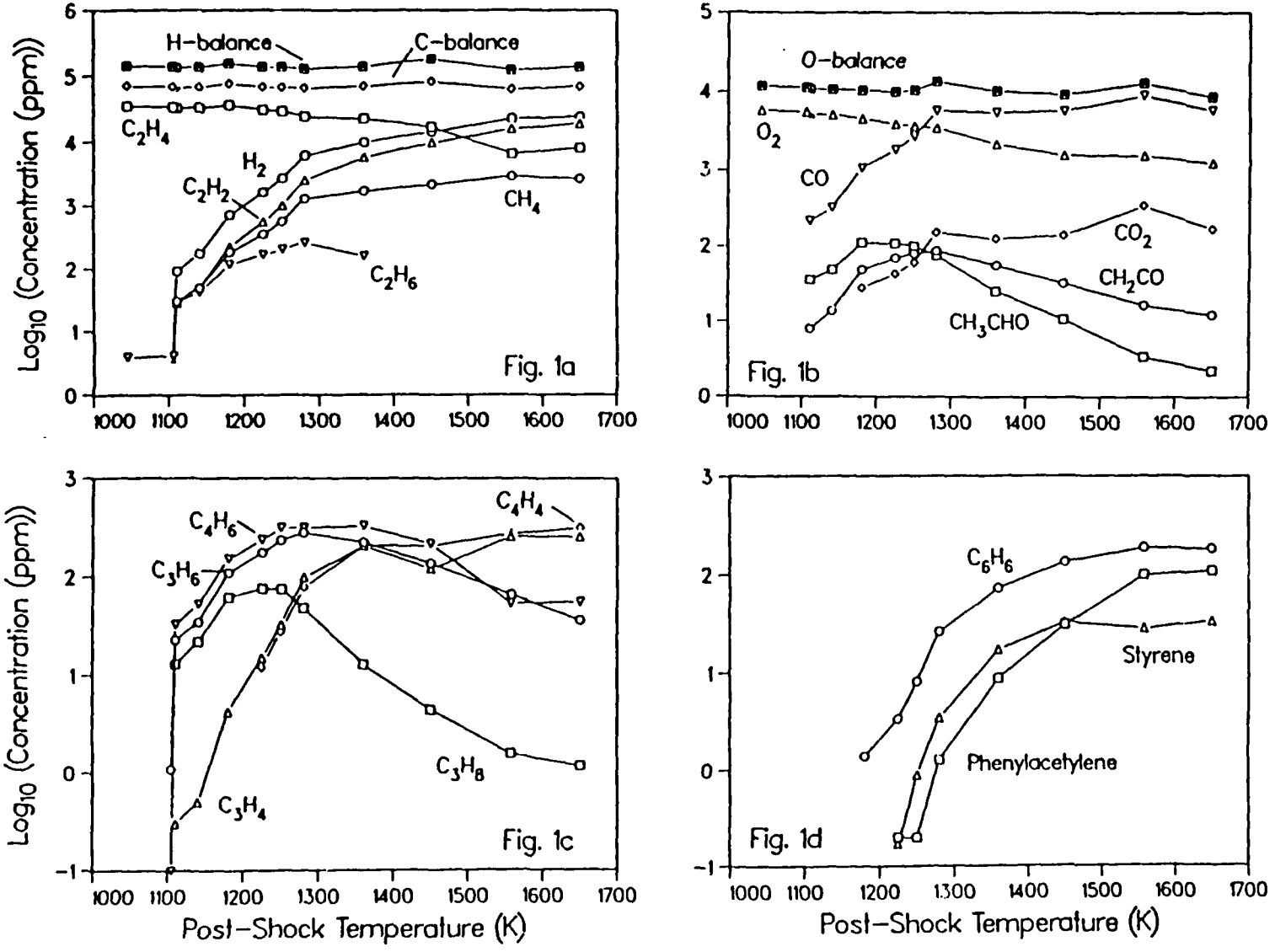

Fig 1. Oxidative Pyrolysis of Ethene in a Single-Pulse Shock Tube - 3.5% C_2H_4, 0.52% O_2 in argon. Dwell Times were approximately 550 microseconds, total pressures were ten atmospheres.

formaldehyde produced in Reaction 4 does not rapidly decompose, Eq. (B) could be a factor of two too high. A preliminary analysis using detailed chemical kinetics indicates that in the temperature range 1100-1200 K, about half of the carbon monoxide produced could be formed (directly or indirectly) from other reactions such as O or OH attack on ethene. In addition, not all of the formaldehyde decomposes to carbon monoxide during the SPST experiments. Consequently, we make the preliminary assessment that rate constants determined from Eq. (B) represent an upper limit and values reduced by a factor of one-third are reasonable estimates for this rate constant. The upper limit and the reduced values are compared to the value obtained by Slagle and co-workers[11] in Fig. 2. In addition, a rate constant was determined from flow reactor data[16] using Eq. (A) (for an experiment of 3.1% ethene, 0.5% oxygen at one atmosphere). The value (also reduced by one-third) is shown in Fig. 2 and agrees well with the SPST data. Overall, these new values are consistent with an extrapolation of the low temperature results, although a stronger decay with increasing temperature is indicated. This negative temperature dependence is not unexpected for addition/rearrangement reactions. As a test for this technique, the same procedure was used in the case when 2.2% ethene and 1.1% acetylene were co-pyrolyzed. Thus, a comparison of rate constants for reactions 1 and 2 could be obtained for comparison to other data. By analogy to the previous derivation,

$$\frac{k_1}{k_2} = \frac{[C_4H_4]_f}{[C_4H_6]_f} \frac{[C_2H_4]_i}{[C_2H_2]_i}$$

This ratio was found to be 1.25±0.3 over the temperature range 1240 to 1360 K, and compares well to the ratio of 1.42 obtained by Fahr and Stein at slightly lower temperatures.

Addition of a little oxygen to ethene pyrolysis (as for many other hydrocarbons) results principally in the acceleration of the reaction: some carbon monoxide, formaldehyde, ketene and other oxidative products are formed, but the identity of the hydrocarbon species and their relative concentrations are similar in the case of pure pyrolysis and oxidative pyrolysis. For SPST experiments at UTRC this situation does not hold in the case of benzene. Based on the following analysis, the difference is due totally to the different fate of the phenyl radical in the pyrolysis versus that in the oxidative pyrolysis. In the pyrolysis,

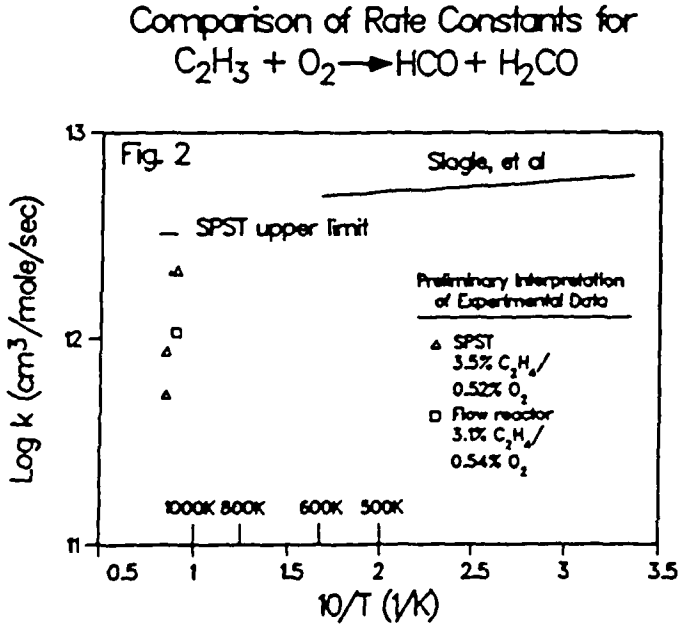

$$C_6H_5 \rightarrow C_4H_3 + C_2H_2 \quad \text{(overall)} \qquad (6)$$

$$C_4H_3 \rightarrow C_4H_2 + H \qquad (7)$$

$$\rightarrow C_2H + C_2H_2 \qquad (8)$$

dominate, leading to the production of C_2H_2 and C_4H_2 as the principal species[17,18]. In the oxidative pyrolysis, however, a sequence similar to

$$C_6H_5 + O_2 \rightarrow C_6H_5O + O \qquad (9)$$

$$C_6H_5O \rightarrow C_5H_5 + CO \qquad (10)$$

$$C_5H_5 + O_2 \rightarrow C_5H_5O + O \qquad (11)$$

$$C_5H_5O \rightarrow C_4H_5 + CO \qquad (12)$$

$$C_4H_5 \rightarrow C_4H_4 + H \qquad (13)$$

$$C_4H_5 \rightarrow C_2H_2 + C_2H_3 \qquad (14)$$

$$C_2H_3 \rightarrow C_2H_2 + H \qquad (15)$$

overrides the pyrolytic ring fracture and phenol, cyclopentadiene, vinylacetylene, and acetylene are principle products. These sequences are qualitatively consistent with observed SPST product distributions. This mechanism for phenyl oxidation is also consistent with and derived principally from the work of Venkat, et al[19]. The explanation for this major difference between the pyrolysis and the oxidative pyrolysis is that, at 1400 K, the lifetime of phenyl based on Reaction 6 is 3500 microseconds, but for decomposition via Reaction 9, the lifetime is just 40 microseconds with only 17 torr O_2. Biphenyl was also observed in the oxidative pyrolysis runs since, for these series of experiments, the sampling system had been modified to collect polyaromatic species. Since biphenyl is formed principally via

$$C_6H_6 + C_6H_5 \leftrightarrow C_{12}H_{10} + H \qquad (16)$$

The relative rates of Reactions 9 and 16 can be written

$$\frac{R_9}{R_{16}} = \frac{k_9}{k_{16}} \frac{[O_2]}{[C_6H_6]}.$$

Assuming negligible back reaction, the integrated value of R_{16} is simply the yield of biphenyl, while that of R_9 can be estimated by either one-half (1) the yields of phenol, cyclopentadiene, and vinylacetylene plus one-half the yield of acetylene or one-half (2) the yield of phenol plus that of carbon monoxide minus the CO produced from Reaction 12 (the yield of vinylacetylene plus one-half of that from acetylene). The correction of one-half is to account for the fact that O-atoms produced in Reaction 6 add to benzene to form phenol. Method (2) produced values for the integrated rate of Reaction 9 about 40% greater than those of method (1). Since additional phenol and hence other products can also be formed from O and OH via

$$H + O_2 \leftrightarrow OH + O$$
$$O + C_6H_6 \leftrightarrow C_6H_5OH$$
$$OH + C_6H_6 \leftrightarrow C_6H_5OH + H,$$

the integrated rate of Reaction 9 calculated using these methods is an upper limit. Using values averaged from methods (1) and (2), the ratio k_9/k_{16} could be calculated. Using a recent measurement[8] of k_{16}, values of k_9 were determined (from a run of 1.1% benzene and 0.2% oxygen) and are plotted in Fig. 3. Also shown on this figure are literature values based on detailed modeling[20] and thermochemical estimates[21]. The SPST upper limits are consistent with the previous results.

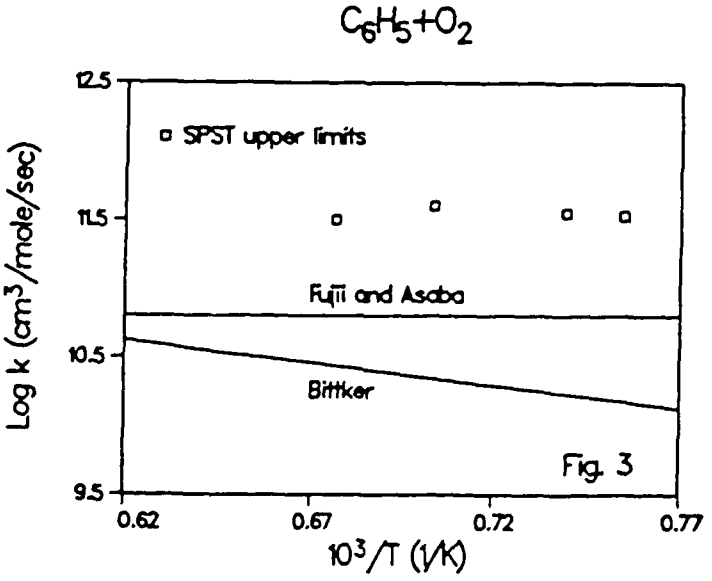

Fig. 3

The drastic difference between products of the pyrolysis and the oxidative pyrolysis of benzene (and quite likely other aromatic hydrocarbons) could have important implications for the mechanisms of soot formation. Cyclopentadienyl, whose stability is resonantly enhanced, is an important and relatively long-lived intermediate during the oxidative pyrolysis of benzene, but is unimportant in the pyrolysis. It is quite reasonable to expect that collisions involving cyclopentadienyl and aromatics (or fused six-membered rings) may lead to growth of aromatic rings. In fact, an unusual result from the present experiments is the production of 1-methylnaphthalene at the early (low temperature) stages of ox-

idative pyrolysis of benzene. Concentrations of this product are nearly a factor of three higher than that of naphthalene and 100 times higher than 2-methylnaphthalene. A possible explanation is the reaction

$$c\text{-}C_5H_5 + C_6H_6 \rightarrow H + 1\text{-}C_{10}H_7CH_3 \quad (1\text{-methylnaphthalene}).$$

Although the rate constant for this reaction might be low due to a complex rearrangement, the net rate could be high due to high concentrations of cyclopentadienyl. In fact, the naphthalene that is observed could be a result of this reaction followed by H-atom substitution of the methyl group rather than acetylene addition to phenyl and then to the benzyne-acetylene radical[22]. Another interesting aspect of oxidation phenomena relates to the question of six-membered vs. five-membered rings in pre-particle kinetics. Thermodynamic and other arguments[23] have been used to suggest that principally six-membered rings exist in pre-particle molecules. These arguments contrast with interpretation of experimental data[24,25] supporting the existence of buckminsterfullerene and similar species which contain a mixture of six- and five-membered rings. Based on (1) the interpretation of benzene (and phenyl) oxidation, which includes formation of either phenoxy and phenol due to attack by O_2, O, or OH followed by loss of a single carbon (to carbon monoxide) and the formation of a five-membered ring and (2) the interpretation by Harris[26] that oxidation of nascent soot particles is a detectable process in fuel-rich premixed flames, we reach the following conclusion: during the growth of PAH's, partial oxidation of these species will occur leading to the production of carbon monoxide and five-membered rings. The resultant compounds will contain mixtures of five- and six-membered rings, some of which will fragment, and others may continue to grow via addition processes.

Soot Oxidation

The focus of this paper thus far has been the oxidation of small hydrocarbon radicals. Oxidation of larger species and soot also play an important role in sooting flames. Harris[26] recently interpreted experimental data to conclude that oxidation competes with surface growth and coagulation during particle inception, and it is generally acknowledged that oxidation can retard growth throughout the life of a particle. The parameter controlling complete burn-out of soot has been determined to be temperature. Kent and Wagner[27] have shown that once the flame temperature decreases below 1400 K, soot oxidation ceases, and a soot trail emerges from the tip of the flame. A physical interpretation of this process can be found by considering a heat balance on an isolated soot particle. Assuming the dominant factors to be radiation loss ($\dot{Q}_{rad}$) and exothermic heat release due to oxidation ($\dot{Q}_{ox}$), the following simplified analysis can be used to explain quantitatively the cessation of soot burn-out.

Radiative loss can be calculated based on an expression from Hall[28]:

$$\dot{Q}_{rad} = 2.97 \times 10^{-10} \text{ watts/cm}^3/\text{K}^5 f_v T^5$$

for radiation from unit gas volume, or

$$\begin{aligned}\dot{Q}_{rad} &= 2.97 \times 10^{-10} \text{ watts/cm}^3/\text{K}^5 T^5 \\ &= 7.1 \times 10^{-14} \text{ kcal/sec/cm}^3/\text{K}^5 T^5\end{aligned}$$

for radiation from unit particle volume. f_v represents the particle volume fraction and the fifth power dependency on temperature arises from a $1/\lambda$ dependency on the particle emissivity. A comparison of oxidation rates indicates (see e.g., Ref. 27) that the oxidation of soot particles is nearly independent of the concentration of molecular oxygen below 2000 K. A fit to measured rates has been reported[27] and the rate of soot oxidation is

$$\frac{dS_m}{dt} = -k_{ox}A$$

$$\text{with} \quad k_{ox} = 91 \times e^{-(39670/RT)} \ g/cm^2/sec$$

and S_m is the soot mass and A is the surface area of the particle. The rate expression is valid only for temperatures below 2000 K. Assuming the reaction sequence to be equivalent to

$$C(s) + 1/2\ O_2 \rightarrow CO,$$

the reaction is 21 kcal/mole (or 1.75 kcal/gm) exothermic. The assumption that carbon monoxide is the principle product is consistent with recent results[29] on carbon oxidation using a diode laser for product detection. The heat release due to oxidation is therefore

$$\dot{Q}_{ox} = (1.75 \text{ kcal/gm}) \times \frac{dS_m}{dt}$$

$$= 160 \times A \times e^{(-39670/RT)} \ kcal/cm^2/sec.$$

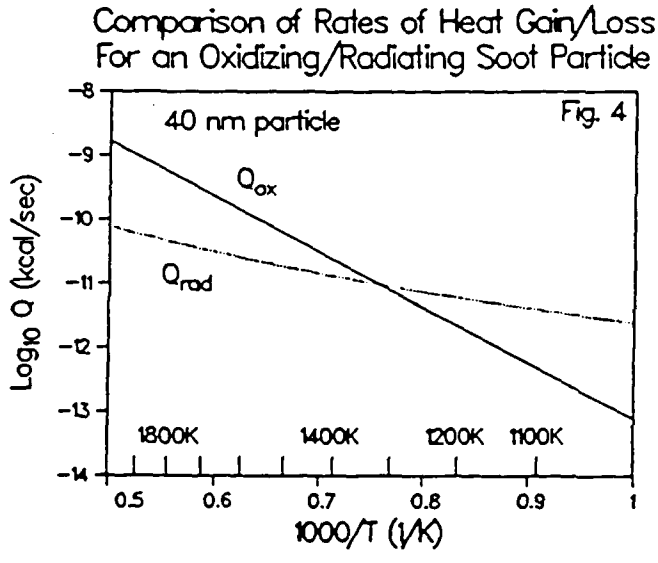

Assuming a particle diameter of 40 nm, $\dot{Q}_{rad}$ and $\dot{Q}_{ox}$ are plotted in Fig. 4 vs. temperature for comparison. As long as the particle temperature exceeds approximately 1400 K, the oxidation process generates sufficient heat to overcome that loss by radiation. Temperatures can rise in this region (see Ref. 30) but usually decay due to other (conductive and convective) losses. Furthermore, the temperature may decrease since heat release due to oxidation may be inhibited by the inability of oxygen to diffuse to the center of the flame. Once the particle temperature reaches about 1400 K, however, the oxidation quenches, as radiation, conductive and convective processes rapidly cool the particle.

Characteristic times for oxidation can also be estimated, assuming the particle is a perfect sphere.

$$\frac{dm}{dt} = -kA$$

substituting for the surface area and integrating

$$\int_{m_o}^{0} \frac{dm}{m^{2/3}} = \int_{0}^{t_{ox}} \frac{4\pi k dt}{\left(\frac{4}{3}\pi\rho\right)^{2/3}}$$

or

$$t_{ox} = \frac{\rho r}{k}$$

$$= 4.0 \times 10^{-8} e^{+39670/RT} \ sec$$

$$= 62 \text{ msec at } 1400 \text{ K}$$

$$= 24 \text{ msec at } 1500 \text{ K}$$

$$= 10 \text{ msec at } 1600 \text{ K}$$

for a particle 40 nm in diameter and with a density of 1.8 gm/cm^3. Considering dwell times in the luminous zone of a co-annular diffusion flame, as well as measured temperatures[31], one can easily argue that once the particle temperature drops below 1500 K, there is insufficient time for complete oxidation. Conductive, convective, and radiation losses slightly dominate over the chemical heat release and the particle cools slowly until 1400 K, at which point heat release from oxidation is too slow, the particle cools very rapidly, and a soot trail is emitted.

ACKNOWLEDGEMENTS

This work has been supported in part by the Air Force Office of Scientific Research under Contract No. F49620-85-C-0012. The author is indebted to Dr. Julian Tishkoff, AFOSR contract monitor, for his support and to P. K. Bonczyk, R. J. Hall, D. J. Seery, and J. J. Sangiovanni for valuable technical discussions. In addition, the author expresses his gratitude to D. Kocum for experimental work and to H. Hollick, K. Wicks, and G. Deske for assistance data in reduction and preparation of the manuscript.

REFERENCES

1. Glassman, I., "Soot Formation in Combustion Processes" to be published in Twenty – Second Symposium (International) on Combustion, The Combustion Institute, Pittsburgh.

2. Hamins, A., Gordon, A. S., Seshadri, K., and Saito, K., Twenty – First Symposium (International) on Combustion, The Combustion Institute, Pittsburgh 1986, p. 1077.

3. Bonczyk, P. K., UTRC, Personal Communication, 1988.

4. Hura, H. S. and Glassman, I., *Combust. Sci. Tech.* 53: 1 (1987).

5. Frenklach, M., Ramachandra, M. K., and Matula, R. A., Twentieth Symposium (International) on Combustion, The Combustion Institute, Pittsburgh 1985, p. 871.

6. Colket, M. B., UTRC, unpublished results, 1988.

7. Frenklach, M., Clary, D. W., Yuan, T., Gardiner, W. C., Jr., and Stein, S., *Combust. Sci. Tech.* 50: 79 (1986).

8. Fahr, A. and Stein, S., to be published in Twenty – Second Symposium (International) on Combustion, The Combustion Institute, Pittsburgh.

9. Weissman, M. A. and Benson, S. W., *J. Phys. Chem.* 92: 4080 (1988).

10. Benson, S. W. and Haugen, G. R., *J. Phys. Chem.* 85: 1735 (1967).

11. Slagle, I. R., Park, J.-Y., Heaven, M. C., and Gutman, D., *J. Am. Chem. Soc.* 106: 4356 (1984).

12. Garo, A., Westmoreland, P. R., Howard, J. B., and Longwell, J. P., *Combust. Flame* 72: 271 (1988).

13. Colket, M. B., Twenty – First Symposium (International) on Combustion, The Combustion Institute, Pittsburgh, 1986, p. 851.

14. Skinner, G. B. and Sokoloski, E. M., *J. Phys. Chem.* 64: 1028 (1960)

15. Kern, R. D., Wu, C. H., Yong, J. N., Pamidimukkala, K. M. and Singh, H. J., "The Correlation of Benzene Production With Soot Yield Determined From Fuel Pyrolysis", ACS National Meeting, Div. Fuel Chem Preprints, 32(2): 456 (1987).

16. Brezinsky, K., Hura, A., and Glassman, I., *Energy and Fuels* 2: 487 (1988).

17. Kern, R. D., Wu, C. H., Skinner, G. B., Rao, V. S., Kiefer, J. H., Towers, J. A., and Mizerka, L.J., Twentieth Symposium (International) on Combustion, The Combustion Institute, Pittsburgh, 1984, p. 789.

18. Colket, M. B., "Pyrolysis of C_6H_6", ACS National Meeting, Div. Fuel Chem. preprints 31(2): 98 (1986).

19. Venkat, C., Brezinsky, K., and Glassman, I., Nineteenth Symposium (International) on Combustion, The Combustion Institute, Pittsburgh, 1982, p. 143.

20. Bittker, D., "Detailed Mechanism of Benzene Oxidation", Poster presentation to the Twenty-Second Symposium (international) on Combustion, P159, Aug, 1988.

21. Fujii, N. and Asaba, T., Fourteenth Symposium (International) on Combustion, The Combustion Institute, Pittsburgh 1973, p. 433.

22. Frenklach, M., Clary, D. W., Gardiner, W. C., Jr., and Stein, S., Twentieth Symposium (International) on Combustion, The Combustion Institute, Pittsburgh 1985, p. 887.

23. Frenklach, M. and Ebert, L. B., *J. Phys. Chem.* 92: 561 (1988).

24. Gerhardt, Ph., Loffler, S., and Homann, K. H., to be published in Twenty – Second Symposium (International) on Combustion, The Combustion Institute, Pittsburgh.

25. Iijima, S., *J. Phys. Chem.* 91: 3466 (1987).

26. Harris, S. J. and Weiner, A. M., *to be published in* Twenty – Second Symposium (International) on Combustion, The Combustion Institute, Pittsburgh.

27. Kent, J. H. and Wagner, H. Gg., *Combust. Sci. Tech.* 41: 245 (1984).

28. Hall, R. J., *Applied Optics* 27: 809 (1988).

29. Brandt, O. and Roth, P., "Shock Tube Measurements of Soot Oxidation Rates Using a Tunable IR-Diode Laser", Poster presentation to the Twenty-Second Symposium (international) on Combustion, P34, Aug, 1988.

30. Boedecker, L. R. and Dobbs, G. M., Twenty – First Symposium (International) on Combustion, The Combustion Institute, Pittsburgh 1986, p. 1057.

31. Santoro, R. J., Yeh, T. T., Horvath, J. J., and Semerjian, H. G., *Combust. Sci. Tech.* 53: 89 (1987).

Appendix B

The Rich Oxidation of Ethylene In a Single-Pulse Shock Tube

The Rich Oxidation of Ethylene in a Single-Pulse Shock Tube

M. B. Colket III
United Technologies Research Center

Second International Conference on Chemical Kinetics
Gaithersburg, MD., July 23-27, 1989

The fate of vinyl radicals during pyrolysis and combustion of hydrocarbons has been a subject of much discussion. Possible reactions include

$$C_2H_3 + C_2H_2 \leftrightarrow (C_4H_5)^* \leftrightarrow C_4H_4 + H \quad (1)$$
$$C_2H_3 + C_2H_4 \leftrightarrow (C_4H_7)^* \leftrightarrow C_4H_6 + H \quad (2)$$
$$C_2H_3(+M) \leftrightarrow C_2H_2 + H(+M) \quad (3)$$
$$C_2H_3 + O_2 \rightarrow HCO + H_2CO \quad (4)$$
$$C_2H_3 + O_2 \leftrightarrow HO_2 + C_2H_2 \quad (5)$$

The relative rates of these reactions will define the fate of vinyl; yet except for the first two, the rate constants for these processes are poorly known. To shed some light on these steps, a series of experiments using a single-pulse shock tube have been completed on the rich oxidation of ethylene. Post-shock temperatures ranged from about 1000 to 1800K and total pressures were 9 to 12 atmospheres. Ethylene and oxygen were mixed in a bath of argon. Concentrations of ethylene were 0.3 to 3.5% and overall stoichiometries varied from 5.25 to about 100. Final products were collected and analyzed using gas chromatography. Measured products include C_1-C_{10} hydrocarbons, carbon oxides, and hydrocarbon oxygenates such as acetaldehyde and ketene. Major hydrocarbon products include acetylene, methane and ethane. Detailed chemical kinetic modeling indicates that the latter is formed principally by the sequence

$$C_2H_4 + H(+M) \leftrightarrow C_2H_5(+M) \quad (6)$$
$$C_2H_5 + C_2H_4 \leftrightarrow C_2H_6 + C_2H_3 \quad (7)$$

Direct evidence for Reaction 4 (oxidation of vinyl) was not obtained but an upper limit for its rate constant was found to be 3×10^{12} cm^3/mole/sec at 1100K which is in good agreement with the determination by Slagle and coworkers (1984). k_5 was estimated to be 5×10^{10} cm^3/mole/sec at 1100K. Large amounts of acetylene are observed and are indicative of either an unusually high rate constant for k_3 or very significant contributions due to reactions, such as:

$$C_2H_4(+M) \leftrightarrow C_2H_2 + H_2(+M) \quad (8)$$
$$C_2H_3 + C_2H_4 \leftrightarrow (C_4H_7)^* \leftrightarrow C_2H_5 + C_2H_2 \quad (9)$$

By copyrolyzing ethylene and acetylene, the ratio k_1/k_2 was determined to be 1.25 ± 0.3 from 1240 to 1360K and agrees well with the ratio of 1.42 obtained from the Fahr and Stein (1989) measurements.

ACKNOWLEDGEMENTS

This work has been supported in part by the Air Force Office of Scientific Research under Contract Nos. F49620-85-C-0012 and F49620-88-C-0051.

Appendix C

The Pyrolysis of Acetylene Initiated by Acetone

COMBUSTION AND FLAME 75: 343–366 (1989)

The Pyrolysis of Acetylene Initiated by Acetone

M. B. COLKET III and D. J. SEERY

United Technologies Research Center, East Hartford, CT 06108

and

H. B. PALMER

Pennsylvania State University, University Park, PA 16802

A detailed, radical chain mechanism is used to model the pyrolysis of acetylene near 1000 K. The initiation process, $C_2H_2 + C_2H_2 \rightarrow C_4H_3 + H$, appears to be inconsistent with thermochemistry. Since experimental evidence indicates the presence of a chain mechanism, alternative sources of initiation are considered. Acetone, a common impurity in "purified" acetylene, was found to dominate radical initiation during the pyrolysis of acetylene near 1000 K despite concentration levels only 0.1% that of acetylene. Modeling results compare favorably with the experimental results of Munson and Anderson for acetylene decay and the formation of products vinylacetylene, benzene, and ethylene. Rate constants for the following reactions were adjusted to be

$C_2H_3 + C_2H_3 \leftrightarrow C_4H_6 \qquad k_4 = 2.0 \times 10^{13}\ cm^3\ mol^{-1}\ sec^{-1}$

$n\text{-}C_4H_5 \leftrightarrow C_4H_4 + H \qquad k_{32} = 1.6 \times 10^{14} \times e^{-(41.4\ kcal\ mol^{-1}/RT)}\ sec^{-1}$

$n\text{-}C_4H_5 + C_2H_2 \rightarrow C_6H_6 + H \qquad k_{33} = 4.5 \times 10^{12} \times e^{-(10.\ kcal\ mol^{-1}/RT)}\ cm^3\ mol^{-1}\ sec^{-1}$

$n\text{-}C_4H_5 + C_4H_4 \rightarrow C_8H_8 + H \qquad k_{35} = 1.2 \times 10^{13} \times e^{-(5.\ kcal\ mol^{-1}/RT)}\ cm^3\ mol^{-1}\ sec^{-1}$

to optimize the fit to the experimental data. A sensitivity analysis shows that the computed results were most sensitive to rate constants for these and a few other reactions. By addition of high-temperature reactions (such as those involving ethynyl radicals), the mechanism was found to be consistent with experimental results using single-pulse shock tubes and the very-high-temperature studies of Frank and Just and Wu, Singh, and Kern. Calculations are quantitatively consistent with the experimental finding that the effect of acetone is negligible at high temperatures (>2000 K) and low concentrations of acetylene ($< 5 \times 10^{-10}$ mol cm^{-3}). The model indicates, however, that at either higher concentrations or lower temperatures, impurities can play a significant role.

INTRODUCTION

Speculation on the mechanism of acetylene pyrolysis has continued for many years. Experiments at low temperature (600–1200 K) during the 1950s and 1960s resulted in a variety of suggestions, including radical chain processes and nonchain dimerizations involving diradical or electronically excited intermediates. During the 1970s, a radical chain mechanism was preferred [1–3] and initiation was assumed to be caused by

$$C_2H_2 + C_2H_2 \rightarrow C_4H_3 + H. \qquad (1)$$

The structure of C_4H_3 was not identified [1] but the overall endothermicity 45.9 kcal/mol was consistent with an early calculation [4] for the heat of formation of the butatrienyl radical (102 kcal/mol). Frenklach and coworkers [5], in a recent modeling study, tracked two of the isomers, namely 1-buten-3-yn-1-yl (n-C_4H_3) and 1-buten-

Published by Elsevier Science Publishing Co., Inc.
655 Avenue of the Americas, New York, NY 10010

0010-2180/89/$0.00

3-yn-2-yl (i-C_4H_3), and used Tanzawa and Gardiner's rate constant [1], but assumed that Reaction 1a was the initiation reaction.

$$C_2H_2 + C_2H_2 \rightarrow n\text{-}C_4H_3 + H, \quad (1a)$$

$$C_2H_2 + C_2H_2 \rightarrow i\text{-}C_4H_3 + H. \quad (1b)$$

Recent estimates [6, 7] for the heat of formation of the product of Reaction 1a (n-C_4H_3) of 124 kcal/mol (see later discussion) indicate that this reaction is about 68 kcal/mol endothermic. Wu et al. [8] noted the descrepancy between the endothermicity of Reaction 1a and the observed activation energy, and suggested that i-C_4H_3 is the product (Reaction 1b). Because isomerization of the (C_4H_4) intermediate is required prior to decomposition, it is probable that the reaction will have a low A-factor and/or an activation barrier in excess of the reaction endothermicity. Their proposed Arrhenius parameters ($A = 2 \times 10^{13}$ cm^3 mol^{-1} sec^{-1}, $E = 44.5$ kcal mol^{-1}) are inconsistent with this constraint.

Discounting the possibility of isomerization and invoking an activation energy of 68 kcal/mol for Reaction 1a, Duran et al. [9] were unable to describe experimental data with detailed chemical kinetic modeling. In addition, Duran and coworkers [10] found their data to be consistent with the assumption that acetylene pyrolyzes by isomerizing to vinylidene which then inserts into a C-H bond of acetylene to form vinylacetylene. The mechanism

$$C_2H_2 + M \leftrightarrow H_2CC: + M, \quad (1c)$$

$$H_2CC: + C_2H_2 \leftrightarrow (C_4H_4)^*, \quad (1d)$$

$$(C_4H_4)^* + M \leftrightarrow C_4H_4 + M \quad (1e)$$

requires that the reverse of the first step be very fast so that vinylidene is always in equilibrium with acetylene. Alternatively, Kiefer et al. [11] find support for the vinylidene mechanism from detailed balancing and interpretation of experimental data on the reverse process, i.e., the decomposition of vinylacetylene.

We cannot disprove a contribution from this nonchain dimerization; however, upon review of our own experimental data as well as that obtained by others we reach the unavoidable conclusion that a radical chain process occurs. In attempts to model experimental data, we have identified the probable role of acetone, a common impurity in acetylene, in initiating a radical chain during laboratory studies of the pyrolysis of acetylene.

In this paper, evidence supporting a radical chain is presented, issues related to acetone-initiation are discussed, and modeling results are compared to existing experimental data near 1000–1500 K. Finally, the proposed model is extended to examine the possible role of acetone under higher temperature conditions (<2000 K).

EVIDENCE FOR CHAIN MECHANISM

Palmer and Cullis's review article [12] cites results such as inhibition by radical scavengers and wall effects as evidence that the thermal decomposition of acetylene is a radical process. Because it is not known whether radical scavengers and walls might effectively remove singlet vinylidene as well as *mono*radicals, other evidence is needed regarding the possible role of vinylidene. The arguments [10, 13] for an extremely short lifetime (with respect to isomerization to HCCH) of vinylidene do strongly suggest that a dominant role for vinylidene is not compatible with the experimental observation of induction periods (see ref. 12) in the pyrolysis; Reaction (1c, −1c) will essentially equilibrate in a time equal to (or less than [13]) the time required for vinylidene to undergo one collision.

Therefore, the observation of induction periods supports the participation of a radical chain in which vinylidene does not play a significant role. [Although a hypothetical chain involving vinylidene can be constructed by adding a fourth reaction,

$$(C_4H_4)^* + C_2H_2 \leftrightarrow H_2CC: + C_4H_4 \quad (1f)$$

to the above three, the "chain length" in this sequence will be insignificant because of the extremely rapid isomerization of H_2CC: to acetylene, i.e., R(1f) cannot compete effectively with R(−1c).]

Evidence for a radical chain also arises from the work of Callear and Smith [14], who investigated the reaction between acetylene and atomic hydrogen in a quartz vessel at 293 K. Atomic hydrogen was generated by decomposing H_2 using a low-pressure mercury discharge lamp. Major products

included ethene, 1,3-butadiene, benzene, and trans-1,3,5-hexatriene. To explain these products, Callear and Smith suggested a reaction mechanism similar to that used in the present study except that in the low temperature, hydrogen-rich investigation, C_2H_3, n-C_4H_5, and l-C_6H_7 (1,3,5-hexatrienl-yl) radicals formed principally C_2H_4, 1,3-C_4H_6, and 1,3,5-C_6H_8 rather than losing H-atoms to form C_2H_2, C_4H_4, and benzene. Some benzene was still formed at low temperatures, presumably because of the high stability of the aromatic. A main conclusion from this low-temperature study was that chain processes exist. If these chain processes exist at room temperature, they are not likely to vanish at elevated temperatures. The principal concerns in extending these results to pyrolysis conditions are the stability of the radical adducts (relative to the reactants) and whether or not sufficient radicals can be generated to initiate the chain and account for the measured rate of acetylene pyrolysis. These aspects can only be addressed properly through detailed chemical kinetic modeling.

At elevated temperatures, there is a multiplicity of products from the thermal decomposition of acetylene. Near 1000 K, using 20% C_2H_2 in helium, Munson and Anderson [15] found vinylacetylene and also benzene, ethene, methane, and hydrogen. Working at even higher temperatures, Ogura [3] detected the same products during pyrolysis in a single pulse shock tube and also diacetylene and traces of 1,3-butadiene, and C_3 and C_5 species. Under similar conditions but with a heated sampling system, Colket [16] detected the same species and benzene, phenylacetylene, and traces of naphthalene as well. Although the vinylidene mechanism apparently explains the overall decomposition rates of the reactant, it does not describe the variety of products that have been observed experimentally. Thus, contributions from a chain sequence are expected.

Further indications of a chain mechanism are provided by additional single-pulse shock tube data in Fig. 1, which compares vinylacetylene and benzene production from three different gases: (a) 2040 ppm biacetyl in argon, (b) 3.7% acetylene in argon, and (c) a mixture of 3.55% acetylene and 1500 ppm biacetyl in argon. It also reveals that the production of C_4H_4 and C_6H_6 is substantially larger from the mixture than would be expected from purely additive considerations. Near 1100 K, the mixture produces an order of magnitude more C_4H_4 and C_6H_6 than is produced from acetylene or biacetyl. Because there is no reason to expect that biacetyl enhances the rate of the vinylidene mechanism, this enhancement must be a result of a chain mechanism initiated by biacetyl decomposition first into acetyl and then into methyl radicals. Mechanisms by which methyl radicals are converted to H-atoms (required for the acetylene chain) are discussed elsewhere in this article. Methyl radical addition to acetylene and to subse-

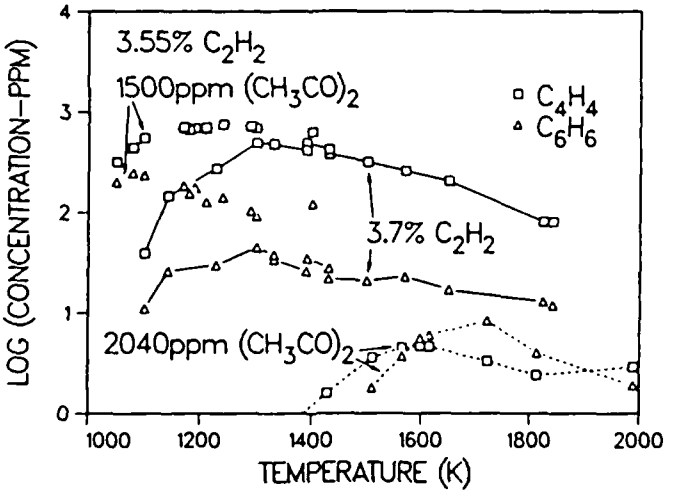

Fig. 1. Comparison of production of vinylacetylene and benzene in a single-pulse shock tube. ——, 3.7% acetylene; ---, 2040 ppm biacetyl; ···, 3.55% acetylene/1500 ppm biacetyl; □, vinylacetylene; △, benzene. Total pressure ~ 8 atmo, dwell times ~ 500-700 μsec.

quent adducts forms a variety of products, e.g., C_3H_4, C_4H_6, C_4H_8, etc., but the concentrations of these species are small relative to those of C_4H_4 and C_6H_6. There appears to be no facile method to produce vinylacetylene and benzene at the observed rates other than from the chain mechanism related to acetylene pyrolysis.

Finally, Ogura [3] shock-heated equimolar mixtures of C_2H_2/C_2D_2 diluted in argon. He found more than 40% of the vinylacetylene in the form of the C_4H_3D and C_4HD_3 isotopes at temperatures as low as 1070 K. It is highly unlikely that such significant scrambling can be accounted for by a vinylidene mechanism. Again a radical chain sequence is favored.

In summary, (1) an induction period has been observed during low-temperature acetylene pyrolysis, (2) a radical chain mechanism has been observed at room temperature, (3) acetylene pyrolysis produces a wide variety of products, (4) a large enhancement in the production of vinylacetylene and benzene is observed when acetylene is copyrolyzed with biacetyl, and (5) significant scrambling was observed during pyrolysis of C_2H_2/C_2D_2 mixtures. Because these phenomena are either indicative of a chain mechanism or can only be explained by a chain mechanism, they support the existence of a chain mechanism during acetylene pyrolysis at temperatures of 900–1400 K. They do not exclude possible contributions of a vinylidene or other nonchain mechanism, nor do they provide information on the relative contributions of the two mechanisms if two coexist. Nevertheless, as recent modeling efforts have focused on a nonchain mechanism, this work focuses solely on chain processes to examine whether or not they describe acetylene decomposition and product formation adequately.

HEATS OF FORMATION OF C_4H_3 ISOMERS

An interesting, although not critical, issue of this analysis is the heats of formation of the isomers of C_4H_3. Most modelers have relied on the early calculations of Cowperthaite and Bauer [4], which were performed for the butatrienyl isomer. Later estimates for the C_4H_3 isomers differ substantially from these calculations. Nevertheless, recent compilations [17, 18] have retained the early results and differences between the isomers are often ignored. For the purpose of this study, we hypothesize two separate isomers of C_4H_3: HCC-CCH_2 (i-C_4H_3) and HCCCHĊH (n-C_4H_3), We assume the first of these to be a resonant-hybrid with the two Kekulé structures: $H\dot{C}=C=C=CH_2$ and $HC\equiv C-\dot{C}=CH_2$. This assumption is consistent with interpretation of electron spin resonance measurements [19].

Recent estimates by Stein [6] and Bittner [7] place the heat of formation ($\Delta H_{f,298}^0$) of n-C_4H_3 near 124 kcal/mol. These estimates are based on the heat of formation of C_4H_4 (about 69 kcal/mol) and the assumption that D(n-C_4H_3-H) is equivalent by analogy to D(C_2H_3-H), i.e., about 108 kcal/mol. Accepting the analogous reasoning, there are remaining uncertanties in both the heat formation of vinylacetylene (C_4H_4) and the C_2H_3-H bond strength. Recent proposals [17, 20] for the heat of formation of C_4H_4 vary between 68 and 74 kcal/ mol. We chose to accept 69 kcal/mol based on the agreement between group additivity calculations and Bittner's analysis [7], which compared experimental heats of hydrogenation for several 3-en-1-yne hydrocarbons. The heat of formation of vinyl and consequently the vinyl-H bond strength has been under much discussion in recent years with most suggested values ranging from 62 [17] to 72 [21] kcal/mol. A midrange value of 67.5 kcal/mol leads to 124(+10, −7) kcal/mol for the heat of formation of n-C_4H_3, where the assigned uncertainties reflect the range in the published values for the heats of formation of vinyl radical and vinylacetylene.

Thermodynamics for i-C_4H_3 have also been estimated by both Stein [6] and Bittner [7]. Stein argues that the difference between n-C_4H_3 and i-C_4H_3 should be approximately equal to the resonant energy in $HCCCCH_2$. An upper limit of this resonant energy is that in the propargyl radical (−8 kcal/mol [58]). He then estimates a lower limit heat of formation of i-C_4H_3 to be 116 kcal/mol. Alternatively, Bittner used the procedure described by Cowperthwaite and Bauer [4] to determine the delocalized electron interactions. Using parameters updated from those used previously [4], Bittner calculates $\Delta H_{f,298}^0$ = 110.6 kcal/mol. It is important to note that as in the case

of n-C_4H_3, both estimates of i-C_4H_3 are dependent on the uncertainties of the heats of formation of C_4H_4 and C_2H_3. Both the Stein and Bittner values are substantially higher than the previous calculation [4] of 102 kcal, although the large estimated uncertainties (+10, −7 kcal) place all three values in "agreement." In the remainder of the present study we have elected to use the lower limit value suggested by Stein. Despite the common use of the early calculation [4] for the heat of formation of C_4H_3, we believe this value is significantly in error due to the updated calculation of Bittner and the recent estimate [20] of 81 kcal/mol for the heat of formation of butatriene, which coupled with 102 kcal/mol for C_4H_3 would predict a rather low (and unlikely) value of 73kcal/mol for the C–H bond strength in butatriene.

PRELIMINARY MODELING

For low-temperature pyrolysis (900–1400 K), Tanzawa and Gardiner [1] invoked bimolecular initiation followed by addition of H-atoms to C_2H_2 to form vinyl radicals. The proposed chain mechanism accounted quite well for the experimental results for acetylene decomposition. However, it did not describe the known production of benzene and higher molecular weight species, which together accounted for more than 50% of the decomposed acetylene (near 1000 K). Frenklach and coworkers [5] extended this mechanism to describe formation of heavier species including PAH and soot formation during pyrolysis of acetylene at higher temperatures. Colket [16], subsequently, used a similar mechanism for comparison to experimental profiles of species with molecular weights up to 102. Each of these studies used Reaction 1 or 1a as the initiation step with Arrhenius parameters as defined by Tanzawa and Gardiner (E = 45.9 kcal, $A = 2 \times 10^{12}$ cm^3 mol^{-1} sec^{-1})

Based on these studies, a simplified, low-temperature sequence can be written (Table 1). This sequence differs from that proposed by Tanzawa and Gardiner [1] in that Reaction 1a is assumed to initiate the reaction and vinyl recombination was found to dominate radical termination. In the earlier modeling [1], the high stability assumed for C_4H_3 led to its important role in

TABLE 1

Simplified Reaction Sequence For Low Temperature Pyrolysis of Pure Acetylene

$C_2H_2 + C_2H_2 \leftrightarrow$ n-$C_4H_3 + H$	(1a)
$H + C_2H_2 \leftrightarrow C_2H_3$	(2)
$C_2H_3 + C_2H_2 \leftrightarrow C_4H_4 + H$	(3a)
$C_2H_3 + C_2H_3 \leftrightarrow C_4H_6$	(4)

termination and C_4H_3 + H dominated. Termination by vinyl recombination has also been suggested by Ogura [3]. Duran et al. [9] and Frenklach et al. [5] also included vinyl–vinyl recombination in their models. In the former study, an unusually high rate constant (10^{14} cm^3 mol^{-1} sec^{-1}) was used which partially explains why their attempts to model acetylene pyrolysis failed. In the latter case, the modeling was performed at temperatures above 1400 K where thermal decomposition of vinyl is fast so alternative recombination processes can compete. A dominant termination step was not identified by Frenklach, et al.

Performing a steady-state analysis on the reactions in Table 1 leads to

$$-\frac{d[C_2H_2]}{dt} = 2k_{3A}\left(\frac{k_{1a}}{k_4}\right)^{1/2}[C_2H_2]^2 + 2k_{1a}[C_2H_2]^2. \qquad \text{(Eq. A)}$$

in agreement with the often quoted experimental observation of second-order decomposition kinetics. Assuming a long chain, the second term in Eq. A can be ignored and the overall activation energy is $E_{ov} = E_{3A} + (E_{1a} - E_4)/2$. Assuming E_{3A} = 4, E_4 = 0 kcal/mol and taking E_{1a} = 68 (in accord with the reaction endothermicity), then E_{ov} = 38 kcal/mol, which agrees with measured values. Substitution of 46 kcal/mol (the previously used value of E_1) for E_{1a} gives a steady-state E_{ov} of 27 kcal/mol, substantially lower than experimental results.

Despite the attractiveness of the "updated" E_{1a}, our attempts to model experimental results of Munson and Anderson [15] were not fully satisfying. The mechanism and rate constants adopted were similar to those used by Colket [16]. Principal differences included values of two rate con-

stants

$$k_{1a}^{high} = 6 \times 10^{14} e^{(-68\ kcal/mol/RT)} cm^3\ mol^{-1}\ sec^{-1}$$

and

$$k_4 = 2 \times 10^{12} cm^3\ mol^{-1}\ sec^{-1}.$$

The first expression is denoted k_{1a}^{high} because it is higher than the maximum value one would expect. The A-factor is obviously much too high for a bimolecular initiation of this type. The value of k_4, for vinyl-vinyl recombination, is more than five times lower than that typically used for this reaction. Thus, despite reasonable agreement of experimental acetylene decay and product formation with the model, these results must be viewed with caution.

INDICATIONS OF ACETONE INITIATION

With concern about the above results and yet with the evidence for the existence of a chain, possible initiation steps were reexamined. Of the likely possibilities

$$C_2H_2 \rightarrow C_2H + H - 128\ kcal\ mol^{-1},$$

$$C_2H_2 + C_2H_2 \rightarrow C_2H + C_2H_3 - 87\ kcal\ mol^{-1},$$

$$C_2H_2 + C_2H_2 \rightarrow i\text{-}C_4H_3 + H - 60\ kcal\ mol^{-1},$$

only the third has a sufficiently low endothermicity, and yet it also would be expected to have a low A-factor in order to form the $H_2C\dot{C}CCH$ radical. This reaction remains a possibility and cannot be ruled out. Further consideration of the initiation problem led us to consider impurities as potential initiators. Acetone, stored in acetylene bottles as an inhibitor of self-detonation, is a well-known impurity of acetylene and coelutes from tanks in concentrations of 1%–20% that of acetylene [23]. Because the vapor pressure of acetone is about one fourth an atmosphere at room temperature and peak cylinder pressures (Matheson) are about 18 atm, nominal acetone concentrations can be estimated to be 1.3% of the value of acetylene. When precautions are taken to reduce the concentration of impurities, acetone concentrations are typically (see, for example, ref. 23) decreased to approximately 0.1% of the acetylene concentration. Assuming that a radical initiation rate of $k_{1a}^{high}[C_2H_2]^2$ is needed to produce sufficient radicals for acetylene pyrolysis, then this rate can be compared to the measured [24] rates of chain initiation by acetone

$$CH_3COCH_3 \rightarrow CH_3 + CH_3CO, \quad (5)$$

$$CH_3CO \rightarrow CH_3 + CO. \quad (6)$$

Assuming [acetone]/[C_2H_2] = 0.001, one obtains

$$\frac{k_5[\text{acetone}]}{k_{1a}[C_2H_2]^2} = 0.004 \times e^{(-4000\ cal/mol/RT)}[C_2H_2]^{-1},$$

with Szwarc and Taylor's expression [24] for k_5 ($= 2.4 \times 10^{14} \exp(-72\ kcal/mol/RT)\ sec^{-1}$). At 20% C_2H_2 and 1000 K (Munson and Anderson's conditions), this ratio is 22 while at $[C_2H_2] = 2.35 \times 10^{-5}$ mol/cm^3 and 1200 K (Ogura), the ratio is 3.2. Because this ratio is greater than 1 at both experimental conditions, radical initiation by thermal decomposition of acetone dominates over that of acetylene.

Considering that k_{1a}^{high} is substantially higher than can be expected from thermodynamic arguments and that the radical initiation rate from acetone is higher than the required rate of initiation, it seems quite reasonable to expect that acetone plays a role in the initiation process. For reference, it is instructive to examine the ratio $k_5[\text{acetone}]/k_1[C_2H_2]^2$ when k_1 is assigned the value determined by Tanzawa and Gardiner [1]. This ratio is then 0.13 and 0.12 for the same conditions cited at the end of the previous paragraph. These values, in all probability, led to early conclusions that acetone initiation contributed negligibly to acetylene pyrolysis. This difference in conclusions suggests a major difference in the values of k_1 and k_{1a} so reasons for this difference need to be examined.

The absolute value of k_1 determined by Tanzawa and Gardiner is nearly two orders of magnitude higher than the k_{1a} found in the present analysis. The principal reason for their higher value is believed to be caused by the low ΔH_f for

the C_4H_3 radical (~20 kcal/mol lower than that used for n-C_4H_3 in the present analysis). The resultant high stability of C_4H_3 radical as used in their model led to high radical concentrations and high rates of radical termination via C_4H_3 + H, the reverse of Reaction 1. This step played only a minor role in the present study; rather vinyl–vinyl recombination dominated termination. Consistent with the interpretation of high radical concentrations (predicted by the Tanzawa and Gardiner model near 1000 K) is they very low rate constant that was used for the principal chain step (Reaction 3a). At 1000 K, their rate constant, $k_{3a} = 1.6 \times 10^{13} e^{-25,100/RT}$, is three order of magnitude below that (for Reaction 3) used in the present study. Although Reaction 3 was found to be nearly equilibrated in the present study, the net rate of Reaction 3 was still more than ten time faster than Reaction 3a.

The important conclusion from this cursory analysis is that acetone decomposition is fast enough to influence the radical concentrations during acetylene pyrolysis.

ISSUES RAISED BY ACETONE INITIATION

Several critical issues must be raised if initiation by acetone contributes. First of all, a rapid mechanism for conversion of methyl radicals to H-atoms must exist; secondly, the "well-known" second-order behavior of acetylene must be addressed, specifically to see if this reaction order can be predicted and if not, why not; and thirdly, if acetone initiation dominates, then why is there such good experimental agreement (see ref. 12) on acetylene decomposition from study to study when initial concentrations of acetone can be expected to vary?

It is readily shown that methyl radicals can be rapidly converted to H-atoms. A mechanism for conversion is shown in Table 2. Rate constants were obtained from the literature where possible. The principal fate of methyl near 1000 K will be its addition to acetylene (R7). According to a recent QRRK analysis [25] the resultant adduct should stabilize under these conditions. Using rate constant (in Tables 2 and 4) and thermodynamic parameters nearly identical to those given by Dean and Westmoreland [25] (see Table 6) the rate of $CH_3\dot{C}HCH$ isomerization to allyl radical relative to its rate of decomposition to methyl acetylene and H is approximately 5. As a consequence of the stability of allyl, its decomposition is slow and principally adds to acetylene to form C_5H_7 (R9). This linear radical can then either decompose to reactants (R(−8)) or form cyclopentadiene plus atomic hydrogen (R10). Thus, methyl radicals produced from acetone decomposition will be rapidly converted to H-atoms. Since the k_5[acetone]/$k_{1a}[C_2H_2]^2$ ratios as previously calculated are significantly greater than 1, production of H-atoms via acetone decomposition appears to be sufficiently fast to initiate the thermal decomposition of acetylene.

At higher temperatures, methyl radical addition to acetylene must compete with methyl recombination (R17). The latter process can become important at high temperatures because its rate is proportional to the square of the concentration of methyl radicals and the rapid decomposition of acetone (at elevated temperatures) quickly produces high concentrations of methyl. Also, methyl can extract hydrogen from acetylene (R16), because at high temperatures thermal energy is available to overcome the substantial endothermicity (~25 kcal/mol) of this reaction. In either high-temperature case, a variety of alternative sequences will again provide H-atoms.

The order n for the overall reaction as defined by

$$-\frac{d[C_2H_2]}{dt} = k_{ov}[C_2H_2]^n$$

is often cited at 2. A steady-state analysis using reactions in Table 1 and Reactions 5–10 in Table 2 leads to

$$-\frac{d[C_2H_2]}{dt} = 2k_{3A}\left(\frac{2k_5}{k_4}\right)^{1/2}[C_2H_2][\text{acetone}]^{1/2},$$

or assuming [acetone]/$[C_2H_2]$ = 0.001, then

$$-\frac{d[C_2H_2]}{dt} = 0.09k_{3A}\left(\frac{k_5}{k_4}\right)^{1/2}[C_2H_2]^{3/2}. \qquad \text{(Eq. B)}$$

TABLE 2

Proposed Set of Reactions and Rate Coefficients for Initiation by Acetone
$\log k = \log A + n \log T - E/R/T/2.303$

	Reactions[a]	Forward rate constant[b] log A	n	E	Reverse rate constant[b] log A	n	E	Ref
5	$CH_3COCH_3 = CH_3CO + CH_3$	14.38	0.0	72.0	11.55	0.0	−5.6	24
6	$CH_3CO = CH_3 + CO$	12.48	0.0	16.7	10.68	0.0	4.6	[c]
7	$CH_3 + C_2H_2 = CH_3CHCH$	11.79	0.0	7.7	12.87	0.0	33.9	48
8	$CH_3CHCH = C_3H_5$	13.15	0.0	36.0	14.10	0.0	57.4	25
9	$C_3H_5 + C_2H_2 = C_5H_7$	12.00	0.0	8.0	13.11	0.0	20.1	est[d]
10	$C_5H_7 - c\text{-}C_5H_6 + H$	10.30	0.0	5.0	0.00	0.0	0.0	est
11	$H + C_3H_4 = CH_3CHCH$	12.76	0.0	3.1	12.52	0.0	38.2	49
12	$H + ALLENE = C_3H_5$	12.60	0.0	2.7	13.13	0.0	60.9	49
13	$2C_3H_5 = C_3H_6 + C_3H_4$	12.70	0.0	0.0	13.20	0.0	30.5	est
14	$C_3H_5 + C_2H_3 = C_5H_8$	12.70	0.0	0.0	15.62	0.0	82.5	est
15	$C_3H_5 + H = C_3H_6$	13.60	0.0	0.0	14.81	0.0	87.0	est
16	$CH_3 + C_2H_2 = CH_4 + C_2H$	12.40	0.0	35.0	13.11	0.0	15.1	est
17	$2CH_3 = C_2H_6$	14.38	−0.4	0.0	16.31	0.0	87.1	[c]
18	$2CH_3 = C_2H_5 + H$	14.90	0.0	26.5	16.92	0.0	16.3	[c]
19	$C_2H_6 + CH_3 = C_2H_5 + CH_4$	−0.26	4.0	8.3	14.71	0.0	25.1	[c]
20	$C_2H_5 = C_2H_4 + H$	13.30	0.0	39.7	12.50	0.0	1.9	[c]
21	$CH_3 + CH_3COCH_3 - CH_4 + CH_2CO + CH_3$	11.60	0.0	9.7	0.00	0.0	0.0	50
22	$H + CH_3COCH_3 - H_2 + CH_2CO + CH_3$	13.28	0.0	6.4	0.00	0.0	0.0	49
23	$C_2H_3 + CH_3COCH_3 - C_2H_4 + CH_2CO + CH_3$	12.48	0.0	6.4	0.00	0.0	0.0	est
24	$CH_2CO = CH_2 + CO$	14.00	0.0	71.0	11.65	0.0	−4.4	[e]
25	$CH_3 + H = CH_2 + H_2$	14.86	0.0	15.1	14.09	0.0	10.1	51
26	$CH_3 + CH_2 = C_2H_4 + H$	13.30	0.0	0.0	15.89	0.0	61.3	51
27	$2CH_2 = C_2H_2 + H_2$	13.30	0.0	0.0	15.65	0.0	128.7	51
28	$CH_2 + C_2H_2 = C_3H_3 + H$	12.26	0.0	0.0	13.36	0.0	11.5	[c]
29	$2C_3H_3 - C_6H_6$	12.70	0.0	0.0	0.00	0.0	0.0	est
30	$CH_2CO + H = CH_3 + CO$	12.85	0.0	3.0	11.87	0.0	37.0	[c]
31	$CH_2CO + CH_3 = C_2H_5 + CO$	12.30	0.0	3.0	13.34	0.0	26.7	est

[a] "=" represents forward and reverse directions included in model. "−" represents forward direction only included in model.
[b] Units for A: $cm^3/mol/sec$. Units for E: kcal/mol.
[c] Rate constant from ref. 29.
[d] Estimate based on thermodynamics and/or analogous reactions.
[e] Rate constant a factor of 3 lower than that reported in ref. 29.

This steady-state result that $n = 3/2$ appears to be a major drawback of the present proposal regarding initiation by acetone. A review of the literature was performed in an attempt to find references in which the reaction order was determined or which provide data from which the order could be computed. A summary of reaction orders is presented in Table 3. Although there is substantial variation in the reaction order, most values fall in the range of 1.5-2.0. The low-temperature data from Silcocks [26] as well as the flow reactor data from Palmer and Dormish [27] were originally interpreted assuming simultaneous homogeneous and heterogeneous processes. Silcocks found the reaction orders to be 2 and 1, respectively, whereas Palmer and Dormish found that this assumption was consistent with their data. An attempt has been made to reinterpret the latter experiments, with a resultant overall order ranging from 1.2 to 1.7. Munson and Anderson's low-

TABLE 3

Experimental Overall Reaction Orders

	Apparatus	Temp (K)	Order (n)
Silcocks [26]	static reactor	625–745	1(het.), 2(hom.)
Cullis and Franklin [28]	static reactor	983	2
Munson and Anderson [15]	flow reactor	873, 923 973–1073	1.7 ± 0.2 1.5 ± 0.1
Palmer and Dormish [27]	flow reactor	1333–1528	1(het.), 2(hom.) [1.2 to 1.7][a]
Ogura [3]	SPST	1000–1670	(~2.3)
Colket [16], this work	SPST	1100–1400	1.6 ± 0.2
Wu, Singh, and Kern [8]	shock tube	1900–2500	1.75 ± 0.2[a]
Aten and Greene [52]	shock tube	1400–2500	1.72 ± 0.1
Cundall et al. [53]	shock tube	1500–2500	1[b]
Gay et al. [54]	shock tube	1600–2400	not 2
Towell and Martin [55]	flow reactor	1220–1400	1.5[b]

[a] Evaluated in present study.
[b] Overall order for formation of products.

temperature experiments [15] exhibit significant scatter in plots of log(rate) vs. log[C_2H_2] but the order appears to be 1.7 ± 0.2. Their higher temperature experiments clearly give n = 1.5 ± 0.1. The results from Colket [16] of n = 1.6 ± 0.2 are from comparison of single-pulse shock tube experiments at 4.9% (unpublished), 3.5% (ref. 11), and 0.2% acetylene (unpublished). The order obtained by Ogura [3] is substantially higher than from other experiments. Results from Cullis and Franklin [28] at 983 K give beautiful agreement with the assumption of a second-order reaction. If indeed a chain mechanism controls the reaction, however, then Cullis and Franklin's data need reinterpretation. They pyrolized pure acetylene at total pressures ranging from 96 to 402 torr. Under these conditions, some critical reactions, particularly H + $C_2H_2 \rightarrow C_2H_3$, can be expected to exhibit pressure dependence (see Warnatz [29]) and will lead to a net decrease in overall reaction rate with decreasing pressure. If pressure dependence is included, a preliminary analysis indicates that Cullis and Franklin's data are no longer inconsistent with the assumption of an overall reaction order of 1.5. Results from other authors listed in Table 3 do not support the "well-known" reaction order of 2.

Thus, with the exception of the very-low-temperature data of Silcocks and the value from Ogura, the assumption of an overall reaction order of 1.5 as suggested by acetone initiation is not unreasonable. In fact, the experimental data seem to support a value of 1.5 as well as or perhaps better than the order of 2.

If acetone is the initiator, then why should experiments performed in many different laboratories, presumably with different initial acetone concentrations, all result in similar overall rate constants? This is a question that we could only partially address. A variety of purification techniques have been used. Often the level of impurities was not determined or not determined with sufficient accuracy. Based on our own experience, the work of Hamins et al [23], and reported purity levels, we estimate that typical purified samples of acetylene contain about 0.1% acetone, with a total range of 0.05% to 0.2%. This variation of a factor of 4 leads to a factor of two variation in overall

decomposition rates (because of the half-order dependence on acetone concentration) and is within the measured experimental uncertainty.

DEVELOPMENT OF KINETIC MODEL

The kinetic model used in this analysis is based on (1) the initiation sequence as indicated in Table 2 largely using published rate constants and (2) an acetylene pyrolysis model as refined by Colket [16] to describe results obtained in a single-pulse shock tube. Model results (using a program based on CHEMKIN [30], LSODE [31], and isothermal, isobaric assumptions) were compared with the flow reactor data of Munson and Anderson [15]. The mechanism and rate constants used to model the flow reactor data are shown in Tables 2 and 4. Bimolecular initiation by acetylene (R1) was included in the model using a rate constant that can be expected to be an upper limit. In the modeling of the Munson and Anderson data, this reaction always had a negligible role. Alternatively, Reaction 1b was not included. Assuming $k_{1b} = 10^{12}e^{-60,000/RT}$, this reaction could be a few times faster than Reaction 1a at 1000 K. Nevertheless this step still plays a negligible role in radical initiation, because $k_{1b}[C_2H_2]^2 \ll k_5[CH_3COCH_3]$ even with acetone one-thousandth the concentration of acetylene. With $E_{1b} = 54$ kcal, consistent with Bittner's thermodynamics for i-C_4H_3, the rate of Reaction 1b is still an order of magnitude less than that of Reaction R5.

A few rate expressions have been adjusted in order to provide better fits to the flow reactor data. Selection of rate constants for modification was accomplished using a combination of a reaction pathway analysis (with computer programs developed at UTRC) and a sensitivity analysis using CHEMSEN [32]. For each rate expression modified, attempts were made to maintain consistency with the SPST modeling results [16] by adjusting both the A-factor and the activation energy. In most cases this was possible because the flow reactor data were most dependent on kinetics over the range 900–1000 K, whereas for the SPST results the range was 1200–1500 K. In the case of the competitive sinks for the n-C_4H_5 radical,

$$n\text{-}C_4H_5 \leftrightarrow H + C_4H_4, \quad (32)$$

$$n\text{-}C_4H_5 + C_2H_2 \rightarrow C_6H_6 + H, \quad (33)$$

this was not possible, but an attempt was made instead to maintain the ratio of rate constants as determined in modeling the SPST data. Reaction 33 has been simplified from the previous three-step reversible sequence involving intermediate formation of l-C_6H_7 and c-C_6H_7, since a QRRK analysis by Westmoreland [33] indicates that at the conditions of the present study the reaction rapidly proceeds as

$$C_2H_2 + n\text{-}C_4H_5 \rightarrow l\text{-}C_6H_7^* \rightarrow c\text{-}C_6H_7^* \rightarrow C_6H_6 + H.$$

Modeling results near 1000 K using the irreversible one-step or the three-step reversible sequence were virtually indistinguishable.

Other differences between the present and previous [16] model include rate expressions for H-atom extraction by phenyl or vinyl from vinylacetylene. These were equated to the expression for vinyl plus 1,3-butadiene suggested by Kiefer et al. [34]. Model results showed little sensitivity to rate constants for these reactions. Vinyl–vinyl recombination (R4) was taken to be 2×10^{13} cm^3/mol/sec based on a fit to the Munson and Anderson data. Rate constants for other alkyl radical terminations were assumed to be equal. The selected value was 5×10^{12} cm^3/mol/sec. After Frenklach et al. [5], the two isomers, n-C_4H_3 and i-C_4H_3, were included; however, there is no ready sink for i-C_4H_3 at the low temperatures of the Munson and Anderson study. To resolve this problem, two reactions were included:

$$n\text{-}C_4H_3 \leftrightarrow i\text{-}C_4H_3, \quad (61)$$

$$i\text{-}C_4\dot{H}_3 + C_4H_4 \rightarrow C_8H_6 + H. \quad (66)$$

The first of these was found to be negligible near 1000 K. The second was the dominant sink for i-C_4H_3 while affecting phenylacetylene slightly. The first reaction was assigned a rate constant similar to a value [35] for the i-$C_3H_7 \leftrightarrow$ n-C_3H_7 isomerization, although a barrier close to the strain energy in cyclopropene was assumed. The resultant activation energy, $E_{61} = 53$ kcal/mol, is rather high (especially if tunneling occurs, as in the case of the vinylidene–acetylene isomerization) so we tested our mechanism with a much

TABLE 4

Proposed Set of Reactions and Rate Coefficients for Acetylene Pyrolysis at Low and Intermediate Temperatures
$\log k = \log A + n \log T - E/R/T/2.303$[a]

		Forward rate constant[b]			Reverse rate constant[b]			
	Reactions[a]	log A	n	E	log A	n	E	Ref
1	$2C_2H_2 = n\text{-}C_4H_3 + H$	13.00	0.0	67.0	12.48	0.0	−2.0	est[c]
2	$H + C_2H_2 = C_2H_3$	12.74	0.0	2.5	13.01	0.0	43.7	56
3	$C_2H_3 + C_2H_2 = n\text{-}C_4H_5$	12.04	0.0	4.0	13.88	0.0	38.4	16
4	$2C_2H_3 = C_4H_6$	13.30	0.0	0.0	16.71	0.0	101.1	pw[d]
32	$n\text{-}C_4H_5 = C_4H_4 + H$	14.20	0.0	41.4	13.60	0.0	3.0	pw
33	$n\text{-}C_4H_5 + C_2H_2 - C_6H_6 + H$	12.65	0.0	10.0	0.00	0.0	0.0	pw
34	$C_2H_3 + C_4H_4 - C_6H_6 + H$	11.60	0.0	0.0	0.00	0.0	0.0	[e]
35	$C_4H_4 + n\text{-}C_4H_5 - C_8H_8 + H$	13.08	0.0	5.0	0.00	0.0	0.0	pw
36	$C_8H_8 + H = C_8H_7 + H_2$	14.60	0.0	7.0	13.65	0.0	12.0	16
37	$C_8H_7 = C_8H_6 + H$	12.85	0.0	45.0	12.95	0.0	0.7	est
38	$C_2H_4 + C_6H_5 = C_8H_8 + H$	11.27	0.0	2.1	12.38	0.0	1.6	[f]
39	$C_6H_6 + H = C_6H_5 + H_2$	14.40	0.0	16.0	12.69	0.0	9.8	29
40	$C_2H_2 + C_6H_5 = C_8H_6 + H$	12.00	0.0	4.0	13.88	0.0	6 0	[e]
41	$C_2H_3 + C_4H_4 = C_2H_4 + n\text{-}C_4H_3$	13.30	0.0	14.5	13.23	0.0	13.4	34
42	$C_4H_4 + C_6H_5 = C_6H_6 + n\text{-}C_4H_3$	13.30	0.0	14.5	13.60	0.0	18.9	34
43	$l\text{-}C_6H_5 = n\text{-}C_4H_3 + C_2H_2$	14.00	0.0	36.0	11.69	0.0	1.0	16
44	$C_6H_5 = l\text{-}C_6H_5$	13.54	0.0	65.0	9.91	0.0	1.1	16
45	$C_2H_3 + C_6H_6 = C_2H_4 + C_6H_5$	13.30	0.0	14.5	12.94	0.0	9.1	[g]
46	$C_2H_3 + H = C_2H_4$	13.60	0.0	0.0	15.55	0.0	105.1	est
47	$C_2H_4 + H = C_2H_3 + H_2$	14.84	0.0	14.5	13.49	0.0	13.8	29
48	$C_2H_3 + H = H_2 + C_2H_2$	13.00	0.0	0.0	13.34	0.0	63.1	29
49	$C_4H_4 + H = n\text{-}C_4H_3 + H_2$	13.90	0.0	14.5	12.49	0.0	12.7	29
50	$C_6H_6 = C_6H_5 + H$	15.70	0.0	107.9	13.39	0 0	−2.6	57
51	$C_6H_5 + C_6H_6 = C_{12}H_{10} + H$	11.80	0.0	11.0	13.04	0.0	8.7	[e]
52	$2n\text{-}C_4H_5 = C_8H_{10}$	12.70	0.0	0.0	16.92	0.0	106.9	est
53	$n\text{-}C_4H_5 + H = C_4H_6$	13.60	0.0	0.0	15.44	0.0	107.9	est
54	$n\text{-}C_4H_5 + C_2H_3 = C_6H_8$	12.70	0.0	0.0	16.33	0.0	104.0	est
55	$C_4H_6 + H = n\text{-}C_4H_5 + H_2$	14.00	0.0	14.5	12.76	0.0	10.9	34
56	$C_4H_6 + C_2H_3 = n\text{-}C_4H_5 + C_2H_4$	13.30	0.0	14.5	13.41	0.0	11.7	[g]
57	$C_6H_5 + C_2H_3 = C_8H_8$	12.70	0.0	0.0	15.76	0.0	104.5	est
58	$i\text{-}C_4H_3 + H_2 = C_2H_2 + C_2H_3$	10.70	0.0	20.0	10.58	0.0	17.8	16
59	$i\text{-}C_4H_3 = C_4H_2 + H$	12.00	0.0	49.0	12.05	0.0	0.6	16
60	$n\text{-}C_4H_3 = C_4H_2 + H$	12.60	0.0	40.0	12.95	0.0	−0.4	16
61	$n\text{-}C_4H_3 = i\text{-}C_4H_3$	13.00	0.0	53.0	13.30	0.0	61.0	est
62	$i\text{-}C_4H_3 + H = C_4H_2 + H_2$	13.00	0.0	0 0	13.65	0.0	56.0	16
63	$C_4H_4 + H = i\text{-}C_4H_3 + H_2$	14.49	0.0	14.5	13.38	0.0	20.7	16
64	$C_6H_5 + C_4H_4 = C_6H_6 + i\text{-}C_4H_3$	13.30	0.0	14.5	13.90	0.0	26.9	[g]
65	$C_2H_3 + C_4H_4 = C_2H_4 + i\text{-}C_4H_3$	13.30	0.0	14.5	13.54	0.0	21.4	[g]
66	$C_4H_4 + i\text{-}C_4H_3 - C_8H_6 + H$	11.60	0.0	0.0	0.00	0.0	0.0	est
67	$H_2 + M = 2H + M$	12.35	−0.5	92.5	9.98	0.0	−13.1	29

[a] "=" represents forward and reverse directions included in model, "−" represents forward direction only included in model.

[b] Units for A: cm^3/mol/sec. Units for E: kcal/mol.

[c] Estimate based on thermodynamics and/or analogous reactions.

[d] Rate evaluated from present work.

[e] See citations in ref. 16. (Reverse rate constants may differ slightly due to differences in the thermodynamics and the temperature range of the fit for the reverse rate.)

[f] Rate constant half of that cited in ref. 16.

[g] See text.

lower activation energy of 5 kcal/mol. Virtually no change was observed in the computations for the Munson and Anderson conditions. Despite the insensitivity of our calculations to this rate constant, we retain the high E_{61} because the isomerization process is more likely analogous to the rearrangement of the vinylidene-acetylene anions (because of the unpaired electron). Calculations [22] for the latter process indicate a barrier of 45-50 kcal/mol in qualitative agreement with the first estimate for E_{61}. Reaction 66 has been proposed [36] as an alternative mechanism for forming phenylacetylene. It is a multistep process requiring a 1,4 H-atom shift, cyclization, and loss of an H-atom and was assigned a rate expression identical to that of Reaction 4 which requires a similar transformation. Neglecting the back reaction is justified since the reverse process is slow at these temperatures. A QRRK analysis [37] has been performed for Reaction 66 and indicates that near 1000 K approximately 50% of the C_4H_4 + i-C_4H_3 adducts will go directly to products prior to stabilization to intermediates. Therefore elimination of the intermediate steps is reasonable.

A third possible sink for i-C_4H_3 not included in the modeling is the addition of i-C_4H_3 to acetylene, cyclization to form a five-membered ring and then isomerization to phenyl.

Third-body effects have been assumed to be small for this analysis. The greatest deviation from this assumption will occur for the H-atom addition to acetylene. Fall-off curves given by Warnatz [29] indicate that the k/k_∞ for this reaction is approximately 0.5 at 1 atm of argon and 1000 K. In the present study, 20% of the gas is acetylene, a more efficient third body, suggesting the k/k_∞ is larger than 0.5; therefore, neglecting pressure effects is believed to result in only a small error. A reduction of k_2 by a factor of two results in a reduction of the overall decomposition rate of about 5%-10%.

Some modeling was also performed for comparison to shock tube results. For these calculations, the kinetic mechanism was expanded to include ethynyl and related radicals (Table 5).

Thermodynamic values are reported in Table 6 and are the same as those used previously [16], except for those of the C_4H_3 isomers, phenyl radical and the C_8-species, which were obtained from Stein [6]. The latter are identical to those used in the study by Frenklach et al. [5].

KINETIC MODEL VS. THEORY

In Figs. 2-5, calculations of acetylene, benzene, vinylacetylene, and ethene yields are compared to experimental profiles as measured by Munson and Anderson [15] in a flow reactor. For these calculations it was assumed that the acetone-acetylene ratio was 0.001. Overall the agreement is quite satisfactory. Benzene is overpredicted at long times for the highest temperature run, presumably because of the conversion of benzene to higher-molecular-weight species. Vinylacetylene is underpredicted at the low temperatures. Hydrogen, not shown, is underpredicted by about a factor of 5-10. Although substantial methane formation was observed, a model for methane formation was not included. Methane produced from methyl directly or via odd-carbon species derived from acetone could only account for a very small portion of the methane observed. Heterogeneous catalysis seem the most likely source of methane although gas-phase reactions are possible. For example, consider addition of the i-C_4H_5 radical ($H_2CCHCCH_2$) to acetylene followed by cyclization to a five-membered ring and isomerization to methylcyclopentadienyl. Subsequent reactions involving methylcyclopentadienyl may then form methyl radicals and/or methane. The i-C_4H_5 radical is generally ignored in kinetic modeling but may play a significant role because it should be formed readily via H-addition to vinylacetylene.

The formation of polyaromatic hydrocarbons is not included in the present model. When reactions including the formation of species up to and including pyrene are added to the reactions in Tables 2 and 4, computed results for acetylene, benzene, and vinylacetylene fit the experimental data almost perfectly for the Munson and Anderson data of 1073 K. There is relatively little change to the model predictions for the lower temperature runs. Reactions involving the high-molecular-weight species are similar to those proposed by Frenklach et al. [5]. Specific reac-

TABLE 5

Proposed Set of Reactions and Rate Coefficients for High-Temperature Acetylene Pyrolysis
$\log k = \log A + n \log T - E/R/T/2.303$

	Reactions[a]	Forward Rate Constant[b] log A	n	E	Reverse Rate Constant log A	n	E	Ref
68	$C_2H_2 + M = C_2H + H + M$	16.62	0.0	107.0	15.21	0.0	−18.2	[c]
69	$C_2H + C_4H_4 = C_2H_2 + i\text{-}C_4H_3$	13.60	0.0	0.0	13.29	0.0	27.0	[c]
70	$n\text{-}C_4H_3 = C_2H_2 + C_2H$	14.30	0.0	57.0	13.42	0.0	0.8	16
71	$n\text{-}C_4H_3 + H = C_4H_2 + H_2$	12.00	0.0	0.0	12.95	0.0	64.0	16
72	$i\text{-}C_4H_3 + H = C_4H_4$	13.78	0.0	0.0	15.49	0.0	98.2	est
73	$C_2H + H_2 = H + C_2H_2$	12.85	0.0	0.0	13.65	0.0	20.8	[c]
74	$C_2H + C_2H_2 = C_4H_2 + H$	13.60	0.0	0.0	14.84	0.0	15.8	[c]
75	$C_4H_2 = C_4H + H$	14.89	0.0	120.0	13.25	0.0	1.9	[c]
76	$C_2H + C_4H_2 = C_6H_2 + H$	13.60	0.0	0.0	15.04	0.0	15.5	[c]
77	$C_4H + C_2H_2 = C_6H_2 + H$	13.30	0.0	0.0	14.97	0.0	8.5	16
78	$C_6H_2 = C_6H + H$	14.89	0.0	120.0	13.02	0.0	5.2	[c]
79	$C_4H + H_2 = H + C_4H_2$	13.30	0.0	0.0	14.34	0.0	13.8	[c]
80	$C_6H + H_2 = H + C_6H_2$	13.30	0.0	0.0	14.56	0.0	10.5	[c]
81	$C_2H + C_6H_6 = C_6H_5 + C_2H_2$	13.30	0.0	0.0	12.40	0.0	14.7	[c]
82	$C_4H + C_6H_6 = C_6H_5 + C_4H_2$	13.30	0.0	0.0	12.63	0.0	7.6	[c]
83	$C_2H_3 + C_4H_2 = C_4H_4 + C_2H$	13.48	0.0	23.0	13.47	0.0	3.1	16
84	$C_4H_4 = C_2H + C_2H_3$	16.00	0.0	105.0	13.37	0.0	−16.2	16

[a] "=" represents forward and reverse directions included in model.

[b] Units for A: $cm^3/mol/sec$. Units for E: kcal/mol.

[c] See citations in ref. 16. (Reverse rate constants may differ slightly due to differences in the thermodynamics and the temperature range of the fit for the reverse rate.)

[d] Estimate based on thermodynamics and/or analogous reactions.

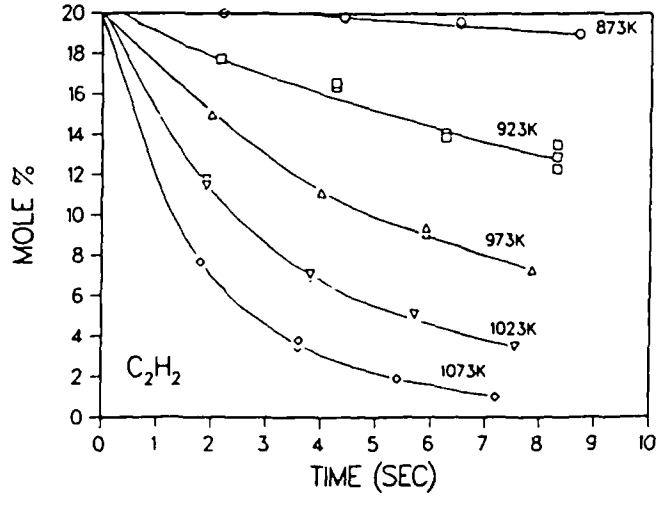

Fig. 2. Comparison of data and model predictions of acetylene decay. Symbols and solid lines are data and best fits from Munson and Anderson (ref. 15). Dotted lines are model predictions from the present study where 1000 ppm acetone in acetylene is assumed.

TABLE 6

Selected Thermodynamics at 300 K[a]

Symbol	Name/structure	S° eu	ΔH_f kcal/mol
$C_{12}H_{10}$	biphenyl	93.6	43.6
C_8H_{10}	octatetraene	90.4	53.2
C_8H_8	styrene	82.6	35.3
C_8H_7	$C_6H_5\dot{C}CH_2$	83.8	83.2
C_8H_6	phenylacetylene	76.4	75.2
C_6H_8	hexatriene	79.4	39.6
C_6H_6	benzene	65.2	19.8
C_6H_5	phenyl	69.1	78.2
C_6H_2	triacetylene	71.1	169.7
C_6H	C_6H	74.3	233.2
C_4H_6	1,3-butadiene	66.6	26.1
n-C_4H_5	$H_2CHCH\dot{C}H$	69.1	82.5
C_4H_4	vinylacetylene	66.1	69.4
i-C_4H_3	$HCC\dot{C}CH_2$	68.1	116.1
n-C_4H_3	$HCCCH\dot{C}H$	69.4	124.1
C_4H_2	diacetylene	59.9	111.7
C_4H	C_4H	62.8	179.0
C_2H_3	vinyl	54.5	65.7
C_2H	ethynyl	49.6	128.5
C_5H_8	1,4-pentadiene	76.6	18.7
C_5H_7	1,4-pentadien-1-yl	79.3	78.2
c-C_5H_6	cyclopentadiene	64.6	32.0
CH_3CO	acetyl	62.0	−6.0
C_2H_5	ethyl	54.6	26.4
CH_3CHCH	$CH_3CH\dot{C}H$	67.5	61.6
C_3H_5	allyl	62.1	39.4
C_3H_4	methylacetylene	59.3	44.4
C_3H_3	propargyl	60.0	81.5
CH_2	methylene	46.4	92.4
CH_2CO	ketene	57.8	−12.4

[a] Thermodynamics of species not listed in this table are essentially identical to those listed in ref. 35.

tions and rate constants have been recently described [36].

Model calculations have also been compared to data obtained in a single-pulse shock tube by Colket [16] at 3.5% and 4.9% acetylene in 5 and 8 atm of argon, respectively. Experimental procedures for the unpublished 4.9% data were similar to those previously described [16]. The acetone concentrations were equated to the measured values, that is, 0.1% and 0.2% the concentration of acetylene for the 3.5% and 4.9% data, respectively. Calculations were performed using a shock tube code modified to account for quenching processes. Again satisfactory agreement (comparable to that achieved in ref. 16) is obtained for most species, including the minor products, styrene and ethylene. The main descrepancy is that the model underpredicts product formation at low temperatures. Of particular interest is Fig. 6, in which only odd-carbon products derivable from the impurity acetone are shown for the 4.9% series of runs. Also plotted is the sum of the concentrations of acetone plus half of all species containing an odd number of carbons. Acetone produces two methyl radicals, each of which could produce an odd-carbon species. The fact that this sum is essentially constant over the range of temperature of experiments lends strong support to a major thesis of this work, namely that acetone produces methyl radicals that convert to H-atoms via addition to acetylene, whereas ethane formation via methyl recombination is small compared to methyl addition to acetylene. Model predictions are not shown in Fig. 6 because prediction of the odd-carbon products is generally poor. This limitation is probably a direct result of the fact that there are very little experimental data on these species, and many of the rate constants in Table 2 were estimated.

Ogura also obtained single-pulse shock tube data at 5% acetylene in about two atmospheres of argon. Model predictions are compared to the Ogura [3] data in Fig. 7 for vinylacetylene, diacetylene, and hydrogen. Again comparison between experiments and theory seem quite satisfactory. For the model calculations, dwell times of 1 msec were assumed and quenching rates comparable to those measured by Colket [16] were used. The acetone–acetylene ratio was assumed to be 0.001. Attempts to fit Ogura's experimental profiles of methane, methylacetylene, allene, and ethylene for experiments with 10% acetylene in argon were also made. The agreement was good for methane and satisfactory for ethylene except at low temperatures when the model significantly underpredicted the experimental data. The model overpredicts the C_3-hydrocarbons by about a factor of two to three. This difference does not seem unreasonable considering the general lack of knowledge regarding pyrolysis of odd-carbon, acetylenic species.

ACETONE-INITIATED PYROLYSIS OF C_2H_2

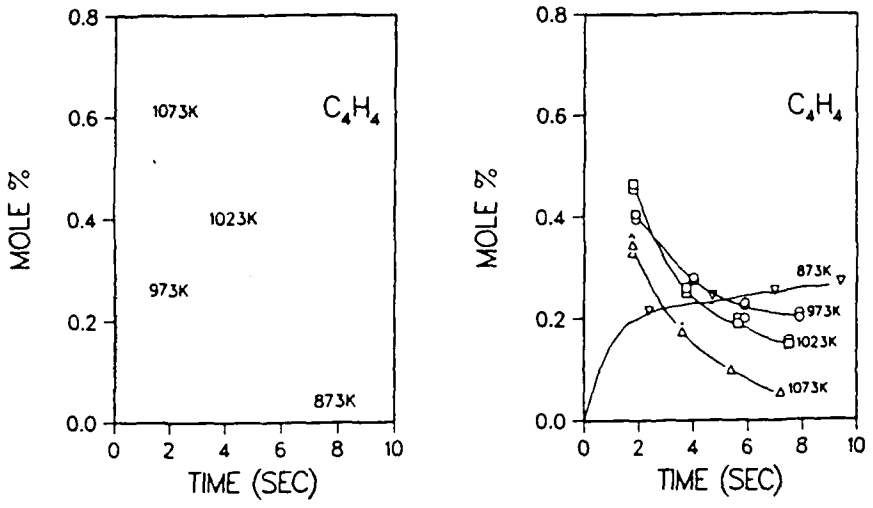

Fig. 3. Comparison of data and model predictions of vinylacetylene formation and decay. (See caption of Fig. 2.)

VINYLIDENE VS. CHAIN

Perhaps the most significant pieces of experimental evidence against a radical chain-mechanism are the results by Hou and Anderson [38] and more recently by Duran et al. [10]. The earlier study involved a molecular-beam, mass-spectrometric analysis of acetylene pyrolysis products from a flow reactor near 1000 K. The usefulness of their facility was "proved" by its ability to detect methyl radicals during pyrolysis of tetramethyl lead and di-t-butylperoxide. They detected no radicals during acetylene pyrolysis. Calculations for their experimental conditions indicate that during acetylene pyrolysis the total radical concentrations were always substantially less than one part per million. It appears unlikely that their facility had the sensitivity to observe species at such low concentrations, whereas methyl radicals readily produced from the test compounds would be expected to achieve substantial concentrations. We think that these early experiments do not disprove a radical chain mechanism.

Recent pyrolysis experiments by Duran et al.

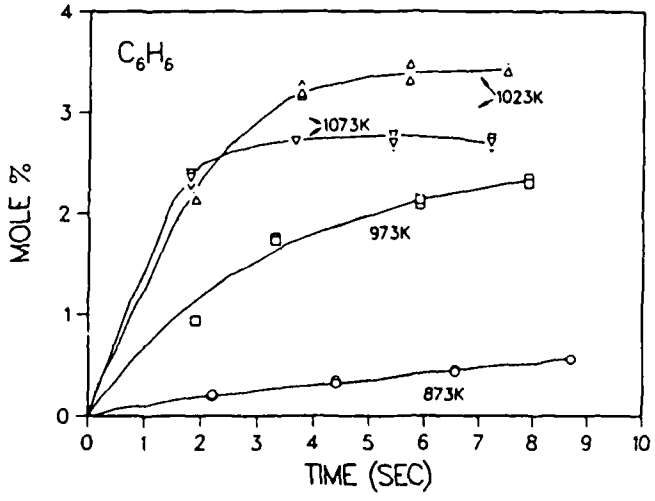

Fig. 4. Comparison of data and model predictions of benzene formation. (See caption of Fig. 2.)

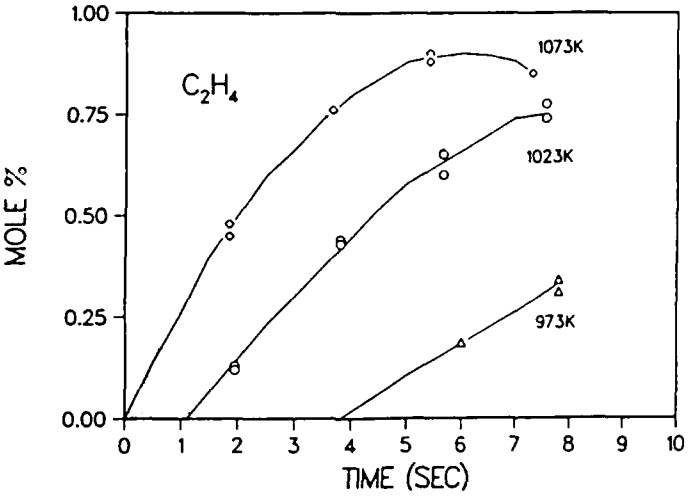

Fig. 5. Comparison of data and model predictions of ethylene formation. (See caption of Fig. 2.)

[10] were also performed in a flow reactor with mass spectrometric analysis. Additions of benzene and toluene showed, respectively, no inhibition and an acceleration. The acceleration, unexplained by the vinylidene mechanism, is easily explained via chain processes since initiation via toluene ($C_7H_8 \rightarrow C_7H_7 + H$) using any of the recently proposed rate expressions (see refs. 39 and 40 and citations contained therein) can be shown to be substantially faster than initiation by acetone. In addition, Duran et al. observed a variety of vinylbenzenes when benzene and acetylene were copyrolyzed. They interpreted these results as evidence for insertion of the carbene (vinylidene) into the benzene ring. Alternatively, these vinylbenzenes may also be the result of the displacement ($C_2H_3 + C_6H_6 \rightarrow H + C_6H_5C_2H_3$), which is similar to the known [41] methyl-substitution in the benzene-toluene system. Copyrolysis of toluene and acetylene produced principally a species at mass 118, interpreted to be methyl styrene. Instead this species may be phenylpropene formed

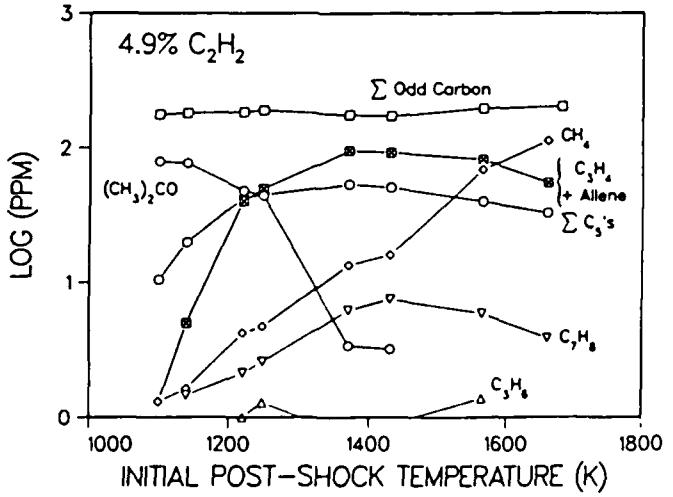

Fig. 6. Single-pulse shock tube data for 4.9% acetylene, 100 ppm acetone in 8 atm of argon. Only odd-carbon species are shown including acetone, allene plus methyl acetylene, four C_3-species (one of two dominant peaks idendified as cylcopentadiene), and toluene Top line is molar sum of the acetone concentration and one-half of all the odd-carbon species.

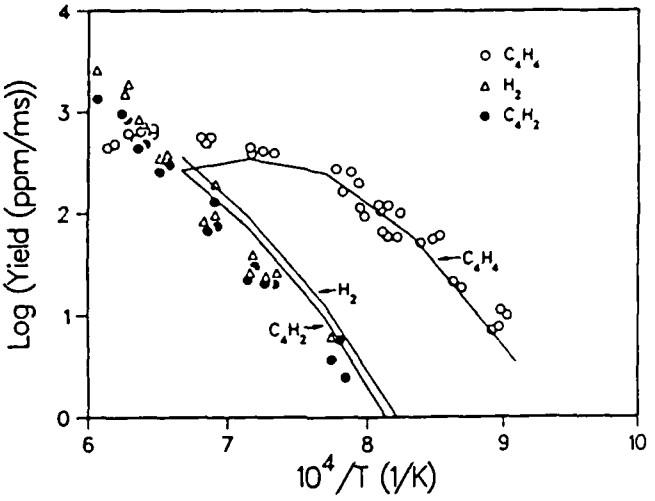

Fig. 7. Comparison of data and model for vinylacetylene, diacetylene, and hydrogen for pyrolysis of 5% acetylene. Single-pulse shock tube data is from Ogura (ref. 3). Solid lines are model predictions assuming 1000 ppm acetone in the acetylene.

by acetylene addition to the stable benzyl radical. Consequently, we question their conclusion of proof for the vinylidene mechanism.

OVERALL REACTION ORDER AND ACTIVATION ENERGY

Reaction order was determined from model predictions by varying the initial concentration (while holding temperature constant at 973 K). Plots of $\log(d[C_2H_2]/dt)_0$ vs. $\log[C_2H_2]_0$ yielded an overall reaction order of 1.43 ± 0.10. The initial rate $d[C_2H_2]/dt]_0$ was taken to be the value immediately after a short induction period (~0.2 sec at 20% acetylene, 873 K). Reaction orders were also determined from plots of predicted $\log(d[C_2H_2]/dt)$ vs. $[C_2H_2]$ as a function of time over the temperature range 873–1073 K. These calculations resulted in a reaction order of 1.43, 1.66, and 1.67 at 973, 1023, and 1073 K, respectively. These values are consistent with the overall order of 1.5 obtained from the steady-state analysis. Assuming this latter value, an overall rate expression was determined using the model prediction for Munson and Anderson's conditions. The rate expression determined was

$$\left.\frac{d[C_2H_2]}{dt}\right)_{ov} = k_{ov}[C_2H_2]^{1.5},$$

where

$$k_{ov} = 10^{11} e^{-40.6\ \text{kcal/mol/RT}} (\text{cm}^3/\text{mol})^{1/2}\ \text{sec}^{-1}$$

at 873–1073 K. This expression can be compared to that obtained from the simplified steady-state expression (sss), Eq. B. Equating k_{3A} to k_3 and using other rates from Tables 2 and 4, this simplified expression becomes

$$\left.\frac{d[C_2H_2]}{dt}\right)_{ov}^{sss} = k_{ov}^{sss}[C_2H_2]^{1.5},$$

where

$$k_{ov}^{sss} = 3.4 \times 10^{11} e^{-40\ \text{kcal/mol/RT}} (\text{cm}^3/\text{mol})^{1/2}\ \text{sec}^{-1}.$$

The lower A-factor from the detailed model is due to a combination of the reverse of R3, additional termination reactions (e.g., R54), and the fact that some acetone decomposes via a chain process rather than R5 (see reactions 21–23 in Table 2).

HIGHER TEMPERATURE MODELING

Preliminary modeling has been performed for shock tube conditions at higher temperatures. The scenario regarding initiation, termination, and the fate of acetone and methyl radicals changes

somewhat. The changes include a greater fraction of acetone decomposing via radical attack. This leads to the production of ketene which also is an effective radical initiator. The resulting sequence,

$$H + CH_3COCH_3 \leftrightarrow CH_2COCH_3 + H_2, \quad (22a)$$

$$CH_2COCH_3 \leftrightarrow CH_2CO + CH_3, \quad (22b)$$

$$CH_2CO \leftrightarrow CH_2 + CO, \quad (24)$$

$$CH_2 + C_2H_2 \leftrightarrow C_3H_3 + H, \quad (28)$$

$$C_3H_3 + C_3H_3 \leftrightarrow C_6H_6, \quad (29)$$

leads to the net production of only one methyl radical (the H-atom is regenerated) compared to the two radicals from initiation directly through acetone decomposition (Reaction 5). This sequence is very dependent on the uncertain high-temperature chemistry of methylene (CH_2) and propargyl (C_3H_3) radicals. In addition to recombination, the latter can add to acetylene to form a C_5H_5 radical whose stability is enhanced by resonance. Other potential complicating features are that some species formed as by-products of acetone decomposition, e.g., cyclopentadienes, have weak C–H bonds because of the resonantly enhanced stability of the hydrocarbon radical (in this case cyclopentadienyl). Consequently, even though acetone may be destroyed early during reaction, some of the products will continue to provide radicals and maintain the decomposition of acetylene. At high temperatures, vinyl recombination no longer dominates radical termination. Methyl radicals and radical adducts formed by addition to acetylene contribute to chain termination.

Recent time-of-flight/shock tube results have also been obtained by Wu et al. [8] at much higher temperatures. They modeled their own as well as other high temperature data using the bimolecular initiation Reaction 1b with an endothermicity of 46 kcal/mol and 102 kcal/mol for the heat of formation of i-C_4H_3, the assumed product. Alternatively, assuming an impurity of 1000 ppm acetone in the acetylene, we attempted to model the data using the reactions in Tables 2, 4, and 5. The experimental decomposition was severely underestimated. An examination of the model results indicated that methyl radicals added to acetylene to eventually form methylacetylene and/or allene (via Reactions 7, 8, 11, and 12). Inclusion of Wu and Kern's [42] reactions and rate coefficients for the thermal decomposition of C_4H_3 resulted in a closer description of the T.O.F. data. A very close match to their data was obtained by increasing the rate constant, k_7, by a factor of 3 and assuming the products of the reaction to be C_3H_4 + H. Using these revisions, acetylene decay can be predicted and is compared to experimental data in Fig. 8a for a range of temperatures. A demonstration of the effect of different assumed levels of acetone is shown in Fig. 8b for the production of diacetylene. Although a pressure dependence is expected for R5, this was not included in the calculations shown in Fig. 8. This omission is of negligible concern because acetone decomposes much faster than the time scale of the experiment and the computed results are insensitive to the value of k_5. Based on uncertainties in thermochemistry, the acetone concentration, and the revisions to Reaction 7, we believe that the good comparison between the experiment and model should be considered qualitative, but strongly suggestive of the fact that impurities also effect experiments of acetylene pyrolysis above 2000 K.

In contrast to these results, Frank and Just [43] found that "purified" and unpurified acetylene produced the same H-atom profiles at 50 ppm acetylene and 2400 K. Using our revised, high-temperature model, H-atom production was calculated assuming both 0% and 1.0% (rather than 0.1% because purification did not effect the experimental results) acetone in the acetylene. The two predicted curves were indistinguishable and matched the experimental data. However, near 2000 K they found that high-concentration runs require purification. Again this result is consistent with our calculations. In fact, our model predicts that the accelerated rate they observe for the initiation process at 1800–2000 K can be explained by the presence of small amounts of acetone (~0.1% in acetylene). The relative effects of acetone are simply explained by the low concentrations in the Frank and Just experiments as well as the amount of H-atoms produced (relative to the concentration of acetylene). The low concentra-

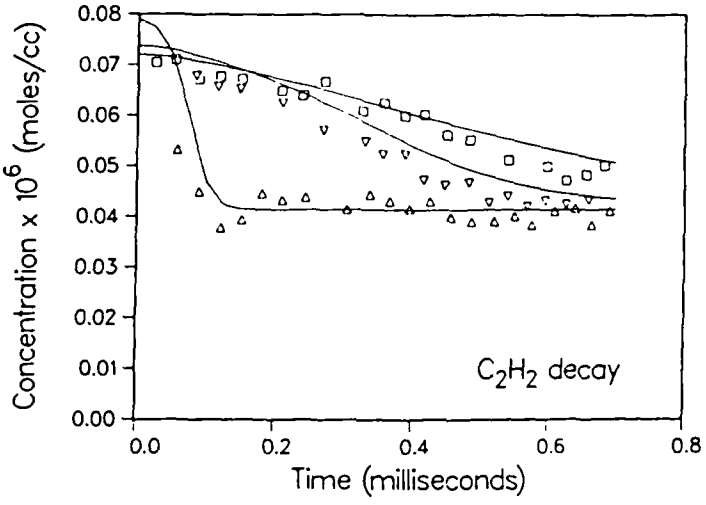

Fig. 8. a. A comparison of T.O.F./shock tube data of acetylene decay obtained by Wu, Singh, and Kern (Fig. 2 of ref. 8) with computations using a revised high-temperature mechanism (see text). An impurity of 1000 ppm acetone in the 3.2% acetylene is assumed for the calculations. Experimental data: □, 2032 K; ▽ 2147 K; △ 2534 K; —— model.

tions favor the initiation process, reaction 68, which is first order in acetylene. Furthermore, at 2420 K, the experimental results show a production of H-atoms (Fig. 3 in Ref. 43) which is approximately 10% of the initial concentration of acetylene. From 1% acetone in the acetylene, one could expect a maximum of 2% H-atoms (one H-atom from each methyl radical), much smaller than the measured value. This situation changes at 2050 K, when H-atoms were found (experimentally) to reach only 0.2% of the initial acetylene concentration. Thus under these conditions, radical production from the decomposition of impurities could perturb that from the pure pyrolysis.

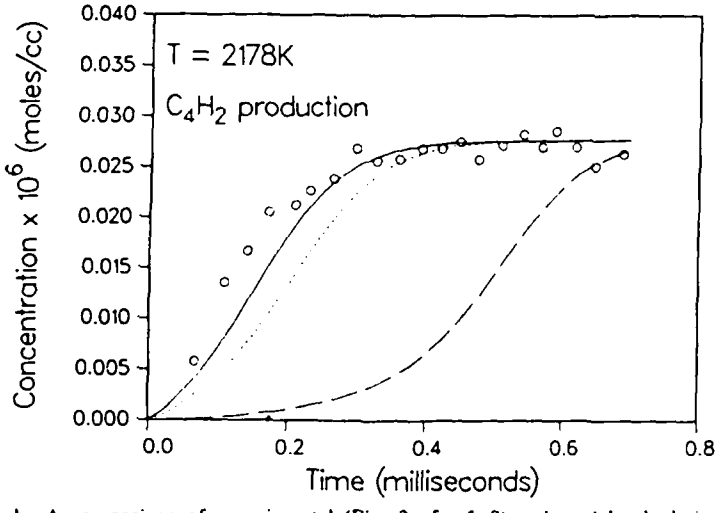

Fig. 8. b. A comparison of experimental (Fig. 3 of ref. 8) and model calculations for the production of diacetylene during the pyrolysis of 6.2% acetylene, at 2178 K, and 0.48 atmospheres. Model calculations were performed assuming 0 (-·-), 500 (---), 1000 (——), and 2000 (···) ppm acetone in the acetylene.

ALTERNATIVE INITIATION STEPS

The focus of this article has been to identify acetone as the principal initiator of radicals during the pyrolysis of acetylene near 1000 K. At higher temperatures, by-products from the acetylene–acetone system, e.g., ketene and allene–methylacetylene, contribute to initiation of radicals (see previous discussion on High-Temperature Modeling). Efforts to perform detailed modeling for this aspect of the acetylene system have been relatively minor because this is not the main point of this article, although this phenomenon can be very important depending on experimental conditions. The explanation of the contribution of these species despite their low concentrations is related to the fact that the energy required for bond cleavage in these and similar species is low (70–90 kcal/mol), especially relative to that required to break the HCC–H bond, i.e., 125–130 kcal/mol. It is also reasonable to expect that thermal decomposition of other product species, particularly olefins such as vinylacetylene and styrene, may contribute to initiation once they attain high concentrations. However, it is difficult to quantify their role in acetylene pyrolysis.

SENSITIVITY AND REACTION PATHWAY ANALYSES

A sensitivity analysis has been performed using CHEMSEN for the isobaric, isothermal conditions of Munson and Anderson. Results of these calculations are reproduced in Table 7 for 973 K after 10% decomposition for the six reactions most sensitive to the computed results for each of the five species listed in Table 7. Rate constants for several of these reactions were determined in this work. Also, a reaction pathway analysis was performed using programs developed at UTRC. Reactant decay and product formation as determined using this analysis are described below.

Acetylene was calculatd to decay principally by three reactions:

$$H + C_2H_2 \leftrightarrow C_2H_3, \tag{2}$$

$$C_2H_3 + C_2H_2 \leftrightarrow n\text{-}C_4H_5, \tag{3}$$

$$n\text{-}C_4H_5 + C_2H_2 \rightarrow C_6H_6 + H. \tag{33}$$

The net rates of the first two are essentially equal whereas the rate of the third is slower because of the decay of $n\text{-}C_4H_5$ to vinylacetylene.

TABLE 7

Normalized Sensitivity Coefficients $(dy/dk \times k/y)^a$

		C_2H_2	C_2H_4	C_4H_4	C_6H_6	H_2
2)	$H + C_2H_2 \leftrightarrow C_2H_3$	−0.014	0.06	0.13	0.09	−0.52
3)	$C_2H_3 + C_2H_2 \leftrightarrow n\text{-}C_4H_5$	−0.030	0.10	0.18	0.21	0.61
4)	$C_2H_3 + C_2H_3 \leftrightarrow C_4H_6$	0.025	−0.42	−0.11	−0.23	−0.55
5)	$CH_3COCH_3 \leftrightarrow CH_3 + CH_3CO$	−0.050	0.85	0.22	0.47	1.11
23)	$C_2H_3 + CH_3COCH_3 \rightarrow C_2H_4 + CH_2CO + CH_3$	—	0.20	−0.01	−0.01	−0.02
32)	$n\text{-}C_4H_5 \leftrightarrow C_4H_4 + H$	−0.020	0.35	0.68	−0.14	0.64
33)	$n\text{-}C_4H_5 + C_2H_2 \rightarrow C_6H_6 + H$	−0.035	0.13	−0.13	0.73	−0.04
34)	$C_2H_3 + C_4H_4 \rightarrow C_6H_6 + H$	—	−0.02	−0.12	0.10	−0.01
35)	$n\text{-}C_4H_5 + C_4H_4 \rightarrow C_8H_8 + H$	—	−0.01	−0.30	−0.10	0.54
36)	$C_6H_6 + H \leftrightarrow C_6H_7 + H_2$	—	−0.08	−0.02	−0.04	0.54
41)	$C_2H_3 + C_4H_4 \leftrightarrow C_2H_4 + n\text{-}C_4H_3$	—	0.18	—	—	—
45)	$C_2H_3 + C_6H_6 \leftrightarrow C_2H_4 + C_6H_5$	—	0.22	—	—	—

[a] As calculated by CHEMSEN at 10% decomposition of acetylene, 973 K, 20% acetylene in 1 atm of argon.

Vinylacetylene is formed almost entirely by H-atom elimination from n-C_4H_5 (Reaction 32). Its decay is due predominantly to

$$n\text{-}C_4H_5 + C_4H_4 \rightarrow C_8H_8 + H, \quad (35)$$

which in turn forms styrene, although H-atom abstraction from vinylacetylene by phenyl or vinyl (R41–42, 64–65) also contributes to vinylacetylene decay. The formation of benzene is from n-C_4H_5 addition to acetylene (R33). As the reaction proceeds, additional benzene is produced by phenyl (from R38) abstracting H-atoms from molecular hydrogen, vinylacetylene or ethene. Ethene arises mainly from H-atom attack on styrene (R38), although some is produced by abstraction of H-atoms from hydrogen and vinylacetylene by vinyl radicals (R47 and R65). According to the proposed model, which underpredicts hydrogen by a factor of 5 to 10, hydrogen is formed by H-atom attack on styrene (R36).

DISCUSSION OF RATE CONSTANTS AND UNCERTAINTIES

In order to fit the Munson and Anderson data, values of four rate constants have been modified from values previously proposed. The reactions are

$$C_2H_3 + C_2H_3 \leftrightarrow C_4H_6, \quad (4)$$

$$n\text{-}C_4H_5 \leftrightarrow C_4H_4 + H, \quad (32)$$

$$n\text{-}C_4H_5 + C_2H_2 \rightarrow C_6H_6 + H, \quad (33)$$

$$n\text{-}C_4H_5 + C_4H_4 \rightarrow C_8H_8 + H, \quad (35)$$

k_4, the rate constant for vinyl-vinyl recombination, was selected to be 2×10^{13} cm^3 mol^{-1} sec^{-1} in this work. This value although slightly high is consistent with rate coefficients for recombination of other low-molecular-weight hydrocarbons (see ref. 44). The value used here is about 50% larger then the expression suggested by Ebert et al. [45]. The rate constant for R32 was based on the thermochemcial estimate by Weissman and Benson [46] but the A-factor was increased by 60% to enhance the fit to experimental data. Equilibrium calculations give a reverse rate constant of about 8×10^{12} cm^3 mol^{-1} sec^{-1} at 1000 K. This value is about a factor of 5 higher than that used for the H + C_2H_2 reactions. Errors in the thermochemistry and possible contributions from reactions involving vinylidene may be the cause of the high rates for R32 and R(−32) as required by this analysis. At 1000 K, the rate constant for the irreversible reaction, R33, is about a factor of 4 [46], 2 [16, 33], and 1.5 [47] lower than values previously proposed. The major difference of this work is the high activation energy (10 kcal/mol) compared to other evaluations: 3.7 [47], 4.9 (from a fit to reported [33] calculations), 6.9 [46], and 9 [16]. Thus, the extrapolated value from the present work is essentially identical to other values [33, 47] near 1200–1300 K. $k_{35} = 1.1 \times 10^{13} e^{-5000/RT}$ as used in this study is substantially lower than the high value suggested by Colket [16] but is about four times larger than the value reported by Cole et al. [47]. As discussed previously, the i-C_4H_5 radical may play a role or C_4H_4–C_4H_4 reactions may contribute.

Rate constants as adjusted in this work are generally within a factor of 4 of other values recently proposed and experimental data for these reactions are extremely limited: usually, rate expressions have been estimated or determined from detailed modeling. Consequently, we believe that the evaluations of rate constants in this study are very reasonable and lend strong support for the general thesis of this article regarding the importance of acetone.

Uncertainties in the analysis include possible contributions because of reactions involving vinylidene and related species. As discussed previously, we are unable to disprove the existence of such mechanisms. The generally good agreement between the modeling (without invoking such mechanisms) and experimental data supports arguments that contributions from these reactions are negligible; instead, the chain mechanism seems to dominate in most cases. It is possible that the vinylidene mechanism contributes to vinylacetylene production at 873 K (Fig. 3) when the chain underpredicts the experimental data. Other uncertainties are related to the lack of a model for

methane formation at low temperatures. At 973 K, Munson and Anderson found that about 1.2% of the initial carbon was converted to methane. Often it is suggested that this methane formation involves heterogeneous catalysis. An alternative and speculative mechanism, described in this paper but not included in the model involves the intermediate formation of the i-C_4H_5 radical. It may be formed by H-atom addition to vinylacetylene or isomerization of the excited n-C_4H_5 radical after its formation by vinyl addition to acetylene. The formation of excited radicals via radical additions to acetylenes is another area of uncertainty in the proposed model. A limited number of QRRK [25] calculations have been performed and indicate that these effects should be included at elevated temperatures. An example is the system

$$C_2H_3 + C_2H_2 \leftrightarrow n\text{-}C_4H_5^*,$$

$$n\text{-}C_4H_5^* \leftrightarrow n\text{-}C_4H_5,$$

$$n\text{-}C_4H_5^* \leftrightarrow C_4H_4 + H,$$

$$n\text{-}C_4H_5^* \leftrightarrow i\text{-}C_4H_5,$$

but for simplicity, these effects have not been included in the present analysis.

Significant uncertainties exist in the kinetics and mechanisms related to the odd-carbon, acetylenic species. This belief is based on the facts that very little experimental data or estimates on such species exist; large uncertainties exist in the thermodynamics of the odd-carbon radicals; and predictions of profiles of odd-carbon species, although qualitative, are not quantitively accurate. Despite these drawbacks, the major conclusion of this article, that is, that acetylene pyrolysis is initiated by a small amount of acteone, should not be altered.

CONCLUSIONS

We are unable to disprove contributions of the vinylidene mechanism or the importance of the initiation Reaction 1b to acetylene decomposition. Recent thermodynamic estimates rule out Reaction 1a as an important contributor to radical initiation. Based on the analysis and detailed modeling presented in this article, we conclude that the pyrolysis of pure acetylene has not been investigated at temperatures below 2000 K. The very high C–H bond strengths in acetylene prevent a rapid initiation of radicals; instead very low concentrations of impurities are the source of radicals which initiate and sustain a chain decomposition. Acetone, a contaminant present in experimental studies of acetylene pyrolysis, has been shown via chemcial kinetic modeling to dominate radical initiation. The overall reaction rate determined both from a simple steady-state analysis and dtailed chemcial kinetic modeling has an activation energy close to 40 kcal/mol and a reaction order close to 1.5. The overall activation enery is consistent with previous experiments whereas the reaction order is lower than the usually assumed value of 2. A detailed review of the literature shows in fact minimal support for a reaction order of 2 while experiments are reasonably consistent with an order of 1.5. A few rate constants have been selected to provide a fit to the Munson and Anderson data. Values of these rate constants are in general consistent with values previously published. The modeling makes no attempt to include reactions involving the vinylidene radical. Although there is no proof against mechanisms involving this carbene, there appears now to be ample evidence in support of a chain mechanism—firstly, experimental evidence from a wide variety of sources and conditions support the presence of a chain and, secondly, a mechanism initiated by thermal decomposition of acetone adequately describes experimental results. Vinylidene-related mechanisms may contribute to acetylene pyrolysis but we believe that a chain mechanism dominates all acetylene pyrolysis above 900 K. The analysis performed in this study is consistent with previous experiments indicating that acetylene pyrolysis is much less sensitive to the presence of impurities at temperatures above 2000 K, but only at very low partial pressures of acetylene. At higher partial pressures as for the case of the data of Wu et al., modeling indicates that acetone impurities can also play a significant role.

This work has been supported in part by the Air Force Office of Scientific Research under

Contract No. F49620-85-C-0012. The authors are indebted to Dr. Julian Tishkoff, AFOSR contract monitor, for his support. We thank Prof. J. Mackie from the University of Sydney for many fruitful discussions and Prof. J. Kiefer from the Univ. of Illinois for his many challenging questions related to this research. Thanks are given to Dr. A. Dean of Exxon and Prof. J. Bozzelli of New Jersey Institute of Technology for their QRRK calculations of the $C_4H_4 + i - C_4H_3$ *system. The able assistance of G. Deske and H. Hollick in the preparation of the manuscript and figures is gratefully acknowledged.*

REFERENCES

1. Tanzawa, T., and Gardiner, W. C., Jr., *J. Phys. Chem.* 84:236 (1980).
2. Back, M. H., *Can. J. Chem.* 49:2119 (1971).
3. Ogura, H., *Bull. Chem. Soc. Jpn.* 50:1044, 2051 (1977).
4. Cowperthwaite, M., and Bauer, S. H., *J. Chem. Phys.* 36:1743 (1962).
5. Frenklach, M., Clary, D. W., Gardiner, W. C., Jr., and Stein, S., *Twentieth Symposium (International) on Combustion*. The Combustion Institute, Pittsburgh, 1985, p. 887.
6. Stein, S. E., National Bureau of Standards, Gaithersburg, MD, Personal Communication, 1987.
7. Bittner, J., A Molecular Beam Mass Spectrometer Study of Fuel-Rich and Sooting Benzene-Oxygen Flames, Ph.D. dissertation, Appendix P, Massachusetts Institute of Technology, 1981.
8. Wu, C. H., Singh, H. J., and Kern, R. D., *Int. J. Chem. Kin.* 19:975 (1987).
9. Duran, R. P., Amorebieta, V. T., and Colussi, A. J., *J. Phys. Chem.* 92:636 (1988).
10. Duran, R. P., Amorebieta, V. T., and Colussi, A. J., *J. Am. Chem. Soc.* 109:3154 (1987).
11. Kiefer, J. H., Mitchell, K. I., Kern, R. D., and Yong, J. N., *J. Phys. Chem.* (in press).
12. Palmer, H. B., and Cullis, C. F., in *Chemistry and Physics of Carbon* (P. L. Walker, Ed.). Marcel Dekker, New York, 1965, Vol. 1, p. 265.
13. Osamura, Y., Schaefer, H. F., Gray, S. K., and Miller, W. H., *J. Am. Chem. Soc.* 103:1904 (1981).
14. Callear, A. B., and Smith, G. B., *J. Phys. Chem.* 90:3229 (1986).
15. Munson, M. S. B., and Anderson, R. C., *Carbon* 1:51 (1963).
16. Colket, M. B., *Twenty-First Symposium (International) on Combustion*. The Combustion Institute, Pittsburgh, 1987, p. 851.
17. Burcat, A., in *Combustion Chemistry* (W. C. Gardiner, Jr., Ed.). Springer Verlag, New York, 1984, pp. 455-504.
18. Kee, R. J., Rupley, F. M., and Miller, J. A., The CHEMKIN Thermodynamic Data Base, Sandia Report, SAND87-8215.UC-4, April, 1987.
19. Kasai, P. H., *J. Am. Chem. Soc.* 94:5950 (1972).
20. Westmoreland, P. R., *American Chemical Society, Fuel Chemistry Preprints* 32:480 (1987)
21. Sharma, R. B., Steno, N. M., and Kosko, W. S., *Int. J. Chem. Kin.* 17:831 (1985).
22. Sakai, S. and Morokuma, K., *J. Phys. Chem.* 91:3661 (1987).
23. Hamins, A., Gordon, A. S., Saito, K., and Seshadri, K., *Combust. Sci. Technol.* 45:309 (1986).
24. Szwarc, M. and Taylor, J. W., *J. Chem. Phys.* 23:2310 (1955).
25. Dean, A. M., and Westmoreland, P. R., *Int. J. Chem. Kin.* 19:207 (1987).
26. Silcocks, C. G., *Proc. R. Soc. Lond.* A242:411 (1957).
27. Palmer, H. B., and Dormish, F. L., *J. Phys. Chem.* 68:1553 (1964).
28. Cullis, C. F., and Franklin, N. H., *Proc. R. Soc. Lond.* A280:139 (1964).
29. Warnatz, J., in *Combustion Chemistry* (W. C. Gardiner, Jr., Ed.). Springer Verlag, New York, 1984, pp. 197-360.
30. Kee, R. J., Miller, J. A., and Jefferson, T. H., CHEMKIN: A General-Purpose, Problem-Independent, Transportable, Fortran Chemical Kinetics Code Package. Sandia National Laboratories, SAND80-8003, March 1980.
31. Hindmarsh, A. C. *ACM Signum Newslett.* 15(4) (1980).
32. Kramer, M. A., Kee, R. J., and Rabitz, H., CHEMSEN: A Computer Code for Sensitivity Anaysis of Elementary Chemical Models. Sandia National Laboratories, SAND82-8230, 1982.
33. Westmoreland, P. R., Ph.D. dissertation, Massachusetts Institute of Technology, 1986.
34. Kiefer, J. H., Wei, H. C., Kern, R. D., and Wa, C. H., *Int. J. Chem. Kin.* 17:225 (1985).
35. Benson S. W., *Thermochemical Kinetics*. Wiley, New York, 1976.
36. Colket, M. B., *American Chemical Society, Fuel Chemistry Preprints* 32:417 (1987).
37. Dean, A. M., Exxon Research Laboratories, Annandale, NJ, Personal communication, 1987.
38. Hou, K. C., and Anderson, R. C., *J. Phys. Chem.* 67:1579 (1963).
39. Pamidimukkala, K. M., Kern, R. D., Patel, M. R., Wei, H. C., and Kiefer, J. H., *J. Phys. Chem.* 91:2148 (1987).
40. Muller-Markgraf, W., and Troe, J., *Twenty-first Symposium (International) on Combustion*. The Combustion Institute, Pittsburgh, 1988, p. 815.
41. Amano, A., Horie, O., and Hanh, N. H., *Int. J. Chem.*

Kin. 8:321 (1976).
42. Wu, C. H., and Kern, R. D., *J. Phys. Chem.*, 91:6291 (1987).
43. Frank, P., and Just, Th., *Combust. Flame* 38:231 (1980).
44. Tsang, W., and Hampson, R. F., *J. Phys. Chem. Ref. Data* 15:1087 (1986).
45. Ebert, K. H., Ederer, H. J., and Isbarn, G., *Int. J. Chem. Kin.* 15:475 (1983).
46. Weissman, M., and Benson, S. W., *Int. J. Chem. Kin.* 16:307 (1984).
47. Cole, J. A., Bittner, J. D., Longwell, J. P., and Howard, J. B., *Combust. Flame* 56:51 (1984).
48. Holt, P. M., and Kerr, J. A., *Int. J. Chem. Kin.* 9:185 (1977).
49. Kerr, J. A., and Moss, S. J., Eds., *CRC Handbook of Bimolecular and Termolecular Gas Reactions.* CRC press, Boca Raton, FL, 1981.
50. Trotman-Dickenson, A. F., and Steacie, E. W. R., *J. Chem. Phys.* 18:1097 (1950).
51. Olsen, D. B., and Gardiner, W. C., *Combust. Flame* 32:151 (1978).
52. Aten, C. F., and Greene, E. F., *Combust. Flame* 5:55 (1961).
53. Cundall, R. B., Fussey, D. E., Harrison, A. J., and Lampard, D., *J. Chem. Soc. Far. Trans. I* 74:1403 (1978).
54. Gay, I. D., Kistiakowsky, G. B., Michael, J. V., and Niki, H., *J. Chem. Phys.* 43:1720 (1965).
55. Towell, G. D., and Martin, J. J., *A. I. Ch. E. J.* 7:693 (1961).
56. Payne, W. A., and Stief, L. J., *J. Chem. Phys.* 64:1150 (1976).
57. Hsu, D. S. Y., Lin, C. Y., and Lin, M. C., *Twentieth Symposium (International) on Combustion.* The Combustion Institute, Pittsburgh, 1985, p. 623.
58. King, K. D., *Int. J. Chem. Kin.* 10:545 (1978).

Received 11 January 1988; revised 2 June 1988

Appendix D

The Pyrolysis of Acetylene and Vinylacetylene In a Single-Pulse Shock Tube

Twenty-first Symposium (International) on Combustion/The Combustion Institute, 1986 pp. 851–864

THE PYROLYSIS OF ACETYLENE AND VINYLACETYLENE IN A SINGLE-PULSE SHOCK TUBE

MEREDITH B. COLKET, III
United Technologies Research Center
Silver Lane, Mail Stop 30
East Hartford, CT 06108

Acetylene and vinylacetylene have been pyrolyzed in a single-pulse shock tube for the temperature range 1100 to 2400°K, at total pressures of approximately eight atmospheres and for dwell times of approximately 700 microseconds. Initial concentrations of the hydrocarbon in argon ranged from about 100 ppm to 4%. Gas samples were collected and analyzed using gas chromatography for hydrogen, and C_1 to C_{10}-hydrocarbons. The data from the pyrolysis of acetylene exhibit substantial production of vinylacetylene, benzene, and phenylacetylene, but agree well with a detailed chemical kinetic model. Data from vinylacetylene pyrolysis and thermochemical arguments suggest a chain mechanism by which H adds to vinylacetylene and the resultant adduct decomposes to acetylene and a vinyl radical. Rate constants for the reverse steps of those occurring during vinylacetylene and benzene pyrolysis have been calculated using thermodynamics and forward rate constants. These reverse rate constants assist in describing the production of vinylacetylene, benzene, and phenylacetylene during acetylene pyrolysis.

Four separate reaction mechanisms for the initial formation of aromatic rings have been identified. The relative importance of each step depends on the ambient temperature and relative concentrations. *Overall* steps can be written as

$$C_2H_2 + n\text{-}C_4H_3 \rightarrow C_6H_4 + H$$
$$C_2H_2 + n\text{-}C_4H_5 \rightarrow C_6H_6$$
$$C_4H_4 + n\text{-}C_4H_5 \rightarrow C_6H_5C_2H_3 + H$$
$$C_4H_4 + C_2H_3 \rightarrow C_6H_6 + H$$

Introduction

Glassman[1] has convincingly argued that the chemistry of fuel pyrolysis plays an important role in sooting diffusion flames. Some pyrolysis steps may be rate-limiting for the production of incipient soot particles, and therefore the total amount of soot.[2] Armed with this information, many research programs have begun to identify the rate-limiting processes. For example, Bittner and Howard,[3] and Bockhorn, et al.[4] have provided experimental confirmation of a variety of high molecular weight polycyclic aromatics present in rich flames. Cole, et al.[5] and Weissman and Benson[6] have suggested mechanisms with rates consistent with thermochemical analysis and experimental data for the production of single-ring aromatics. Frenklach, et al.[7] has modeled soot formation from acetylene pyrolysis in shock tubes using a detailed chemical mechanism. The mechanism includes production of aromatic rings and continual growth of polycyclic aromatics. Qualitative success has been obtained in this substantial effort despite the lack of confirming experimental data describing profiles of intermediates for confirmation/support of the proposed model.

It is the objective of the present work to extend these earlier works in order to help elucidate pyrolysis steps and chemical mechanisms related to the formation and break-up of aromatic rings. A single-pulse shock tube[8,9] was selected for this study, not only because shock tubes are one of the few devices capable of generating conditions of importance to soot formation in diffusion flames, but also to extend the information on soot production already generated through optical studies in shock tubes.[10–13]

Preliminary versions of the modeling work have been described separately for acetylene[14] and vinylacetylene.[15] The present work combines the earlier models, including a recent one for benzene pyrolysis,[16] into one model which satisfactorily describes both decomposition (of the parent hydrocarbons) and product forma-

tion. Required revisions include slight adjustments to rate constants and to assumed thermodynamic parameters.

Description of Fa :ilities

The SPST used in this program is 2E5 cm long and has a diameter of 3.8 cm (i.d.). The driver is 88 cm in length and can be turned by shortening its length in 3.8 cm increments; the driven section is 197 cm long. An 11.7 liter "dump tank" is located in the driver (lower pressure) section 30 cm downstream of the diaphragm. Pressure profiles were determined using Kistler pressure transducers located 15.25 and 2.50 cm from the end wall. Arrival times were measured to within one microsecond using digitized pressure traces. Calculated quench rates are typically 10^5 K/sec or higher in the rarefaction wave. Starting pressures prior to filling are 0.2μ and leak rates are less than 1μ/min. Post-shock temperatures were calculated based on the measured incident shock velocity and normal shock wave equations.

The procedures for performing an experiment are similar to those described by Tsang,[17] except for an automated sampling system. The sample is collected at the endwall of the shock tube using 0.045 inch i.d. tubing heated to over 85°C. Approximately 30 milliseconds after the gas has been shock heated and cooled, a solenoid valve opens to the evacuated sample cell and then closes after 300 milliseconds. The sample storage vessel is all stainless steel with an internal volume of 25 cc.

The sampling volume is directly coupled to a low volume (<3cc), heated inlet system of a Hewlett Packard 5880 A gas chromatograph. Valves, detectors and software integration routines as described previously[14] enable this system to provide automatic quantitative detection of hydrogen and hydrocarbon species up to C_{10}-hydrocarbons. Based on repeated injections of calibrated samples, overall accuracies are estimated to be three percent. Calibration gases were stored in stainless steel cylinders with degreased valves and were heated to approximately 60°C prior to injection.

Argon (99.999% pure) was obtained from Matheson and was the principal diluent. Compressed acetylene, also from Matheson, contained about 1 to 2% acetone (added for stability) depending on bottle conditions. Acetylene was purified by repeated freezing and thawing at liquid N_2 temperatures and retaining only the middle 50%. Final samples still contained 0.1 to 0.2% acetone. Vinylacetylene was obtained from Wiley Organics and contained an unidentified hydrocarbon with a concentration of approximately 8000 ppm.

Model Description

Detailed chemical kinetic calculations have been performed using CHEMKIN,[18] LSODE,[19] and a version of a shock tube code originally developed by Mitchell and Kee[20] but modified to include quenching effects in an SPST. Quenching rates are determined using experimental pressure traces, assuming adiabatic expansion, and using the equation

$$\frac{dT}{dt} = \frac{T}{P}\frac{\gamma-1}{\gamma}\frac{dP}{dt}.$$

Calculated quenching rates vary as a function of shock strength and time. Initial quenching rates are as high as 2×10^6K/sec for shocks producing initial post-shock temperatures of 2000°K, but only 25% of that rate for shocks producing reflected shock temperatures near 1200°K.

The chemical kinetic model used in this work is reproduced in Table I and is based on proposed mechanisms for the pyrolysis of acetylene[21] and ethene.[22] The reaction set includes the identification of the C_4H_3 isomers following Frenklach, et al.[7] The radicals are denoted n-C_4H_3 for the (normal) isomer with the unpaired electron on the terminal vinylic carbon and i-C_4H_3 for the (iso)isomer with the radical site on the interior carbon atom. n-C_4H_5 (radical on end carbon) was the only C_4H_5 isomer considered in this work. Also, the mechanism includes the forward and reverse processes of the predominant path for decomposition of benzene, i.e.,

$$C_6H_6 + H \rightleftarrows C_6H_5 + H_2 \qquad (39)$$
$$C_6H_5 \rightleftarrows \ell\text{-}C_6H_5 \qquad (56)$$
$$\ell\text{-}C_6H_5 \rightleftarrows \text{n-}C_4H_3 + C_2H_2 \qquad (55)$$

where ℓ-C_6H_5 has been suggested[16] to be the 1-hexyne-3,5-dien-6-yl radical. The rate constants (R55,R56) have been revised slightly from the previous work[16] in order to be consistent with the reverse processes.

As required, thermodynamic estimates of some species were made using group additivity techniques.[23] Otherwise, data from readily available sources were used.[24,25] Both estimates of rate parameters and those calculated using equilibrium constants are dependent on the selected thermodynamics. Of particular concern during the present research is the apparent uncertainty in the heat of formation of

TABLE I
Proposed Set of Reactions and Rate Coefficients
logk = logA + nlogT − E/R/T/2.303 *

	Reactions	Forward Rate Constant			Reverse Rate Constant			Ref
		logA	n	E	logA	n	E	
1	C2H4 + M=C2H3 + H + M	16.16	0.0	81.8	14.24	0.0	−23.0	22
2	C2H4 + H =C2H3 + H2	14.84	0.0	14.5	13.53	0.0	14.0	21
3	H + C2H2=C2H3	12.74	0.0	2.5	13.01	0.0	43.8	21
4	C2H3 + H=H2 + C2H2	13.00	0.0	0.0	13.34	0.0	63.2	21
5	H2 + M=2H + M	12.35	−.5	92.5	11.74	−.5	−11.9	21
6	C2H2 + M=C2H + H + M	16.62	0.0	107.0	15.25	0.0	−17.9	21
7	2C2H2=n−C4H3 + H	12.30	0.0	45.9	11.67	0.0	−25.0	21
8	i−C4H3 + H2=C2H2 + C2H3	10.70	0.0	20.0	11.41	0.0	17.1	PW*
9	C4H4=i−C4H3 + H	15.20	0.0	85.0	12.72	0.0	−12.1	PW
10	C4H4=n−C4H3 + H	15.00	0.0	100.0	12.93	0.0	−7.7	PW
11	C2H + C4H4=C2H2 + i−C4H3	13.60	0.0	0.0	12.48	0.0	27.9	21
12	n−C4H3=C2H2 + C2H	14.30	0.0	57.0	13.56	0.0	3.0	PW
13	i−C4H3=C4H2 + H	12.00	0.0	49.0	12.86	0.0	−0.2	PW
14	n−C4H3=C4H2 + H	12.60	0.0	40.0	13.04	0.0	1.4	PW
15	n−C4H3 + H=i−C4H3 + H	13.48	0.0	0.0	13.06	0.0	10.7	PW
16	i−C4H3 + H=C4H2 + H2	13.00	0.0	0.0	14.47	0.0	55.2	PW
17	n−C4H3 + H=C4H2 + H2	13.00	0.0	0.0	14.05	0.0	65.9	PW
18	C4H4 + H=i−C4H3 + H2	14.49	0.0	14.5	12.62	0.0	21.9	26,PW
19	C4H4 + H=n−C4H3 + H2	13.90	0.0	14.5	12.45	0.0	11.2	26,PW
20	C2H3 + C2H2=n−C4H5	12.04	0.0	4.0	13.79	0.0	37.7	PW
21	C2H + H2=H + C2H2	12.85	0.0	0.0	13.60	0.0	20.5	22
22	C2H + C2H2=C4H2 + H	13.60	0.0	0.0	14.78	0.0	15.4	21
23	C4H2=C4H + H	14.89	0.0	120.0	13.28	0.0	2.1	22
24	C2H + C4H2=C6H2 + H	13.60	0.0	0.0	14.97	0.0	15.1	21
25	C4H + C2H2=C6H2 + H	13.30	0.0	0.0	14.91	0.0	8.1	21,PW
26	C6H2=C6H + H	14.89	0.0	120.0	13.05	0.0	5.3	22
27	C4H + H2=H + C4H2	13.30	0.0	0.0	14.30	0.0	13.5	22
28	C6H + H2=H + C6H2	13.30	0.0	0.0	14.53	0.0	10.3	22
29	C2H + H=C2 + H2	12.00	0.0	23.0	11.55	0.0	3.8	PW
30	C2H + M=C2 + H + M	16.67	0.0	124.0	15.61	0.0	0.4	36
31	C4H4 + C6H5=C6H6 + n−C4H3	12.00	0.0	0.0	12.56	0.0	3.1	PW
32	C4H4 + C6H5=C6H6 + i−C4H3	12.00	0.0	0.0	12.14	0.0	13.8	PW
33	C2H + C6H6=C6H5 + C2H2	13.30	0.0	0.0	12.05	0.0	14.1	34
34	C4H + C6H6=C6H5 + C4H2	13.30	0.0	0.0	12.29	0.0	7.0	34
35	C2H3 + C4H2=C4H4 + C2H	13.48	0.0	23.0	13.46	0.0	3.1	PW*
36	C2H3 + C4H4=C2H4 + n−C4H3	11.70	0.0	16.3	11.55	0.0	13.4	35,PW
37	C2H3 + C4H4=C2H4 + i−C4H3	11.70	0.0	16.3	11.13	0.0	24.1	35,PW
38	C6H6=C6H5 + H	16.18	0.0	107.9	13.55	0.0	−3.0	16
39	C6H6 + H=C6H5 + H2	14.40	0.0	16.0	12.39	0.0	9.5	34
40	2C6H5=C12H10	12.48	0.0	0.0	16.57	0.0	108.3	17
41	C6H5 + C6H6=C12H10 + H	11.80	0.0	11.0	13.27	0.0	8.4	37
42	n−C4H3 + C6H5−C10H8	13.00	0.0	0.0	0.00	0.0	0.0	PW
43	C2H2 + C6H5=C8H6 + H	12.00	0.0	4.0	13.50	0.0	3.1	38,PW
44	C2H4 + C6H5=C8H8 + H	11.57	0.0	2.1	12.99	0.0	1.6	38
45	C2H3 + C4H4−C6H6 + H	11.60	0.0	0.0	0.00	0.0	0.0	PW
46	n−C4H5=C4H4 + H	14.00	0.0	41.4	13.42	0.0	3.2	6
47	n−C4H5 + C2H2=*l*−C6H7	12.81	0.0	9.0	14.80	0.0	44.4	6,PW
48	n−C4H5 + H=C4H4 + H2	13.00	0.0	0.0	13.03	0.0	66.2	PW
49	C4H6 + H=n−C4H5 + H2	14.00	0.0	14.5	12.80	0.0	11.2	26,PW
50	C6H6 + C2H=C8H6 + H	12.00	0.0	0.0	12.25	0.0	13.2	PW
51	C4H4=C2H + C2H3	16.00	0.0	105.0	13.46	0.0	−15.5	PW

TABLE I (*Continued*)

	Reactions	Forward Rate Constant logA	n	E	Reverse Rate Constant logA	n	E	Ref
52	C4H4 + n−C4H5−C8H8 + H	13.90	0.0	3.0	0.00	0.0	0.0	PW
53	C8H8 + H−C8H6 + H + H2	14.60	0.0	7.0	0.00	0.0	0.0	PW
54	C6H5 + C2H3=C8H8	13.00	0.0	0.0	16.34	0.0	104.4	PW
55	*l*−C6H5=n−C4H3 + C2H2	14.00	0.0	36.0	11.71	0.0	−0.1	PW
56	C6H5=*l*−C6H5	13.54	0.0	65.0	10.22	0.0	1.4	PW
57	C6H6 + H=c−C6H7	13.60	0.0	4.3	13.12	0.0	24.6	PW
58	c−C6H7=*l*−C6H7	14.48	0.0	50.0	11.36	0.0	0.4	PW

*NOTES: Units for A: cc,moles,sec.
Units for E: kcal/mole.
"=" represents forward and reverse directions included in model.
"−" represents forward direction only included in model.
PW indicates rate evaluted from the present work.

vinyl[26,27] and related (e.g. n-C_4H_3 and n-C_4H_5) radicals. Uncertainties in the heats of formation and entropies of these radicals directly translate into errors in proposed rate constants. Thermodynamic parameters at room temperature for species included in this work are presented in Table II.

Results and Discussion

Several series of runs of the pyrolysis of acetylene and vinylacetylene have been completed. Each series represents approximately 10 to 15 separate experiments and each experiment in a series has the same initial concentration in argon. For each run, a chemical analysis is performed of final product distribution. Initial post-shock temperatures for runs from a given series typically range from 1100 to 2400°K. Detailed chemical kinetic model calculations have been performed for most series and the numerical results for selected series are compared to the experimental data in Figs. 1,3–5. Mass balance data were presented previously.[14] A detailed discussion of the experimental data and kinetic mechanism follows.

Acetylene

The decomposition of 3.7% acetylene in argon and production of the major species, i.e. C_4H_2, H_2, and C_6H_2, agree well with existing kinetic models. As seen in Fig. 1, vinylacetylene (VA), benzene and phenylacetylene are also observed and may play a critical role in the growth and production of polycyclic aromatics. The bimolecular reaction $2C_2H_2 \rightarrow C_4H_4$ is thought to occur at low temperatures. Extrapolation of low temperature rate constants provided quantitative agreement with the experimental profile. In addition, the activation energy for this process (~40 kcal/mole) is in reasonable agreement with the assumption of intermediate formation of the C_4H_4 diradical, which is approximately 35 to

TABLE II
Selected Thermodynamics at 300K

Species	*Heat of Formation* (kcal/mole)	*Entropy*
$C_{12}H_{10}$	43.6	93.7
$C_{10}H_8$	36.0	79.5
C_8H_6	78.3	79.6
$\ell-C_6H_7$	97.4	81.8
$c-C_6H_7$	49.9	72.1
C_6H_6	19.9	65.2
C_6H_5	78.5	69.4
$\ell-C_6H_5$	139.2	80.0
C_6H_2	169.7	71.1
C_6H	233.2	74.3
C_4H_6	26.1	66.6
$n-C_4H_5$	82.5	69.1
C_4H_4	69.4	66.1
$n-C_4H_3$	125.1	68.7
$i-C_4H_3$	115.2	71.6
C_4H_2	111.7	59.9
C_4H	179.0	62.8
C_2H_4	12.6	52.4
C_2H_3	65.7	54.5
C_2H_2	54.2	48.1
C_2H	128.5	49.6
C_2	200.2	47.7

43 kcal more energetic than two molecules of acetylene.[28] Unfortunately, this mechanism does not provide a plausible, parallel path for the formation of benzene; yet the similarity in profiles of benzene and VA strongly suggest a parallel mechanism. Stein[29] suggested an alternative chain process initiated by H-atom addition to acetylene to form VA, i.e.,

$$C_2H_2(+H) \rightarrow C_2H_3(+C_2H_2) \rightarrow n\text{-}C_4H_5(-H) \rightarrow C_4H_4$$

This sequence is identical to the first steps in the ring formation process proposed by Frenklach, et al.[7] The final steps of the proposed process include

$$C_4H_4(-H) \rightarrow n\text{-}C_4H_3(+C_2H_2) \rightarrow \ell\text{-}C_6H_5 \rightarrow \text{phenyl}$$

followed by subsequent formation of benzene or phenylacetylene.

Detailed chemical kinetic modeling of the present experimental data, however, strongly suggests that early (i.e. low temperature) benzene formation arises principally from acetylene addition to the normal-butadienyl radical, not the $n\text{-}C_4H_3$ radical, i.e.,

$$n\text{-}C_4H_5(+C_2H_2) \rightarrow \ell\text{-}C_6H_7 \rightarrow c\text{-}C_6H_7(-H) \rightarrow C_6H_6$$

where $\ell\text{-}C_6H_7$ is defined to be the 1,3,5-hexatrien-1-yl radical.

Preliminary calculations using this mechanism have also been performed for comparison to the flow reactor data on acetylene pyrolysis obtained by Munson a. d Anderson.[30] Semiquantitative agreement for the production of benzene and VA was achieved and thus the bimolecular reaction involving intermediate formation of a C_4H_4 diradical is not necessary to describe lower temperature acetylene pyrolysis.

Above 1500°K, cyclic compounds are formed principally by acetylene addition to $n\text{-}C_4H_5$ in agreement with the proposal by Frenklach, et al.[7] Previously it was assumed, however, that $n\text{-}C_4H_3$ was formed through path A, whereas (R-12) was the dominant route under the present conditions

$$n\text{-}C_4H_5(-H) \rightarrow C_4H_4(-H) \rightarrow n\text{-}C_4H_3 \quad A$$
$$C_2H_2 + C_2H \rightarrow n\text{-}C_4H_3 \quad (-12)$$

This conclusion arises from results discussed later in this paper which show that VA decomposition principally involves H-atom addition to C_4H_4, not H-atom abstraction. As temperature increases, the abstraction route will become more significant; however, the concentration of C_2H will also increase so (R-12) still remains competitive. Furthermore (R-12) is a straightforward process for producing the normal radical and, in Fig. 1, assists in adequately describing the production of benzene and phenylacetylene. Demonstration of the relative sources of $n\text{-}C_4H_3$ can be seen in Fig. 2, where reaction sources and sinks are plotted as a function of time for two different temperatures.

Figure 1 shows that the model overpredicts observed benzene and phenylacetylene concentrations above 1600°K. Coincidentally, this is the same temperature at which a significant deficit in recovered mass first appears.[11] Some phenylacetylene and benzene above 1600°K is probably converted to higher molecular weight species which are not observed and not accounted for by the model.

Vinylacetylene

Mixtures of 0.01, 0.115 and 1.0% VA in argon were pyrolyzed over the temperature range 1100 to 2500°K. The data for the lowest and highest concentrations are presented in Figs. 3, 4 and 5. The other species not shown in these figures were observed at concentrations less than 2% of the parent. These species include methane, ethylene, allene/methylacetylene, several unidentified C_4 species, C_6H_4, toluene, and a C_9-hydrocarbon (possibly indene). Data on the series with intermediate concentration have been presented previously.[15] The most significant information is that at low temperatures and

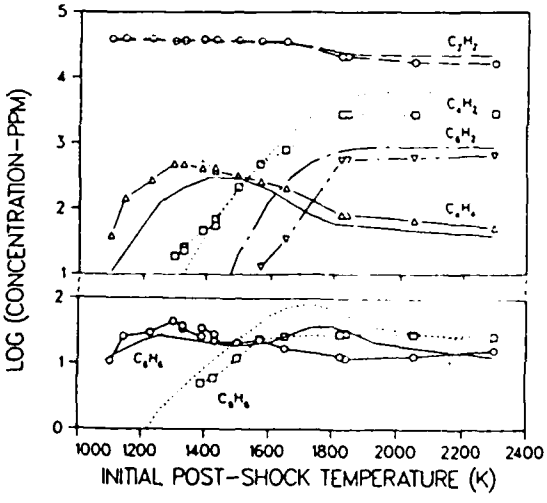

FIG. 1. Experimental and Model Results for Pyrolysis of 3.7% Acetylene in Argon. Dwell Time = 700×10^{-6} sec. Total pressure ≈ 8 atm.

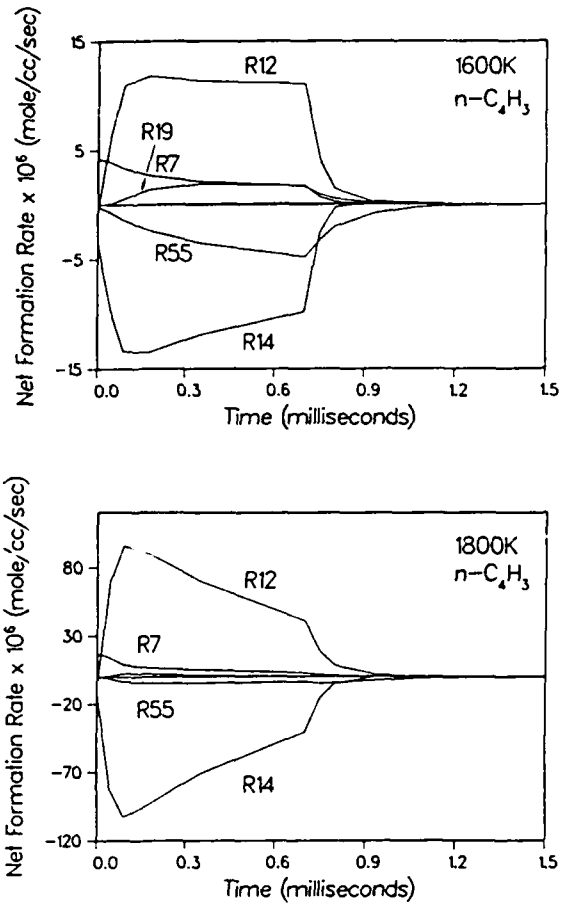

FIG. 2. Net Formation Rate for Production/Destruction of the n-C_4H_3 Radical. 2a) at 1600K, 2b) at 1800K.

Contributing reactions:

R7 $C_2H_2 + C_2H_2 \rightleftarrows n\text{-}C_4H_3 + H$

R12 $n\text{-}C_4H_3 \rightleftarrows C_2H_2 + C_2H$

R14 $n\text{-}C_4H_3 \rightleftarrows C_4H_2 + H$

R19 $C_4H_4 + H \rightleftarrows n\text{-}C_4H_3 + H_2$

R55 $1\text{-}C_6H_5 \rightleftarrows n\text{-}C_4H_3 + C_2H_2$

Quenching wave arrives at 700×10^{-6} sec. Total pressure ≈ 8 atm. Pyrolysis of 3.7% acetylene.

low initial concentrations, acetylene is the predominant product, while diacetylene (as well as H_2) is produced at levels approximately ten times less than that of acetylene. Aromatics are produced at higher temperatures and concentrations, but not in quantities sufficient to encourage rapid growth of polycyclics and severe mass imbalance. Relatively little data have been presented previously for comparison to this SPST data. Lundgard's[31] review has identified one previous work which overlaps the present temperature range. Yampol'skii, et al.[32] examined VA pyrolysis between 1023 and

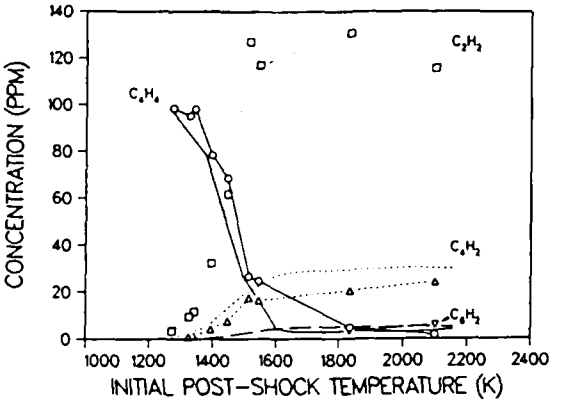

FIG. 3. Experimental and model results for 100 ppm Vinylacetylene in Argon. Dwell time ≈ 700×10^{-6} total pressure ≈ 8 atm.

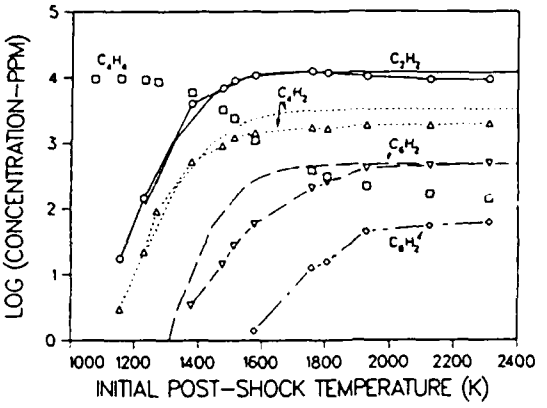

FIG. 4. Experimental and Model Results for Aliphatic Species during Pyrolysis of 1% Vinylacetylene in Argon. Dwell time ≈ 700×10^{-6}sec, total pressure ≈ 8 atm.

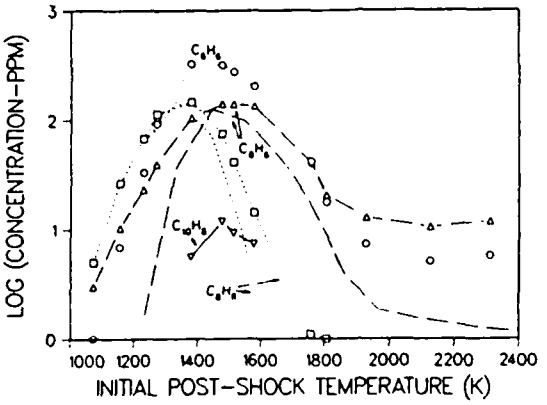

FIG. 5. Experimental and Model Results for Aromatic Products during Pyrolysis of 1% Vinylacetylene in Argon. Dwell time ≈ 700×10^{-6}sec, total pressure ≈ 8 atm.

1273°K and produced qualitatively similar results to the SPST work. The main low temperature aliphatic found by Yampol'skii was acetylene with traces of methane and ethene, although diacetylene was not detected. Benzene was also observed previously, as well as a polymer whose precursor may be styrene. The overall decomposition of VA observed by Yampol'skii, et al., $k = 1.6 \times 10^{11} \exp(-52{,}800 \text{cal/RT})$ sec^{-1} is approximately five times higher than the SPST results.

Kinetic modeling requires the identification of the initiation step and a chain process which describes the predominant formation of acetylene with minor production of diacetylene, styrene, benzene and phenylacetylene. The three possible initiation processes are

R9 $C_4H_4 \rightarrow i\text{-}C_4H_3 + H$ − 98 kcal/mole
R10 $C_4H_4 \rightarrow n\text{-}C_4H_3 + H$ −111 kcal/mole
R51 $C_4H_4 \rightarrow C_2H + C_2H_3$ −122 kcal/mole

where the estimated endothermicities may each be in error by as much as 10 kcal/mole due to uncertainties in heats of formation of the hydrocarbon radicals. In this work, the principal initiation process was assumed to be Reaction 9, which required a rate expression of $10^{15.2} \exp(-42800/T)$ sec^{-1}, although the A-factor seems high and E_{act}, low, for the C-H bond scission. It is important to note that the model results were relatively insensitive to the absolute magnitude of the initiation rate or its temperature dependence. A factor of three change in the initiation rate resulted in approximately a 20–30% change in the overall rate of decomposition and the formation of products. The explanation for this phenomenon is that the decomposition of VA in the range 1200–1400°K is controlled by a chain mechanism:

		$log_{10}A$	E_{act}
R9			
initiation	$C_4H_4 \rightleftarrows i\text{-}C_4H_3 + H$	15.2	85000.
R-46			
chain	$H + C_4H_4 \rightleftarrows n\text{-}C_4H_3$	13.0	1370.
R-20			
chain	$n\text{-}C_4H_3 \rightleftarrows C_2H_3 + C_2H_2$	14.0	43360.
R-3			
chain	$C_2H_3 \rightleftarrows H + C_2H_2$	13.0 cc,mole,sec	43710. cal mole

where the last three reactions account for the majority of the decomposition of the parent and the predominance of acetylene in the low-temperature products. This chain is not only important specifically to understanding the pyrolysis of vinylacetylene; but, as discussed earlier in this paper, also to the mechanism of ring formation during acetylene pyrolysis. Explanations for elimination of other mechanisms are presented below.

Alternative chain mechanisms for decomposition of VA would include H-atom abstraction from C_4H_4 resulting in $\dot{C}:CCH:CH_2$, $HC:C\dot{C}:CH_2$, or $HC:CCH:\dot{C}H$. Formation of the first of these can be neglected from thermodynamic considerations. In addition, direct formation of two acetylene molecules from this structure seems unlikely. The second isomer, $i\text{-}C_4H_3$, should decompose principally into diacetylene, since breakage of the C-C bond would have a high activation barrier due to the formation of vinylidene as an intermediate. The last isomer, $n\text{-}C_4H_3$, may decompose into $C_4H_2 + H$ or $C_2H + C_2H_2$. Estimated rates

	$Log\ k$ (1300°K)	$Log_{10}A$	E
R12			
$n\text{-}C_4H_3 \rightleftarrows C_2H + C_2H_2$	4.72	14.3	57000.
R14			
$n\text{-}C_4H_3 \rightleftarrows C_4H_2 + H$	5.88	12.6	40000.

suggest that Reaction 14, i.e. production of C_4H_2, is faster by a factor of 14 near 1300°K where VA decomposition is observed. At higher temperatures the two rates approach one another. These relative rate estimates are supported by experimental decomposition data of benzene pyrolysis from Kern, et al.[33] Those researchers found that the initial ratio of products C_2H_2/C_4H_2 at 1700°K, is approximately two to one. Assuming the overall decomposition path

$$C_6H_6(-H) \rightleftarrows C_6H_5 \rightleftarrows n\text{-}C_4H_3 + C_2H_2,$$

then the C_2H_2/C_4H_2 product ratio suggests that the branching ratio k_{14}/k_{12} is also approximately two to one. The calculated ratio using the above rates is three (3) at 1700°K. Thus, if $n\text{-}C_4H_3$ is the principal intermediate from VA decomposition, then the initial production rate of C_4H_2 would be similar to or higher than that of C_2H_2 during VA pyrolysis. Such a prediction is not substantiated by the SPST experiments.

H-atoms may add to VA at locations other than to the secondary acetylenic carbon. Addition to the other carbons would form $H_2C:\dot{C}CHCH_2$, $HC:CCHCH_3$, or $HC:CCH_2\dot{C}H_2$. However, each of these radicals would be expected to reform VA, decompose into products other than two acetylenes or involve energetic intermediates. Thus it appears that the decomposition chain involving $n\text{-}C_4H_3$ will dominate. Detailed chemical kinetic calculations using the

specific rate constants in Table I are consistent with this analysis.

Production of diacetylene is described by

$$R + C_4H_4 \rightarrow i\text{-}C_4H_3 + RH$$
$$R + C_4H_4 \rightarrow n\text{-}C_4H_3 + RH$$

followed by decomposition of C_4H_3 into diacetylene plus H-atoms. R may be an H-atom or a hydrocarbon radical.

As shown in Fig. 5, reasonable agreement with experimental profiles of aromatic species were obtained using the reaction sequence of Table I. The apparent underprediction of VA at elevated temperatures is presumably an experimental problem due to partial gas sampling of boundary layers which contain the unheated parent hydrocarbon. Above 1600°K, phenyl is formed from the $n\text{-}C_4H_5 + C_2H_2$ recombination and is followed by conversion to benzene or phenylacetylene. At lower temperatures, the predominate formation routes of aromatics are

R45 $C_4H_4 + C_2H_3 \rightarrow C_6H_7$
(1,3,5-hexatrien-3-yl)
$C_6H_7 \rightarrow c\text{-}C_6H_7$
$c\text{-}C_6H_7 \rightarrow C_6H_6 + H$

for benzene formation, and

R52 $C_4H_4 + n\text{-}C_4H_3 \rightarrow C_8H_7$
$C_8H_7 \rightarrow c\text{-}C_8H_6$
$c\text{-}C_8H_6 \rightarrow C_8H_5 + H$

to produce styrene. PA is produced principally by

R53 $C_8H_5 + H \rightarrow C_8H_7 + H_2$
$C_8H_7 \rightarrow C_8H_6 + H$

near 1500°K and below, but at higher temperatures, acetylene addition to phenyl also occurs. Reactions 45, 52, and 53 were assumed to be overall processes and nonreversible. For the conditions (radical concentrations and temperatures) at which these reactions contribute, preliminary calculations confirmed the validity of these assumptions. Despite the good agreement with the experimental data, there are several unsettling features of these proposals. Reaction 45 requires a 1,3 or 1,4 H-atom shift prior to cyclization and Reaction 47, which has been proposed previously[3] should be a preferred route for aromatization. However, $k_{47} \approx 10^{11}$ cc/mole-sec would be required to explain the experimental data. This rate is significantly higher than the rate in Table I, 2×10^{11} cc/mole-sec, required by the acetylene modeling, and previous determinations [7.5×10^{10} (Ref. 5) and 2.7×10^{11} (Ref. 6) at 1300°K].

Another concern of the modeling results is that the value of k_{52} required to match the experimental data is approximately 100 times higher than a previous determination using data from a low pressure, premixed butadiene flame. Rate determinations from the SPST data are subject to errors due to boundary-layers, quenching effects, and modeling complexity. However, the flame determination is expected to be a lower limit since, when evaluating the rate constant, Cole, et al.[5] assumed that the $n\text{-}C_4H_3$ radical was the dominant C_4H_3 species. Other isomers, particularly $H_2C{:}CHCCH_2$, which is less reactive and more stable by 3 kcal/mole, can contribute significantly to mass 53.

The assumption of the predominance of $n\text{-}C_4H_3$ in the flame work would only partially explain the difference between the two evaluations. Uncertainties in heats of formation and entropies for $n\text{-}C_4H_3$ and/or vinyl, which may affect the $n\text{-}C_4H_3$ concentration via

$$C_2H_2 + C_2H_3 \rightleftharpoons n\text{-}C_4H_3$$

may also help to alleviate the difference; but probably by no more than a factor of five. Alternatively, reactions not considered in the present work may describe production of aromatics or significantly enhance the concentration of $n\text{-}C_4H_3$.

Conclusions

Single-pulse shock tube data have been obtained for the pyrolyses of acetylene and vinylacetylene. The data have been used to support previous proposals for acetylene and benzene pyrolysis with some revisions. A decomposition model for vinylacetylene involving H-atom addition to vinylacetylene has been proposed in order to explain product formation. Severe constraints imposed by simultaneously modeling decomposition of each of the parent hydrocarbons as well as five or more product species have been satisfied with the proposed model. Vinylacetylene, benzene, and phenylacetylene are observed during acetylene pyrolysis. The sequence

$$C_2H_2 + H \rightleftharpoons C_2H_3$$
$$C_2H_2 + C_2H_3 \rightleftharpoons n\text{-}C_4H_3$$
$$n\text{-}C_4H_3 \rightleftharpoons C_4H_4 + H$$
$$C_2H_2 + n\text{-}C_4H_3 \rightarrow t\text{-}C_6H_7$$
(1,3,5-hexatrien-1-yl)
$$t\text{-}C_6H_7 \rightarrow c\text{-}C_6H_7$$
$$c\text{-}C_6H_7 \rightarrow C_6H_6 + H$$

describes the low temperature formation of vinylacetylene and benzene (1100–1400°K). Reverse rates calculated from thermodynamics for the first three steps describe the decomposition of vinylacetylene. At temperatures above 1500°K, phenyl is formed by

$C_2H_2 + H \rightleftarrows C_2H + H_2$
$C_2H_2 + C_2H \rightleftarrows n\text{-}C_4H_3$
$C_2H_2 + n\text{-}C_4H_3 \rightleftarrows \ell\text{-}C_6H_5$
(1-hexyne-3,5-dien-6-yl)
$\ell\text{-}C_6H_5 \rightleftarrows$ phenyl

and is followed by formation of benzene or phenylacetylene. Reverse rates calculated from thermodynamics are consistent with a previous proposal for decomposition of phenyl during benzene pyrolysis.

Aromatic formation during vinylacetylene pyrolysis at low temperatures is described by

$C_2H_3 + C_4H_4 \rightarrow C_6H_7$
(1,3,5-hexatrien-3-yl)
$C_6H_7 \rightarrow c\text{-}C_6H_7$
$c\text{-}C_6H_7 \rightarrow C_6H_6 + H$
and $n\text{-}C_4H_5 + C_4H_4 \rightarrow \ell\text{-}C_8H_9$
$\ell\text{-}C_8H_9 \rightarrow c\text{-}C_8H_9$
$c\text{-}C_8H_9 \rightarrow C_8H_8 + H$

The proposed rate constant for the first step is low, but the reaction requires an H-atom shift. The required rate for the addition of the normal butandienyl radical to vinylacetylene is approximately 100 times higher than a previous measurement. Consequently, it is possible that calculated concentrations of $n\text{-}C_4H_5$ are inaccurate or that other mechanisms are significant.

Acknowledgements

This work has been supported in part by the Air Force Office of Scientific Research (AFSC) under Contract No. F49620-85-C-0012. The United States government is authorized to reproduce and distribute reprints for governmental purposes, notwithstanding any copyright notation herein. The author is indebted to Dr. D. J. Seery and Prof. H. Palmer for their constant support and suggestions throughout this research. The author is also grateful to Dr. P. R. Westmoreland for many fertile discussions and his sharing of technical/thermodynamic information. The authors of CHEMKIN and LSODE should be acknowledged, since these computer routines substantially increased the capability for performing the model calculations; particular thanks should go to Dr. R. J. Kee for his suggestions and guidance in modifying the codes. The experimental research has been completed only with the able assistance of D. Kocum. His assistance is greatly appreciated.

REFERENCES

1. Glassman, I.: "Phenomenological Models of Soot Processes in Combustion Systems," Department of Mechanical and Aerospace Engineering Report 1450, Princeton University, NJ (1979).
2. Harris, S.J. and Weiner, A.M.: Combustion Science and Technology, *31*, 155 (1983). Also *32*, 267 (1983).
3. Bittner, J. and Howard J.B.: *Eighteenth Symposium (International) on Combustion*, p. 1105, The Combustion Institute, Pittsburgh (1981).
4. Bockhorn, H., Fetting, F. and Wenz, H.W.: Ber.Bunsenges.Phys.Chem., *87*, 1067 (1983).
5. Cole, J.A., Bittner, J.D., Longwell, J.P. and Howard, J.B.: Combustion and Flame, *56*, 51 (1984).
6. Weissman, M. and Benson, S.W.: Int'l.J.Chem. Kin., *16*, 307 (1984).
7. Frenklach, M., Clary, D.W., Gardiner W.C., Jr., and Stein, S.: *Twentieth Symposium (International) on Combustion*, p. 887, The Combustion Institute, Pittsburgh (1985).
8. Glick, H.S., Squire, W., and Hertzberg, A.: *Fifth Symposium (International) on Combustion*, p. 393, Reinhold Publishing Corp., New York, (1955).
9. Lifshitz, A., Carroll, H.F. and Bauer, S.H.: J.Chem.Phys., *39*, pp. 1661–1665 (1963).
10. Graham, S.C., Homer, J.B. and Rosenfeld, J.L.J.: Proc.R.Soc.London A344,259 (1975).
11. Wang, T.S., Matula R.A., and Farmer, R.C.: *Eighteenth Symposium (International) on Combustion*, p. 1149–1158, The Combustion Institute, Pittsburgh (1981).
12. Frenklach, M., Ramachandra, M.K. and Matula, R.A.: *Twentieth Symposium (International) on Combustion*, p. 871, The Combustion Institute, (1984).
13. Rawlins, W.T., Cowles, L.M. and Krech, R.H.: *Twentieth Symposium (International) on Combustion*, p. 879, The Combustion Institute, (1985).
14. Colket, M.B.: *Shock Waves and Shock Tubes, Proceedings of the Fifteenth International Symposium on Shock Waves and Shock Tubes*. Ed. by D. Bershader and R. Hanson, Stanford University Press, Stanford, p. 311 (1986).
15. Colket, M.B.: "Pyrolysis of Vinylacetylene," Paper No. 53, presented at Eastern Section/Combustion Institute, Fall Technical Meeting, Philadelphia, November 1985.
16. Colket, M.B.: "Pyrolysis of C_6H_6," presented at American Chemical Society, New York City National Meeting, Division of Fuel Chemistry preprints *31* (2), p. 98, April 13–16, 1986.

17. Tsang, W.: Shock Waves in Chemistry, Ed. by A. Lifshitz, Marcel Dekker, Inc., New York, pp. 59–129 (1981).
18. Kee, R.J., Miller J.A. and Jefferson, T.H.: "CHEMKIN: A General-Purpose, Problem-Independent, Transportable, Fortran Chemical Kinetics Code Package," Sandia National Laboratories, SAND80-8003, March 1980.
19. Hindmarsh, A.C.: "LSODE and LSODI, Two New Initial Value Differential Equation Solvers," ACM *SIGNUM* Newsletter, *15*, No. 4, Dec. 1980.
20. Mitchell, R.E. and Kee, R.J.: "A General-Purpose Computer Code for Predicting Chemical Kinetic Behavior behind Incident and Reflected Shocks," Sandia National Laboratories, SAND 82-8205, March 1982.
21. Tanzawa, T. and Gardiner, W.C., Jr.: Combust. Flame *39*, 241 (1980), also J.Phys.Chem. *84*, 236 (1980).
22. Kiefer, J.H., Kapsalis, S.A., Al-Alami, M.Z., and Budach, K.A.: Combust. Flame *57*, 79 (1983).
23. Benson, S.W.: *Thermochemical Kinetics*, J. Wiley and Sons, New York (1976).
24. Stull, D.R. and Prophet, H., JANAF Thermochemical Tables, 2nd Ed., U.S. Dept. of Commerce, Nat.Bur.Stand., Washington, D.C. (1971).
25. Burcat, A.: in *Combustion Chemistry*, p. 457, ed. by Gardiner, W.C., Springer-Verlag, New York (1984).
26. Kiefer, J.H., Wei, H.C., Kern, R.D. and Wu, C.H.: Int.J.Chem.Kin. *17*, 225 (1985).
27. Sharma, R.B., Serno, N.M. and Koski, W.S.: Int.J.Chem.Kin. *17*, 831 (1985).
28. Kollmar, H., Carrion, F., Dewar, M.J.S., and Bingham, R.C.: J.American Chemical Society *103*, 5292, 1981.
29. Stein, S.E.: private communication (1984).
30. Munson, M.S.B. and Anderson, R.C.: Carbon *1*, 51 (1963).
31. Lundgard, R.A.: "The Pyrolysis of Vinylacetylene," Ph.D. Thesis, Pennsylvania State University, available from University Microfilms International, Ann Arbor, Michigan (1983).
32. Yampol'skii, Yu. P., Maksimov, Yu V., and Lavroskii, K.P.: J.Phys.Chem. USSR (English translation) *182*, 940 (1968).
33. Kern, R.D., Wu, C.H., Skinner, G.B., Rao, U.S., Kiefer, J.H., Towers, J.A., and Mizerka, L.J.: *Twentieth Symposium (International) on Combustion*, The Combustion Institute, p. 789 (1984).
34. Kiefer, J.H., Mizerka, L.J., Patel, M.R., and Wei, H.-C., J.Phys.Chem. *89*, 2013 (1985).
35. Ebert, K.H., Ederer, H.J. and Isbarn, G.: Int.J.Chem.Kin. *15*, 475 (1983).
36. Miller, J.A., Mitchell, R.E., Smooke, M.D. and Kee, R.J.: *Nineteenth Symposium (International) on Combustion*, The Combustion Institute, p. 181 (1982).
37. Fujii, N. and Asaba, T.: *Fourteenth Symposium (International) on Combustion*, The Combustion Institute, Pittsburgh, p. 433 (1973).
38. Mallard, W.G., Fahr, A., and Stein, S.E.: "Rate Constants for Phenyl Reactions with Ethylene and Acetylene," Paper No. 92, Chem.Phys.Proc. Comb., ES/CI, Clearwater Beach, Fla., Dec. 3–5, 1984.

COMMENTS

F. Temps, MPI F. Stromungsforschung, West Germany. Would the author please comment on the possible role of vinylidene (singlet or triplet) or triplet acetylene on the acetylene pyrolysis?

Author's Reply. Vinylidene appears to be a strong candidate for initiation of acetylene, since it lies only about 44 kcal/mole above the ground state of acetylene and since the intermediate transition state is only two (2) to four (4) kcal/mole above vinylidene[1]. A subsequent step:

$$H_2C - C: + HCCH \rightarrow H_2C\dot{C}CH\dot{C}H \rightarrow i\text{-}C_4H_3 + H$$

is endothermic (overall) by about 15 kcal/mole (or 69 kcal/mole above two acetylene molecules). The overall endothermicity of this sequence is lower than other proposed bimolecular initiators which form $C_2H + C_2H_3$ or $n\text{-}C_4H_3 + H$, which are about 86 and 79 kcal endothermic, respectively. Unfortunately, the endothermicity of the sequence involving vinylidene is still about 13 kcal higher than the activation energy of the bimolecular initiator (Reaction 7) used in the present work.

Vinylidene could also play a role if the above intermediate, $H_2C\dot{C}CH\dot{C}H$, undergoes a 1,4 H-atom shift to produce vinylacetylene. Although this route was considered in the present work, there is no apparent parallel pathway to benzene, which adequately describes experimental profiles. It is, of course, possible that this mechanism contributes to the production of vinylacetylene. A possible role of triplet acetylene was not considered in the above analysis.

REFERENCE

1. Carrington, T., Hubbard, L.M., Schaefer, H.F., and Miller, W.H.: J. Chem. Phys. *80* (9), 1 (1984).

•

S.E. Stein, Chemical Kinetics Div, National Bureau of Standards, U.S.A. How do you interpret the unusually high rate constant for styrene formation?

Author's Reply. As summarized in the conclusions of the manuscript, the rate expression $k_{45} = 7.9\times10^{13}$ exp(−3000/RT) cc/mole-sec, is about a factor of 100 too high, when compared to rate constants of comparable addition processes. The interpretation is that either other mechanisms dominate styrene formation or that rate coefficients and/or thermodynamics for several of the reactions/species are in error. The most likely alternative mechanism is a dimerization process; the most likely errors associated with rate coefficients and thermodynamics probably involve vinyl and butadienyl radicals.

There is presently insufficient information available to ascertain which of the above (or if all) contribute to the discrepancy. Consequently, the data are presented as is.

•

K.H. Homann, Technische Hochschule Darmstadt, West Germany. Did you consider a dimerization step as the first reaction in the pyrolysis of C_2H_2 and C_4H_4? In a recent study of C_4H_2 pyrolysis at 100°C we found that the homogeneous initiation step was $2\,C_4H_2 \rightarrow C_8H_4$. Addition of H atoms to the reaction system had no effect on the products[1].

1. Homann K.H. and Pidoll U.V.: Ber. Bunsenges. Phys. Chem. 1986, in press.

Author's Reply. In an early analysis of this work, the dimerization of acetylene was considered as the predominant mechanism for vinylacetylene formation. The rate constant ($k = 3.6=10^{14}$ exp(-44100/RT) cc/mole-sec) reported by Bradley and Kistiakowsky[1] was found to describe nicely the low temperature formation of C_4H_4. Coincidentally, the overall activation energy of this process is similar to the endothermicity for the formation of HĊCHCHĊH, the diradical intermediate. The endothermicity of this process was estimated to be 35 to 43 kcal/mole by interpreting results from Kollmar, et al.[2]. Despite the good agreement with experiment and reasonable mechanistic explanations (see also the response to Prof. F. Temps regarding the role of vinylidene) several problems arose. First, the Bradley and Kistiakowski data were shown[4] to be misinterpreted, leaving doubt regarding their reported rate constants. Secondly, there appears to be no parallel pathway to the formation of benzene at low temperature which describes the experimental results. In support of the chain mechanism during acetylene pyrolysis is that production of C_4H_4 and C_6H_6 can be explained using the proposed chain which includes rate constants very much consistent with previously proposed rate constants and thermochemistry. Additionally, many other products were not reported due to their relatively low concentrations; but their existence is strongly indicative of radical, chain mechanism. Further support for the chain mechanism is drawn from the fact that the proposed mechanism qualitatively predicts the product distributions observed during low temperature pyrolysis of acetylene[4] (allowing for a small change in the initiation rate and for pressure dependence of addition reactions).

Finally, Callear and Smith[5] have shown convincingly that processes very similar to those described in this work occur at room temperature when H-atoms are added to acetylene. The conclusion of the present work is that a radical, chain mechanism adequately describes the observed dominant products using mechanisms and rates which are reasonable. Dimerization processes cannot as yet be ruled out absolutely (and they may play a contributing role), but it does not seem necessary to invoke their existence to explain the observed results.

As strong a case against dimerization processes cannot be made in the case of vinylacetylene, since it is necessary to add a reaction (#45) which had not been proposed previously and (most disconcerting) to use an unusually high rate for the addition of n-C_4H_5 to C_4H_4 (R52)(see response to question by Dr. S. Stein).[4] However, with the lack of evidence of dimerization processes occurring during high temperature acetylene processes, the author favors a chain mechanism for explaining the product distribution. The vinylacetylene data can be fitted reasonably if one assumes dimerization processes dominate aromatic formation. For example, by reducing k_9, k_{45}, k_{52}, and k_{53} by factors of 2, 2, 100, and 2 respectively and including:

$$2C_4H_4 \rightarrow C_8H_8(a) \text{ and } 2C_4H_4 \rightarrow C_8H_6 + 2H \text{ (b)}$$

(as irreversible steps) with respective rate constants of:

$$k_a = 9\times10^{13} \exp(-40000/RT)$$

and

$$k_b = 3\times10^{12} \exp(-35000/RT) \text{ cc/mole-sec}$$

then experimental profiles can be predicted reasonably (although benzene is overpredicted at low temperatures). k_a, in comparison, is approximately two to three times higher than an extrapolation of Lundgard and Heicklen's(6) expression:

$$k = 3\times10^{11} \exp(-29200 \text{ cal/mole/RT}) \text{ cc/mole/sec}$$

for the net formation of "dimerized" products, formed via a combination of molecular and radical processes. The radical process at low temperatures was assumed to involve formation of a diradical intermediate, although possible contributions from

the chain process as suggested in this paper should not be necessarily ignored.

REFERENCES

1. Bradley, J.N. and Kistiakowsky, G.B.: J. Chem. Phys. *35*, 264 (1961).
2. Kollmar, H., Carrion, F., Dewar, M.J.S., Bingham, R.C.: J. Am. Chem. Soc. *103*, 5292 (1981).
3. Gay, I.D., Kistiakowsky, G.B., Michael, J.V. and Niki, H.: J. Chem. Phys. *43*, 1720 (1965).
4. Ref. #30 of manuscript.
5. Callear, A.B. and Smith, G.B.: J. Phys. Chem. *90*, 3229 (1986).
6. Lundgard, R. and Heicklen, J.: Int. J. Chem. Kin. *16*, 125 (1984).

●

S.J. Harris, General Motors Research Labs, U.S.A. Are C_2H_2 and C_4H_2 equilibrated in your system? At what temperatures? If they *are* equilibrated, then you cannot obtain mechanistic information from the contractions. If they are not equilibrated, are they far enough away from equilibrium so that you have confidence that *the mechanism is controlling the* products?

Author's Reply. For the dwell times (500–800 microseconds) of these pyrolysis experiments, the acetylenes are equilibrated only above 1500–1700 K, depending on the concentration and identity of the reactant. Major conclusions of the present work are dependent strongly on the experimental result that products of low temperature (1100–1300 K) pyrolysis of vinylacetylene are principally acetylene, diacetylene, and hydrogen with the product ratios C_2H_2/C_4H_2 and C_2H_2/H_2 approximately ten to one. Perturbations of these product ratios by equilibration reactions would significantly alter the conclusions of this paper. The "non-equilibration" of acetylene at low temperatures and short times can be demonstrated by the following modeling study and by comparison to experiments on benzene pyrolysis.

In an artificial modeling exercise of C_4H_4 pyrolysis, rate coefficients for Reactions 46 and 20 were decreased while coefficients of Reactions 13 and 18 were increased by factors of ten (10) *or more*. The net result was to convert the overall decomposition pathway from:

$$C_4H_4 \rightarrow 2C_2H_2$$

to

$$C_4H_4 \rightarrow C_4H_2 + H_2$$

The modeling results below 1400 K indicated final C_4H_2/C_2H_2 *ratios of approximately one hundred* (100) to one which is 2½ orders of magnitude above equilibrium. Consequently, this modeling exercise indicates the relative unimportance of equilibrating reactions under the low temperature conditions at which the decomposition mechanism was deduced.

Experimental evidence for *non-equilibration* at low temperatures can be inferred from recent data on benzene pyrolysis. At 1500K, several hundred degrees higher than the temperatures at which mechanistic information was obtained in the present work, Colket[1] found an initial C_2H_2/C_4H_2 ratio of approximately three (3) to one (1), a value lower than the equilibrated ratio of about five (5) to one (1) (depending on assumed thermochemistry). The experimental ratio is similar to the value (two to one) obtained by Kern, et al.[2], at yet higher temperatures (1704 K). Consequently, both modeling and experimental data support arguments that early (i.e. initial) formation of acetylenic products are not equilibrated.

REFERENCES

1. Colket, M.B., "Pyrolysis of C_6H_6," Preprints of the Division of Fuel Chemistry, American Chemical Society, *31* (2), 98 (1986).
2. Ref. 33 of manuscript.

●

J.H. Kiefer, Univ. of Illinois at Chicago, U.S.A. In answer to Dr. Harris' question, current models of high-temperature acetylene pyrolysis require C_2H radicals for C_4H_2 equilibration, and the formation of this radical seems unlikely at these temperatures. I also have questions for the speaker. First, for your chain production of C_2H_2 to proceed sufficiently I suspect you may well need the high rate of vinyl dissociation you assumed. Otherwise the fast process $C_2H_3+H \rightarrow C_2H_2+H_2$ would very effectively terminate the chain. Do you think you could stand the low rate of vinyl dissociation of your butadiene work[1]? Finally, if the heat of formation of C_4H_3 were about 130 kcal/mol, as has been suggested to me by Karl Melius, could your model still provide sufficient conversion of C_4H_4?

REFERENCE

1. Kiefer, J.K., Wei, H.C., Kern R.D., and Wu, C.H.: Int. J. Chem.Kin., *17*, 225 (1985).

Author's Reply. The philosophy for selection of reactions and corresponding rate constants presented in Table I was to use well-established mechanisms and rate constants while selecting other mechanisms and rate constants as required by the experimental results, but consistent (in most cases) with thermochemistry. Vinyl decomposition was assumed to be

pressure independent and its rate constant was not varied in the analysis described by the manuscript. A preliminary examination of the effect of the use of a lower rate for vinyl decomposition was examined by using Kiefer's rate expression which is more than 100 times slower than that used in the present analysis. In the modeling of vinylacetylene, the overall decomposition rate of the parent decreased by only 20%, although the "quasi-steady" concentration of vinyl radicals increased by nearly a factor of 100. The overall route of vinylacetylene decomposition changed only slightly from that described in the manuscript. Main problems that arise are: (1) diacetylene and ethene are overpredicted by about a factor of two and five, respectively; and (2) early formation of both vinylacetylene and benzene from acetylene pyrolysis are underpredicted each by about an order of magnitude. Some features suggest that an intermediate value for vinyl decomposition might be reasonable. The data on vinylacetylene and acetylene from this work, however, do not support the low rate constant as determined in your analysis of my butadiene data.

If C_4H_5 radicals have a heat of formation of 130 kcal/mole, it would tend to support present arguments that H-atoms add to vinylacetylene rather than abstract H-atoms from vinylacetylene. By using this high heat of formation in modeling, however, two major problems will arise. First, the effective activation energy of the initiation process ($C_4H_4 \rightarrow i\text{-}C_4H_3 + H$) was 85 kcal/mole in this work. This low value is questionable as it stands, but would be nearly impossible to reconcile if the overall endothermicity were 113 kcal/mole. A second problem results from the fact that the high heat of formation (vs. 125 kcal/mole assumed in this work) would substantially reduce the "quasi-steady state" concentration of $n\text{-}C_4H_5$. Thus, the formation of phenyl via $n\text{-}C_4H_5$ addition to acetylene would be substantially reduced and benzene and phenylacetylene significantly underpredicted.

•

W.C. Gardiner, University of Texas U.S.A. Inclusion of irreversible steps in polymer formation mechanisms has to be regarded with special care, particularly in the case of soot formation, where the diversity of pathways and unsuspected reversibility of quite exoergic steps make the points of no return first appear at molecular sizes well beyond those considered in this paper[1].

In order to make valid comparisons between computed and measured yields of one-ring and two-ring aromatic compounds, the reaction mechanism must be extended—under provision for reverse reaction—to still larger species, as a minimum to acenapthalene. For this reason it would appear that the rate constants used in this paper to model formation of aromatic rings have to be regarded as artificial.

REFERENCE

1. Frenklach, M., Clary, D.W., Gardiner, W.C., and Stein, S.E.: 20th Symp. (Int.) on Combustion, p. 887, The Combustion Institute, Pittsburgh, 1985.

Author's Reply. In general, your comment is very reasonable and should be considered for long reaction times or conditions which allow conversion of significant matter to larger species. However, for the conditions at which the modeling was applied in this work, this effect is relatively unimportant. In the present study, the kinetics analysis was performed for short reaction times (700 microseconds) and low temperatures (<1600 K) for which early formation kinetics (of aromatics) could be observed. Under these conditions, relatively small fractions of the observed aromatics undergo growth processes. For example, in the case of 3.5% acetylene pyrolysis, 10 ppm of benzene was observed at 1100 K, the lowest temperature at which the mixture was pyrolyzed. Concentrations of phenylacetylene at this temperature can be estimated to be 1½ to 2 orders of magnitude lower and do not achieve a comparable concentration until 1500 K (for the same dwell time). Based on data using higher initial concentrations of acetylene (4.9%), naphthalene concentrations are more than an order of magnitude below those of phenylacetylene at these temperatures. An analysis of mass balance indicates good recovery of initial carbon below 1650 K. These results may not be proof, but they indicate strongly that the processes observed in this study are descriptive of the initial formation steps (of aromatics) and perturbation due to lack of inclusion of subsequent growth processes are negligible.

•

M. Frenklach, Pennsylvania State Univ., U.S.A. Our mechanism (1,2) to which the author refers, was composed of a very large variety of reaction pathways including all those discussed by the author. No assumptions about the importance of individual elementary reactions in the mechanism were made; our conclusions about dominant reaction pathways leading to polycyclic aromatic hydrocarbons and soot were drawn instead from the results of computer experiments described in the cited references. Thus, contrary to the author's assertion, the pathway

$$n\text{-}C_4H_5 \rightarrow C_4H_4 + H$$
$$C_4H_4 + H \rightarrow n\text{-}C_4H_5 + H_2 \qquad (1)$$

was not *assumed* but *deduced* to be the dominant pathway for the production of $n\text{-}C_4H_5$ for the conditions of "soot" formation in shock-tube pyrolysis of acetylene. Although we found the reaction

$$C_2H_2 + C_2H \rightarrow n\text{-}C_4H_3 \qquad (2)$$

to be fast at very short reaction times, it quickly gave way to the sequence (1) that became dominant for soot appearance. The competition between (1) and (2) is sensitive to experimental conditions; e.g., reaction (2) plays a more prominent role in the presence of oxygen (3). Hence, differences in experimental conditions and different assumptions about thermochemical values are the likely sources of the different relative fluxes of (1) and (2) noted in this paper.

REFERENCES

1. Frenklach, M., Clary, D.W., Gardiner, W.C., Jr., and Stein, S.E.: *Twentieth Symp. (Int.) on Combustion*, p. 887, The Combustion Institute, Pittsburgh, 1985.
2. Frenklach, M. Clary, D.W. and Ramachandra, M.K., "Shock Tube Study of the Fuel Structure Effects on the Chemical Kinetic Mechanisms Responsible for Soot Formation, Part II", NASA Contractor Report 174880, May 1985.
3. Frenklach, M., Yuan, T., Clary, D.W., Gardiner, W.C., Jr., and Stein, S.E.: *Combust. Sci. Technol.*, in press.

Author's Reply. As suggested by Dr. Frenklach, the manuscript should be changed to read: "Previously, it was *deduced* . . . that n-C4H3 was formed through path A, whereas (R-12) was the dominant route under the present conditions." In both the present and previous work, it should be remembered that the authors have been forced to estimate—or assume—values of absolute rate constants for which either no data or little data are available. Oftentimes, substantial uncertainty exists in estimation techniques. Consequently, this procedure, by its very nature, leads to *assumptions* about the importance of individual elementary reactions. Conclusions reached or deduced in any work usually are only as good as the initial assumptions.

•

A.M. Dean, Exxon Res. & Eng. Co., U.S.A. Given the fast rate constant for $C_2H_3 + C_4H_4$ (with no activation energy) that was needed to explain C_6H_6 formation, is it not possible to conclude that the rapid rate of aromatics formation is still a puzzle?

Author's Reply. The rate constant for k_{45} was determined to be 4×10^{11} cc/mole-sec, which is about two orders of magnitude below collision frequency and is similar in magnitude to rate constants determined for other addition reactions. The only unusual feature regarding Reaction 45 is that the linear intermediate, 1,3,5-hexatrien-3-yl, must undergo an H-atom shift and convert to the 1,3,5-hexatrien-1-yl radical prior to cyclization. It is believed, however, that this H-atom shift is not rate controlling. The size of the rate constant, in the opinion of the authors therefore, does not appear to be unreasonably large. The activation energy could not be determined in this experiment; and so none was assigned, although it would not be unreasonable to assume an effective activation energy of at least several kcal/mole.

Certain features of aromatics formation certainly can be considered to be unresolved, or at least under discussion. See, for example, the other questions and responses to this paper. Certainly more experimental and modeling work needs to be performed. One critical area of research is the accurate determination of enthalpies and entropies (and their temperature dependencies) for important radical intermediates.